People's Democratic Republic of Algeria

Ministry of Higher Education and Scientific Research

20th August 1955 University – SKIKDA

Faculty of Technology
Department of Petrochemistry

Dissertation

With a view to obtaining the diploma in

Master

Field: Petrochemical Industries

Specialty: Petrochemical Engineering

Theme :

Neural Network Modeling and Development of an Application for Optimizing Flare Gas Recovery Module in Skikda Refinery RA1K

Students :

- SAAD DJABALLAH Wiam
- BRAHIMI Aicha Zina

Supervised by :

- Dr. BOUSSOUF Ibtissam
- Dr. BENDIB Riad

University Year 2024/2025

Acknowledgement

*Before our words seek out human names, we begin by thanking **Allah**, the Most Merciful, Source of all wisdom and strength. By His will this journey began, and by His grace it finds completion.*

*To our beloved **parents, sisters and brothers,** your love, prayers, and unwavering support have been our greatest strength. Thank you for being our light through every challenge.*

*Our sincere gratitude goes to **our supervisors: Dr. BOUSSOUF Ibtissam & Dr. BENDIB Riad**, for their guidance, patience, and encouragement throughout this work. their support shaped both its direction and our growth.*

*We would also like to express our sincere gratitude to **Mr. KERBOUAA** and **Mr. NEDJRAN** for their valuable help and support throughout this work*

*And to our **friends**, thank you for the shared struggles, the late nights, and the laughter that made it all easier.*

To everyone who has, in one way or another, contributed to this accomplishment. thank you. May Allah bless you all abundantly.

Dedications

For all those who stand behind the quiet moments of success, I dedicate this work

*To my loving **parents**, who have always been the foundation of my strength, and whose endless support made every step possible.*

*To my amazing **sisters**, who brought joy, encouragement, and calm through every challenge.*

*To my **research partner and dearest friend, Aicha,** thank you for walking every step beside me, for the motivation, the laughter, and the resilience we built together. Alone we can do so little, together we can do so much.*

*To my true **friends**, who shared the stress, the hope, the long nights, and the quiet victories.*

*To the dedicated **professors** who guided me with patience, challenged me to do better, and helped shape the person I've become.*

*To my **PETROCHEMICAL ENGINEERING** family, the **PROMO 2020-2025**, and our **DEPARTEMENT: PETROCHEMICAL INDUSTRY**, where I learned, grew, failed, succeeded, and found my voice.*

And to the person I'm becoming, may I never forget where I started.

Wiam

Dedications

First and foremost, I would like to thank my mother the one who has been there through it all. Thank you for understanding me like no one else ever could, no matter how messy or ridiculous the situations I got myself into.

Most importantly, thank you for being my best friend the one who listens to my thoughts, my dramas, and supports me without hesitation. You are, without a doubt, the greatest mom of all time.

To my father thank you for being by my side throughout these five years. Your presence and support have shaped the person I am today.

To my brothers I love you. Thank you for always making me feel special, for being my protectors, and yes, sometimes even my helpers just as I deserved.

To my Wiwi, my partner in crime it's been five years since we met, and I still remember it like it was yesterday. The crazy memories we've made together, and now, the fact that we're graduating side by side it's truly on another level. Thank you for being not just a great classmate and friend, but a true ride-or-die.

To Meram, Madjda, and Marwa I wouldn't have made it through without you. You've made my life brighter and lighter. Thank you for giving me some of the happiest moments I'll carry with me forever. Every corner of the university, every seat on the bus, every little memory is filled with your laughter and love. You are the reason I believe that love and friendship are very real.

To Nisrine and Marwa God may not have given me sisters by blood, but He gave me you. You know how much I've longed for that bond, and I found it with you.

Thank you for every shared moment, every comforting word, and every burst of laughter.

Finally, to my beautiful self-Nina only you and Allah know how difficult these five years have been. But through every storm, every moment of doubt, you stood back up when no one thought you would. Life taught us how hard it is to be there for everyone you love while still having to fight for yourself in silence. So today, I want to thank myself for choosing the right path, for holding on to faith, and for becoming the person I am today. You made it. You're graduating. You're closing a chapter with strength and grace.

And to the future me, when you come back and read this I hope you're everything you dreamed of becoming. I hope your life is as beautiful as your soul.

Finally, I want to thank every person who has crossed my path during this journey the ones I loved, who showed me what love truly feels like, and even the ones I disliked, who reminded me that pain, mistrust, and disappointment are part of life too.

I thank my teachers, my classmates, the people I've shared memories with, and even the strangers I passed on the street because I truly believe that everyone we meet, no matter how briefly, is meant to teach us something.

As I close this chapter, I hold on to the hope that over these five years, I have learned everything I needed to learn in order to move forward stronger, wiser, and ready for what comes next.

Aicha

ABSTRACT

This memory presents the modeling and optimization of the Flare Gas Recovery (FGR) module, focusing on the GTK unit at Skikda Refinery RA1K, using artificial neural networks (ANNs) and process simulation. The goal is to develop a predictive model and a MATLAB application to make the unit smarter, helping engineers reduce gas flaring, improve energy efficiency, and make better operational decisions. The operational goal is to maximize LPG recovery in unstabilized naphtha, while minimizing energy losses and emissions related to flaring. The GTK module was simulated with ASPEN HYSYS to understand its behavior and generate reference data. Real operational data from the DCS were used to train and test the ANN model. The developed application integrates this model with a user-friendly interface for prediction and scenario analysis. Results confirm the accuracy of the approach ($R^2 > 0.99$) and its potential to minimize flaring losses. This work shows how combining simulation and AI tools can support more sustainable refinery operations.

Keywords: Artificial Neural Networks; Flare Gas Recovery; Aspen HYSYS; Smart Refinery; Dynamic Simulation; LPG - Unstabilized Naphtha.

Résumé

Ce mémoire présente la modélisation et l'optimisation du module de récupération des gaz de torche (FGR), en particulier le module GTK de la raffinerie RA1K de Skikda, en utilisant les réseaux de neurones artificiels (RNA) et la simulation de procédé. L'objectif est de développer un modèle prédictif et une application MATLAB pour rendre l'unité plus intelligente, afin d'aider les ingénieurs à réduire le torchage, améliorer l'efficacité énergétique et prendre de meilleures décisions opérationnelles. L'objectif opérationnel est de maximiser la récupération du GPL dans le naphta instable, tout en minimisant les pertes énergétiques et les émissions liées au torchage. Le module GTK a été simulé avec ASPEN HYSYS afin de générer des données de référence. Des données réelles du DCS ont permis d'entraîner et de tester le modèle. L'application intègre ce modèle via une interface conviviale pour la prédiction et l'analyse de scénarios. Les résultats confirment la précision ($R^2 > 0.99$) de l'approche et son potentiel de réduction des pertes par torchage. Ce travail montre l'intérêt de combiner simulation et IA pour une exploitation plus durable des raffineries.

Mots clés : Réseaux de neurones artificiels ; Récupération des gaz de torche ; Aspen HYSYS ; Raffinerie intelligente ; Simulation dynamique ; GPL - naphta instable.

ملخص

يعرض هذا البحث نمذجة وتحسين وحدة استرجاع غازات الشعلة (FGR)، مع التركيز على وحدة GTK في مصفاة سكيكدة RA1K، بالاعتماد على الشبكات العصبية الاصطناعية (ANN) ومحاكاة العمليات. يهدف هذا العمل إلى تطوير نموذج تنبؤي وتطبيق برمجي في بيئة MATLAB بهدف جعل الوحدة أكثر ذكاءً، ومساعدة المهندسين على تقليل عمليات الحرق وتحسين الكفاءة الطاقوية واتخاذ قرارات تشغيلية أفضل. الهدف التشغيلي هو رفع نسبة استرجاع الغاز البترولي المسال في النافثا غير المستقرة، مع تقليل الخسائر في الطاقة والانبعاثات الناتجة عن عملية الحرق. تمّت محاكاة وحدة GTK باستخدام برنامج ASPEN HYSYS لتوليد بيانات مرجعية وفهم سلوك الوحدة. كما استُخدمت بيانات تشغيلية حقيقية من نظام التحكم الموزّع (DCS) لتدريب واختبار النموذج العصبي. يدمج التطبيق هذا النموذج عبر واجهة استخدام بسيطة تتيح التنبّؤ وتحليل السيناريوهات. أظهرت النتائج دقّة المنهجية ($R^2 > 0.99$) وقدرتها على تقليل الفواقد الناتجة عن الحرق. يبرز هذا العمل أهمية توظيف المحاكاة مع أدوات الذكاء الاصطناعي لدعم التشغيل المستدام للوحدات الصناعية.

الكلمات المفتاحية : الشبكات العصبية الاصطناعية؛ استرجاع غازات الشعلة؛ Aspen HYSYS ؛ المصفاة الذكية؛ المحاكاة الديناميكية؛ GPL - نافثا غير مستقرة.

Table of Contents

Abbreviations List

ANN: Artificial Neural Network.

Bcm: Billion Cubic Meters.

CDU: Crude Distillation Unit.

GHG: Green House Gases.

GTK: Gas Torches compresseur.

LNG: Liquified Natural Gas

LPG : Liquified Pteroleum Gas.

NG: Natural Gas.

U10: Atmospheric Distillation Unit 10.

UNFCCC: United Nations Framework Convention on Climate Change.

ANN: Artificial Neural Networks

Tables List

Figures List

Annexes List

Annex 01: GTK Module PFD (Process Flow Diagram).

Annex 2: GTK Module Streams Composition and Parametrs “Design

Annex 03: GTK Streams Composition and Parameters “Real Case”.

Annex 04: DCS DATA “15/04/2025”.

GENERAL INTRODUCTION

Petroleum refining is the industrial process of transforming crude oil a complex mixture of hydrocarbons into valuable finished products such as gasoline, diesel, kerosene, jet fuel, and petrochemical feedstocks. Modern refineries operate as integrated systems that use various processes including distillation (to separate crude into fractions based on boiling points), thermal and coking units (to convert heavy residues into lighter products), catalytic processes (like cracking and reforming to improve fuel quality and yield), and treatment units (to remove impurities and meet environmental standards) [1].

Each unit plays a vital role in ensuring operational efficiency, meeting the global demand for energy and chemical products, environmental compliance, and resource optimization. In this context, the Skikda refinery stands out not only for its significant refining capacity but also for its commitment to modern recovery technologies. A prime example of this is the GTK module, an essential component designed to recover flare gas and reduce emissions, and this is what we focused on.

The GTK module is designed to recover valuable hydrocarbons from gases that would otherwise be flared, helping reduce environmental pollution and energy waste. It mainly handles gases coming from the overhead of the atmospheric distillation unit and processes them through a system composed of a separator drum, compressor, cooler, and final separation**.** The recovered gases, such as LPG and light hydrocarbons, are routed for further processing. By reducing flaring and increasing product recovery, GTK contributes to improving refinery efficiency, enhancing environmental protection, and boosting economic gains through the recovery of valuable intermediate products like LPG and naphtha**.** [2]. The GTK equipment plays an important role in Unit 10 of the Skikda refinery due to the problems it helps solve and the value it adds. Therefore, we chose it as the focus of our study, which aims to transform this equipment into a smart one.

To bring this vision to life, we followed a structured multi-step approach. First, Aspen HYSYS was used to simulate the GTK unit and gain a deeper understanding of the process. At the same time, real industrial data was collected from the Distributed Control System (DCS) at the refinery. This data served as the foundation for training an Artificial Neural Network (ANN), computer models inspired by the brain. They learn from data by adjusting connections between simple processing units (neurons), making them useful for recognizing patterns and

making predictions [3] in MATLAB, with the goal of predicting and optimizing the volume flow of unsterilized naphtha. Finally, the developed model was integrated into a smart application, effectively transforming the GTK unit into an intelligent, self-optimizing system.

This dissertation contains five chapters:

- The first discusses gas flaring.
- The second presents the exploration of neural networks: key concepts and practical application.
- The third provides a description of Unit 10 and the GTK Module of the Skikda refinery.
- The fourth shows the simulation of the design and real cases of the GTK Module.
- The fifth explains the optimization of the GTK Module through neural network-based modeling of the LPG fraction.

References:

[1]. Al-Qahtani, K. Y. (2009). Petroleum refining and petrochemical industry integration and coordination under uncertainty (Doctoral dissertation, University of Waterloo).

[2]. Bouzaouit, A., & Bendjama, C. (2022). Simulation and study of new configuration for flare gas unit (GTK) Skikda (Master's thesis, University of 20 August 1955 Skikda). Faculty of Technology, Department of Petrochemistry and Process Engineering.

[3]. Sathelly, B. (2018). An artificial neural network approach to predict liver failure likelihood (Master's thesis, University of Toledo).

CHAPTER I

Gas Flaring

I.1 Introduction

In the world of oil and gas processing, efficiency and sustainability are more critical than ever. A significant challenge that continues to confront refineries and petrochemical plants is the handling of flare gases—a by-product generated during routine operations and emergency pressure relief events. These gases, if not managed properly, are simply burnt off via flaring, leading to environmental pollution, energy wastage, and economic loss [1].

Flare gases primarily consist of hydrocarbon vapors, often including valuable components like methane, ethylene, propane, and heavier compounds. Traditionally, these gases have been flared to ensure safety and prevent over-pressurization, but with increasing environmental regulations and rising energy costs, this once-common practice is no longer sustainable [1].

I.2 Gas flaring in industry

I.2.1 Definition of gas flaring

Flaring is defined by Canadian Association of Petroleum Producers as the controlled burning of natural gas that cannot be processed for sale or use because of technical or economic reasons.

Flaring can also be defined by the combustion devices designed to safely and efficiently destroy waste gases generated in a plant during normal operation [2].

I.2.2 Definition of flare gas

When oil is extracted, it often comes to the surface accompanied by water and gas, known as "associated gas." After being separated from the oil, the gas may be *flared,* meaning it is burned on site, a process that is visible as a flame coming from a flare stack [3].

I.2.3 Flare gas composition

Flare gas consists of a mixture of different gases. The composition depends upon the source of the gas going to the flare. Associated gases released during oil-gas production mainly contain natural gas (NG). NG is more than 90 % methane (CH_4) with ethane and a small amount of other hydrocarbons; inert gases such as N_2 and CO_2 may also be present.

Flare gas from refineries and other process operations will commonly contain a mixture of hydrocarbons and in some cases hydrogen. However, landfill gas, biogas or digester gas is a

mixture of CH_4 and CO_2 along with small amounts of other inert gases. There is in fact no standard composition and it is therefore necessary to define some group of flare gas according to the actual parameters of the gas [2,3].

I.2.4 Flare gas sources

The sources of gas emissions into the atmosphere are [3]:

- ✓ Gases associated with crude oil in oil fields.
- ✓ Gases from gas processing units.
- ✓ Gases from LNG units and refineries.
- ✓ Gases released during the commissioning of an oil or natural gas well.
- ✓ Gases emitted during operational difficulties or power outages.

I.3 State of global flaring

Global flaring estimates based on satellite data are useful for assessing global, regional, and country-level flaring trends. The World Bank has published such data on global flaring volumes since 2012. The data shows the total volume of gas flared from upstream oil and gas in 2023 was 145 billion cubic meters (bcm).

Flaring rose by 9 bcm from 2022 to 2023 while oil production only grew by one percent, resulting in an increase in flaring intensity from 4.7 m^3/ bbl to 5 m^3/bbl [4].

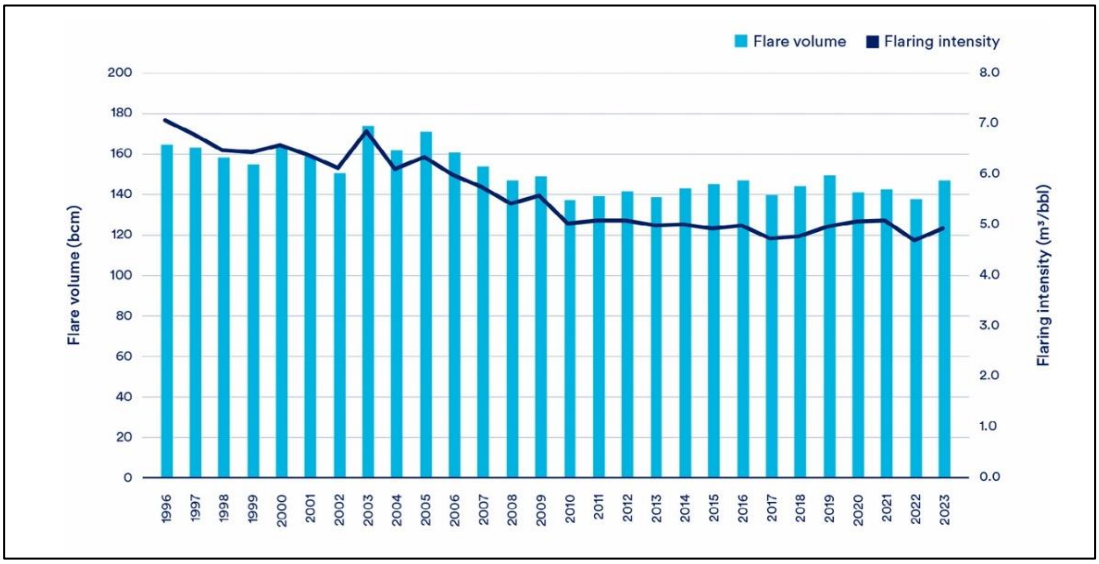

Figure I.1: World Bank Global Flaring and Methane Reduction Partnership (GFMR) [4].

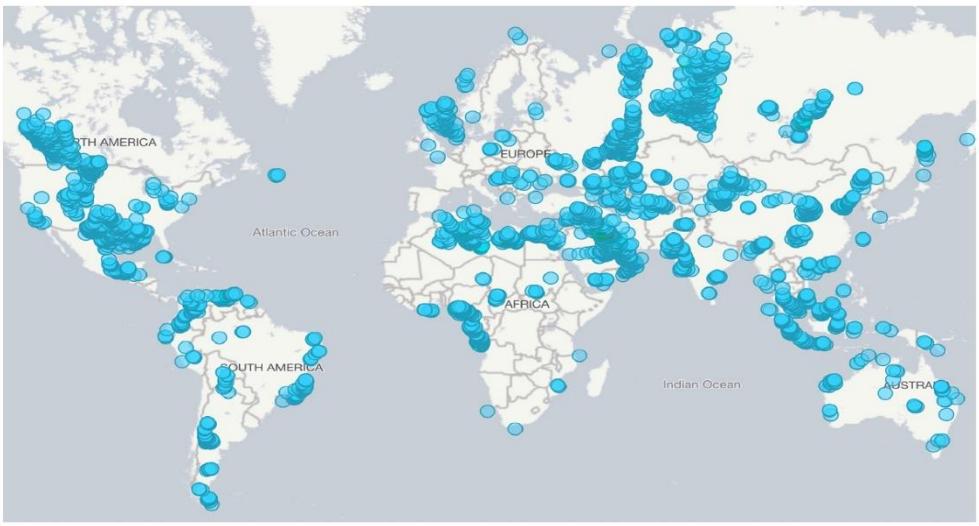

Figure I.2: Locations of Flares Observed by Satellite, from World Bank Global Gas Flaring Tracker [4].

I.3.1 Gas flaring in the Arab region

Algeria, Iraq and Libya accounted for close to 80% of the Arab region's total gas flaring. If we add Egypt, Oman and Saudi Arabia, the total gas flaring of this group of six countries represents over 90% of all the gas flared in the Arab region [5].

Gas flaring volumes in Algeria and Oman are the equivalent of 21% and 10%, respectively, of their gas consumption levels in 2018. Despite the much lower percentage levels compared with Iraq and Libya, the flared volumes remain relatively high for countries facing natural gas supply constraints [5].

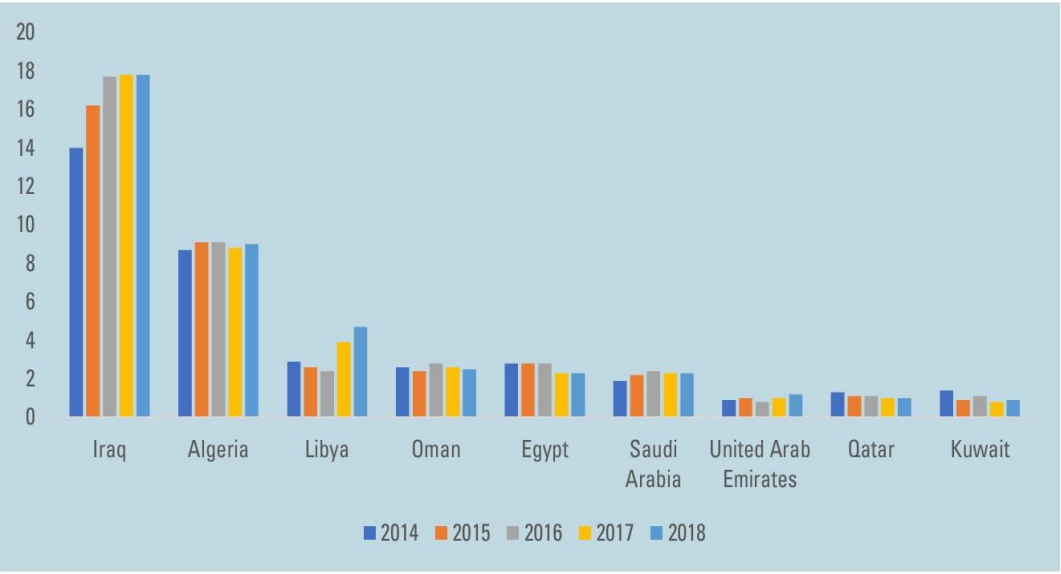

Figure I.3: Gas flaring in Arab countries (bcm), 2014-2018 [5].

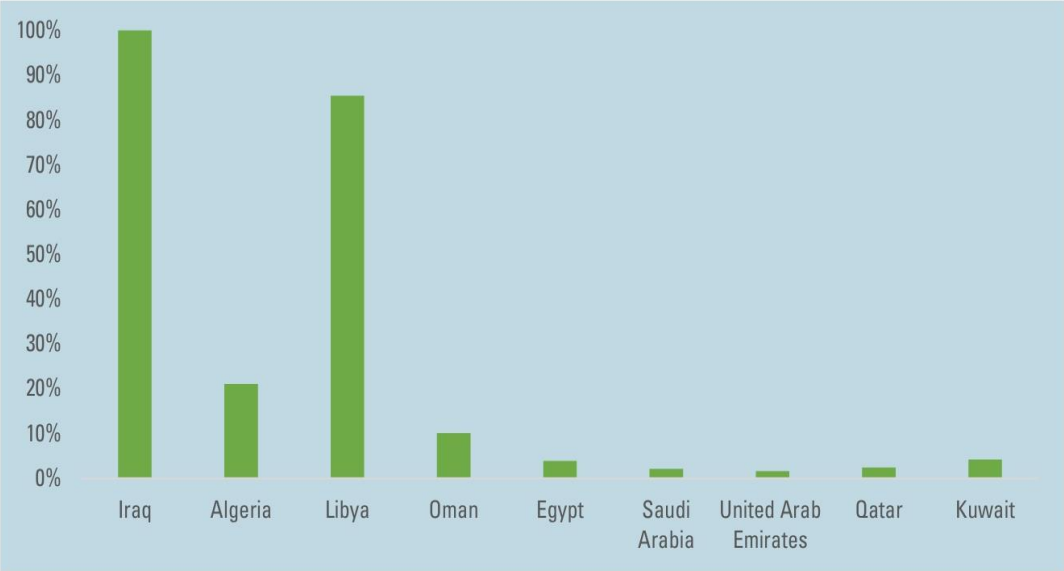

Figure I.4: Gas flaring as a percentage of 2018 gas consumption [5].

I.4 Gas flaring types

Depending on the rationale for its application, flaring can be categorized as Routine, Safety and Non-Routine [6].

- Routine flaring is undertaken during normal oil production operations in the absence of sufficient facilities or amenable geology to reinject the produced gas, use it on-site, or dispatch it to a market. For instance, an upstream operator may flare because the sale of associated das to end consumers is hindered by the remoteness and topology of the drilling location, low gas price in accessible market, or a time lag between the development of the field and connection to a gas pipeline.
- Safety flaring is done to purge flare lines, to ensure safe operation of the facility, or to do both, and includes emergency shutdown.
- Non-Routine flaring can occur for a range of reasons outside od routine and safety, such as equipment maintenance, initial field start-up or start-up after a shutdown, temporary failure at gas collection facilities, and well testing and maintenance.

I.5 Gas flaring emissions

A large number of hydrocarbons are produced when waste oil-gas and oil-gas-water solutions are flared. Flaring is inefficient with combustion being most affected by ambient winds and heating value of the fuel. Inefficient burning releases raw fuel. The efficiency of flares can be dependent on several factors like composition of the flare stream, Flow rate of

flare gases, wind velocity, ambient turbulence, presence of hydrocarbon droplets in the flare stream and presence of water droplets in the flare stream [7].

These operational and compositional factors can adversely affect flame stability and combustion completeness, resulting in the formation of soot and carbon monoxide (CO) due to incomplete oxidation of hydrocarbons [8].

The goal of flare is to convert, through oxidation, substances in the flare gas stream to their safest form possible. In the case of hydrocarbons, the most desirable products are carbon dioxide and water vapour. Sulphur in compounds like hydrogen sulphide is converted to sulphur dioxide. Other oxides, like the oxides of nitrogen, or partially oxygenized compounds like carbon monoxide or formaldehyde are less desirable. Toxic compounds like poly-nuclear aromatic hydrocarbons PAHs, aromatics and volatile organic compounds formed in these diffusion flames may not be fully consumed [7].

I.6 Gas flaring regulation in Arab countries

The lack of regulatory frameworks or effective and enforceable regulation to reduce and eventually stop associated gas flaring is a key challenge faced by Arab hydrocarbon-producing countries. As shown in table, this ranges from cases where there is no specific regulation of gas flaring, to cases where a country's oil and gas regulation clearly addresses the issue of gas flaring reduction or elimination and sets non-compliance penalties or taxes [5].

- **Regulation in Algeria:**

Article 52 of the 2013 Hydrocarbons Law prohibits gas flaring. However, routine flaring authorizations could be granted exceptionally for limited periods of time [5].

Article 158 of the new 2019 Hydrocarbons Law prohibits the flaring and venting of gas. As stipulated in the previous law, routine flaring authorizations could be granted exceptionally for limited periods of time. Flaring required for safety reasons does not require such authorizations, but a detailed report must be submitted to the relevant regulatory authorities 10 days after the flaring [5].

The new hydrocarbons law has been approved by the lower and upper houses of parliament, it became effective on December 22, 2019, upon its publication in the Official Journal, as established by Law No. 19-13 of December 11, 2019, which sets the legal framework for oil and gas activities in Algeria [9].

- **Penalties or flaring taxes :**

Any operator requesting this exceptional authorization will have to pay a non-deductible specific tax to the treasury of 8,000 Algerian dinars/1000 m^3 of flared gas. For isolated areas, a different flaring tax system applies. In the new 2019 Hydrocarbons Law, the above penalty has been increased to 12,000 Algerian dinars/1000 m^3 to take into consideration the depreciation of the Algerian dinar [5].

I.7 Impacts of gas flaring

The effects of gas flaring under this heading are multifaceted. These effects, have received the most attention and corrective action worldwide. Although the impacts are seen more in developing countries like Nigeria, Angola, Libya etc. where technology for utilization of such energy are only recently just be employed at a snail pace [7].

The impacts on human, the environment and the economy remain that of a global concern. Nigeria and Russia have been mentioned to be the highest gas flaring countries in all the literatures reviewed with more literatures on the Niger Delta region of Nigeria as it concerns these impacts of gas flaring. Current developments in these countries to mitigate the effects of gas flaring have been discussed under trends of gas flaring [7].

I.7.1 Environmental degradation

The environmental problems caused by flaring are mainly global, but to some extent also regional and local. For example, flaring/venting during oil production operations emits CO_2, methane and other greenhouse gases which contribute to global warming causing climate change, and this affects the environmental quality and health of the vicinity of the flares. This negates commitments made by countries under the United Nations Framework Convention on Climate Change (UNFCCC) and Kyoto Protocol. Global environmental impact is due to the burning of associated or solution gas, which produces carbon dioxide (CO_2) and methane (CH_4). These emissions increase the concentration of greenhouse gases (GHG) in the atmosphere, which in turn contributes to global warming [7].

Gas flaring contributes to climate change, which has serious implications for the world. Gas flaring is a major source of greenhouse gases (GHG) contributing to global warming which could accelerate the problem of climatic change and harsh living conditions on earth, if not checked.

Moreso, flaring may further contribute to local and regional environmental problems, such as acid rain with attendant impact on agriculture, forests and other physical infrastructure.

The acid rain which results in environmental degradation including soil and water contamination, and roof erosion.

The incineration of sour gas produces sulphur oxides, which are released into the atmosphere. The end result of these compounds when they combine with atmospheric compounds, namely oxygen and water is what is called acid rain, which produces a lot of negative environmental effects [7].

I.7.2 Health implications for humans

The health impacts of air pollution spreads across a wide area, and those who rely on locally produced food whether from their own production or bought at market, risk contamination. The flares contain widely-recognized toxins, such as benzene, which pollute the air. Local people complain of respiratory problems such as asthma and bronchitis. There have been over 250 identified toxins released from flaring including carcinogens such as benzopyrene, benzene, carbon disulphide (CS_2), carbonyl sulphide (COS) and toluene; metals such as mercury, arsenic and chromium; sour gas with H_2S and SO_2; Nitrogen oxides (NOx); Carbon dioxide (CO_2); and methane (CH_4) which contributes to the greenhouse gases [7].

Environmental contaminants have also been related to endocrine dysfunction, immune dysfunction, reproductive disorders and autoimmune rheumatic diseases. Gas flaring causes surrounding communities to suffer from increased health risks including premature deaths, respiratory illnesses, asthma and cancer. Another effect that should be addressed is thermal pollution, since there is a limit to which the human body can tolerate the fluxes released during gas flaring. Furthermore, both habitat and structural buildings nearby also have heat threshold [7].

Table I.1: Thermal and noise emissions from flaring [2].

Distance (m)	Thermal radiation (kW/m^2)	Noise level (dB)
10	5.66	86.3
20	5.87	86.19
30	6.04	86.02
40	6.14	85.78
50	6.17	85.50
60	6.14	85.18
70	6.04	84.83
80	5.88	84.46
90	5.67	84.08
100	5.42	83.68

Table I.2: Pollutants of flare and their health effect [2].

Chemical name	Health effect
Ozone in land	In low densities eye will stimulate and in high densities especially children and adults it will cause respiratory problems.
Sulphide hydrogen	In low densities it will effect on eye and nose which result in insomnia and headache.
Dioxide nitrogen	It will effect on depth of lung and respiratory pipes and aggravates symptoms of asthma. In high densities it will result in meta hemoglobin which prevents from absorption of oxygen by blood.
Particles matter	There is this believe that it will result in cancer and heart attack.
Dioxide of Sulphur	It will stimulate respiratory system and as a result aggravating asthma and bronchitis.
Alkanes: Methane, Ethane, Propane	In low densities it will result in swelling, itching and inflammation and in high densities it will result in eczema and acute lung swelling.
Alkenes: Ethylene, Propylene	It will result in weakness, nausea and vomit.
Aromatics: Benzene, Toluene, Xylene	It is poisonous and carcinogenic. It influences on nerve system and in low densities it will result in blood abnormalities and also it will stimulate skin and result in depression.

I.7.3 Economic effects

From an economic perspective, the flaring of this associated gas is a colossal waste to the communities. The economic cost of total gas flared is quite staggering which implies great investment opportunities for the private sector. Hence, more gas intensive modes of production, greater private sector investment are encouraged in the sector and governments should recycle and seek for more trading opportunities for the gas sector. Apart from the release of greenhouse

gases into the atmosphere, gas flares are said to release some 45.8 billion kilowatts of heat into the atmosphere of the Niger Delta from gas flared daily.

As a result of this incineration of the environment, gas flaring has raised temperatures and rendered large areas uninhabitable [7].

I.8 The flare

The flare is a last line of defense in the safe emergency release system in a refinery or chemical plant. It is used to dispose of purged and wasted products from refineries, unrecoverable gases emerging with oil from oil wells, vented gases from blast furnaces, unused gases from coke ovens, and gaseous water from chemical industries. Flares are also used for burning waste gases from sewage digesters process, coal gasification, rocket engine testing, nuclear power plants with sodium, water heat exchangers, heavy water plants, and ammonia fertilizer plants.

The flare provides a means of safe disposal of the vapor streams from its facilities, by burning them under controlled conditions such that the adjacent equipment or personnel are not exposed to hazards, and at the same time obeying the environmental regulation of pollution control and public relations requirements [10].

I.8.1 Flare types

In industrial plants the most common utilized flare systems are elevated flares and ground flares. Selection of the type of flare is influenced by several factors, such as availability of space; the characteristics of the flare gas (composition, quantity and pressure); economics; investment and operating costs; public relations and regulation [10].

I.8.1.1 Elevated flare

Elevated flare is the most commonly used type in refineries and chemical plants. They have larger capacities than ground flares. The waste gas stream is fed through a stack from 32 ft to over 320 ft tall and is combusted at the tip of the stack. The elevated flare, can be steam assisted, air assisted or non-assisted [10].

The elevated flare can utilize steam injection / air injection to made smokeless burning and with low luminosity up to about 20%+ of maximum flaring load.

The disadvantage of steam injection / air injection is it introduces a source of noise and may cause noise pollution. If adequately elevated, this type of flare has the best dispersion characteristics for malodorous and toxic combustion products. Capital costs are relatively high,

and an appreciable plant area may be rendered unavailable for plant equipment, because of radiant heat considerations [10].

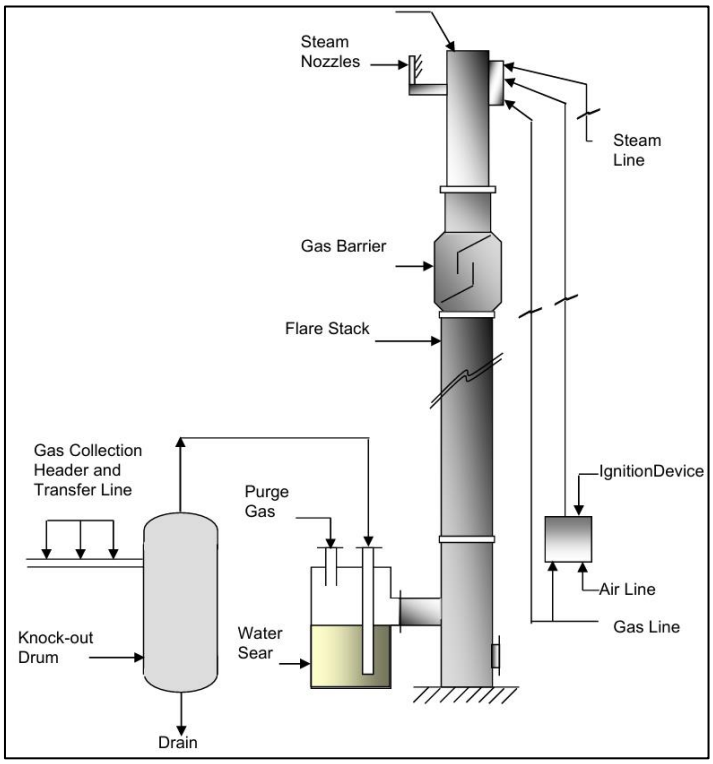

Figure I.5: Steam Assisted Elevated Flare System [10].

I.8.1.2 Ground flare

A ground flare is where the combustion takes place at ground level. It varies in complexity, and may consist either of conventional flare burners discharging horizontally with no enclosure or of multiple burners in refractory-lined steel enclosures.

The type, which has been used almost exclusively, is the multijet flare (enclosed type). Compare to elevated flare, ground flare can achieve smokeless operation as well, but with essentially no noise or luminosity problems, provided that the design gas rate to the flare is not exceeded.

However, it has poor dispersion of combustion product because its stack is near to ground, this may result in severe air pollution or hazard if the combustion products are toxic or in the event of flame-out. Capital, operating and maintenance requirements cost are higher [10].

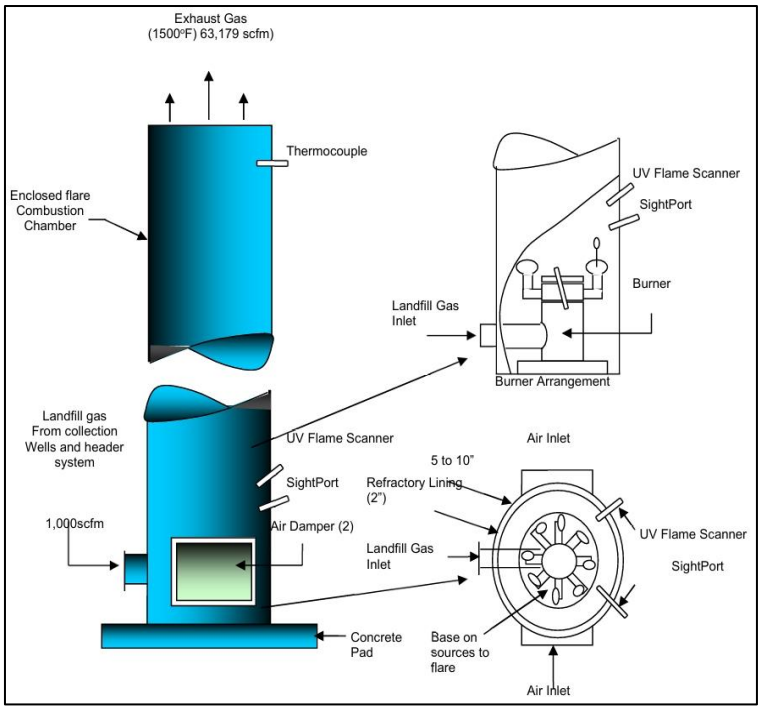

Figure I.6: Typical Enclosed Ground Flare [10].

I.8.2 Flare system

Typical flare system consists of [10]:

- Gas collection header and piping for collecting gases from processing units.
- A knockout drum to remove and store condensable and entrained liquids.
- A proprietary seal, water seal, or purge gas supply to prevent flash-back.
- A single or multiple burner unit and a flare stack.
- Gas pilots and an igniter to ignite the mixture of waste gas and air.
- A provision for external momentum force (steam injection or forced air) for smokeless flaring.

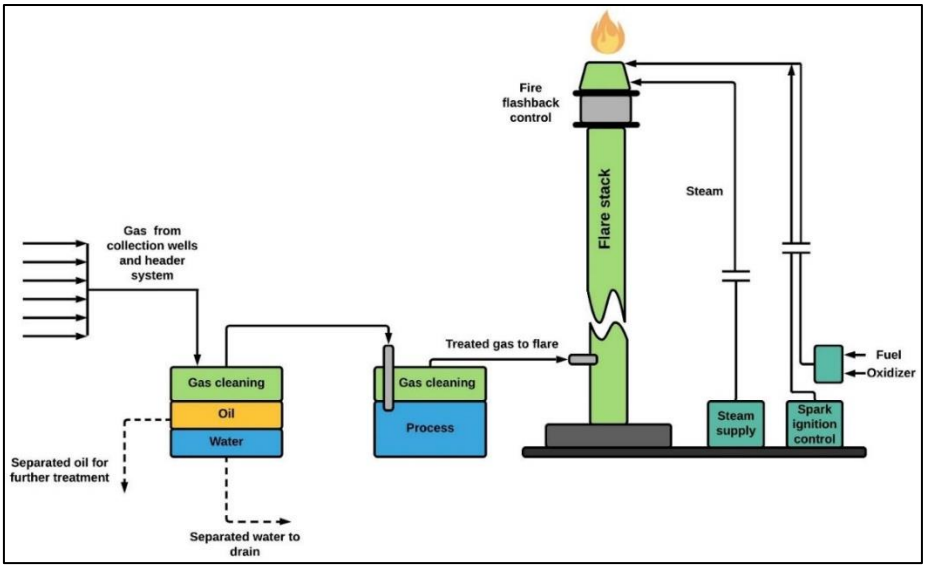

Figure I.7: Flare system design [11].

I.9 Flare Gas Recovery technologies

Flare gas recovery systems lower emissions by recovering flare gases before they are combusted by the flare. In practice, a flare gas recovery system collects gas from the flare header before it reaches the flare, compresses the gas and cools it for re-use in the refinery-fuel gas system. Otherwise depending on the composition of the flare gas, the recovered vapors may also be recycled as a refinery feed stock. A flare gas recovery system offers other benefits through reduced fuel gas costs, visible flame, odors and auxiliary flare utilities, such as steam for smoke suppression [10].

Refinery operators recognized that implementing this recovery system required both careful evaluation of existing flare operations and design of the recovery unit. The recovery system must process the flare gases safely and efficiently without compromising the safety and operability of the existing flares. Therefore, the refinery developed a total project strategy that included facility process data analysis; review of existing flare equipment; technology review and selection; supplier selection; detailed system design fabrication and installation; commissioning; training and performance testing [12].

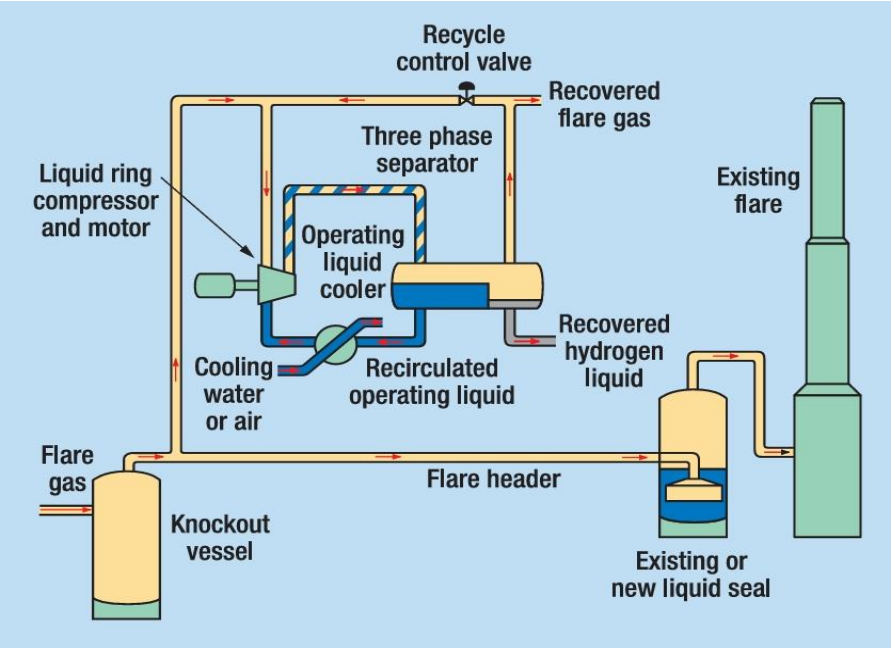

Figure I.8: Simplified representation of a flare gas recovery unit integrated with an existing flare system [12].

I.10 Conclusion

In this chapter, we have explored the issue of gas flaring from various perspectives, ranging from its fundamental definitions to its technical characteristics and global implications. As a widespread practice in the oil and gas industry, gas flaring plays a crucial role in ensuring operational safety, yet poses significant environmental and economic challenges.

We examined the composition and sources of flare gases, along with the different types of flaring and their roles in industrial operations. Global and regional trends, especially in the Arab world, were also discussed to highlight the scale of the issue. The environmental and health impacts of flaring were presented, reinforcing the need for stricter regulations and cleaner technologies. Lastly, we looked at flare systems and recovery technologies as potential solutions to reduce emissions and waste.

In summary, gas flaring remains a critical issue in modern industrial practice. Understanding its mechanisms, consequences, and possible solutions is essential for improving energy efficiency, protecting the environment, and moving towards a more sustainable future in the oil and gas sector.

CHAPTER II

Neural Networks: Key Concepts and Practical Application

II.1 Introduction

Neural networks play a crucial role in identifying complex patterns, addressing intricate problems, and adapting to dynamic environments [13]. In this chapter, we focus on the application of neural networks.

Neural networks are a type of machine learning model designed to replicate how the human brain processes information. They consist of layers of interconnected units, known as neurons, that work together to analyze data, detect patterns, and perform tasks such as image recognition or decision-making.

Neural networks are transforming key sectors including finance, healthcare, and the automotive industry. Because these artificial neurons mimic the functioning of the human brain, they are well-suited for applications like image recognition, character recognition, and stock market prediction [14].

II.2 Neural Network technology

Neural-network technology can provide solutions to a wide variety of science and engineering problems that involve extracting useful information from complex or uncertain data. Although neural networks have long been a topic of academic research, the recent developments of effective learning algorithms and special-purpose computational hardware and the demonstrations of their applications have suggested that neural networks can provide useful tools for solving practical problems [15].

II.2.1 Definition

An artificial neural network (ANN), also known as neural network, is a computational model capable of processing information to tackle tasks such as classification and regression. It is the component of artificial intelligence inspired by the human brain and nervous system [16].

According to Sammut and Webb, 2011 [17] artificial networks are computer models built on the basis of biological neural networks, such as those seen in the human brain [19].

According to Adamowski et al. 2012 [18], The computational model can be thought of as a network of neurons with basic processing abilities that can do simple mathematical calculations. The data-driven approach using artificial neural networks (ANNs) and

mathematical algorithms can leverage the relationship between the input and output data to solve complex, nonlinear problems [19].

ANNs were first created to simulate the information-processing capabilities of a brain network of neurons [19].

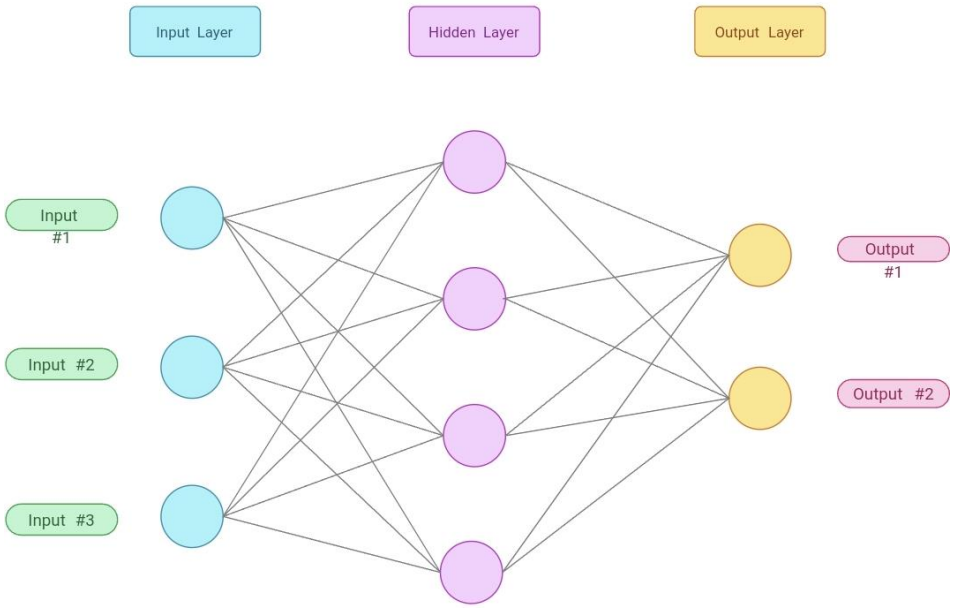

Figure II.1: Neural Network Diagram [20].

II.2.2 Artificial Neural Network Architecture

There are three layers in the Artificial Neural Network Architecture [21]:

- The Input Layer A neural network's input layer is made up of a collection of artificial input neurons. They send information from the initial neuron layers to the system for processing. The neural network's input layer initiates the workflow.
- Hidden Layer The artificial neural network's hidden layer is made up of input and output layers, and the input and output of the artificial neurons are weighted by the number of inputs.
- The Output Layer The last neurons layer is an output layer in an artificial neural network that provides specific outputs in the programmer. Because they are the network's final "performer" nodes, neurons in the output layer can be built and treated differently.

II.2.3 Benefits of Neural Networks

Neural networks, with their remarkable ability to derive meaning from complicated or imprecise data, can be used to extract patterns and detect trends that are too complex to be noticed by either humans or other computer techniques. A trained neural network can be thought of as an "expert" in the category of information it has been given to analyses. This expert can then be used to provide projections given new situations of interest and answer "what if" questions. Other benefits include [21]:

- ✓ Adaptive Learning: The capacity to learn how to do tasks based on data provided for training or prior experience.
- ✓ Self-Organization: An ANN may organize or represent the information it gets during learning time on its own.
- ✓ Real-Time Operation: ANN calculations may be performed in parallel, and specific hardware components that take advantage of this feature are being created and built.
- ✓ Fault Tolerance: through Redundant Information Coding: Partial network breakdown results in performance reduction. Even if the network is severely damaged, certain network functions may be kept.

Since neural networks are best at identifying patterns or trends in data, they are well suited for prediction or forecasting needs including.

II.2.4 Types of Neural Network

II.2.4.1 Feed Forward Neural Network

The feed-forward neural network is the most fundamental artificial neural network utilized for typical recurring and characterization issues. There is no circling in the network. Data goes in just one way via each tier of the network. Information travels in just one direction in this organization, from the underlying hubs to the disguised hubs and yield hubs. Perception is a basic single-layer feedforward network, while multi-layer perception (MLPs) are used for more complex tasks. It is also used in supervised learning. Figure 2 depicts the architecture of the feed-forward neural network [21].

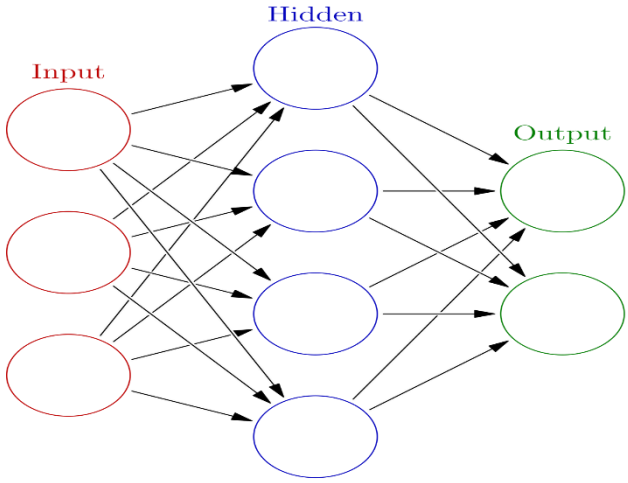

Figure II.2: Feed-Forward Neural Network [22].

II.2.4.2 Cascade Neural Network

Cascade-forward neural networks are a type of neural network similar to feed-forward networks but with additional connections. In this architecture, each layer is not only connected to the next one but also to all previous layers, including the input layer. For example, in a three-layer network, the output layer receives inputs not only from the hidden layer but also directly from the input layer. This structure allows the network to better capture complex, non-linear relationships between inputs and outputs by preserving both linear and non-linear dependencies throughout the network. [21].

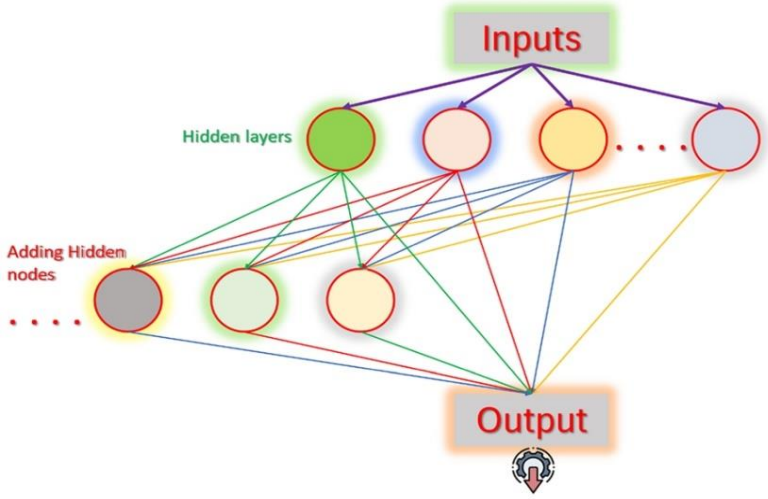

Figure II.3: Network of cascade correlation neural network [23].

II.2.4.3 FitNet Shallow Neural Network

A neural network contains beginning layers, as well as input and output layers that might be termed hidden layers. These might be referred to as encoders. These layers are buried within a thin network. There are several research that show how to fit any function into a shallow network. It must be completely overweight. A number of parameters are generated by the fit net shallow neural network. In summary, a "shallow" neural network is one that generally includes only one hidden layer [21].

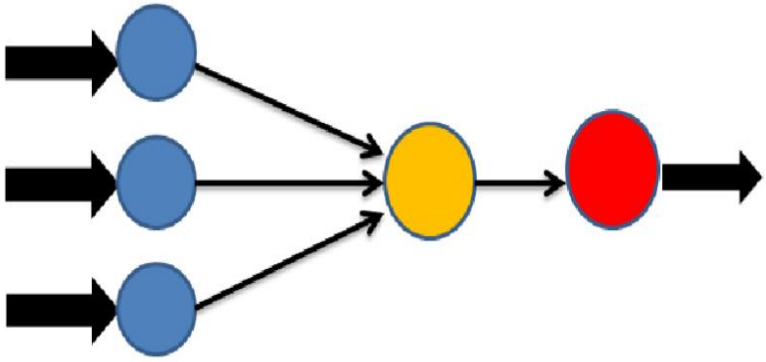

Figure II.4: FitNet Shallow Neural Network [21].

II.2.4.4 Shallow Neural Networks

In summary, "shallow" neural networks contain only one hidden layer, whereas "deep" neural networks include several hidden layers of varied types. Shallow neural networks include only a few layers, generally just one hidden layer. The figure below depicts a basic neuron with R inputs. A weight of w is applied to each input. The input to the transfer function b is the sum of the weighted inputs plus the bias. Any differentiable transfer function b, can be used by neurons to create output [21].

II.2.4.5 Recurrent Neural Network

A recurrent neural network is a network that has backward linkages from the output to the input and a hidden layer. Recurrent neural networks are frequently used in deep learning, model construction, and simulation of human brain neural activity. A recurrent neural network (RNN) is an advanced artificial neural network (ANN) with a direct memory cycle. The ability to construct new network types using fixed-size input vectors.

The recurrent neural networks use these input vectors. RNNs are used in image processing, language processing, and even modelling programmers that add characters to text

one at a time. Essentially, you have an input that is processed by a neural network, and then you have an output. The layers between input and output are known as hidden layers, and they allow data to be modified [21].

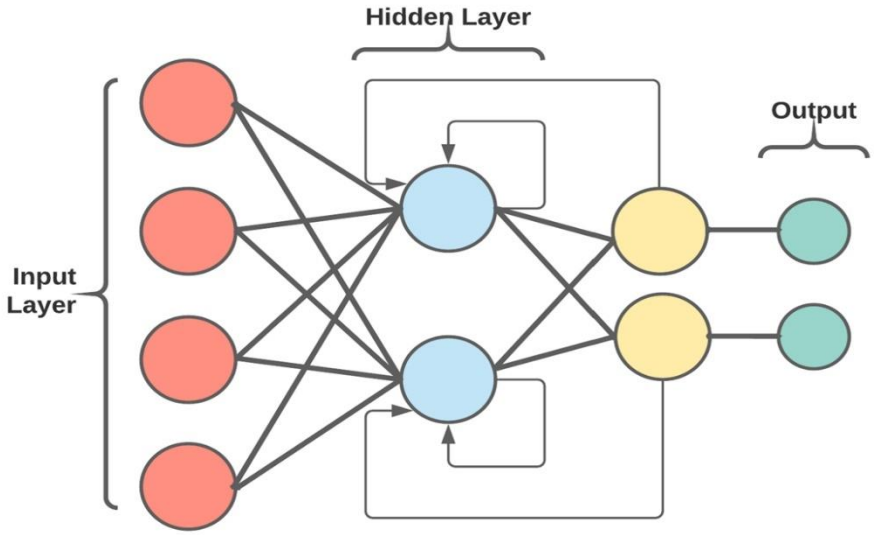

Figure II.5: Recurrent neural network architecture diagram [24].

II.2.4.6 Convolutional neural networks

Convolutional Neural Networks (CNNs) are deep learning models that use convolutional layers, often with pooling or fully connected layers, to detect patterns in visual data. By applying matrix operations, CNNs generate feature maps that analyze specific image regions, making them highly effective for AI-powered image recognition. They are widely used in applications such as facial recognition, NLP, OCR, image classification, and signal processing [25].

II.2.4.7 Deconvolutional neural networks

Deconvolutional Neural Networks operate in reverse of Convolutional Neural Networks, aiming to recover features or signals that may have been lost during initial processing. They are particularly useful in applications such as image analysis and synthesis, where reconstructing or enhancing visual data is essential [25].

II.2.4.8 Modular neural networks

Modular Neural Networks are made up of multiple independent modules, each responsible for a specific part of a larger task. These modules work separately with unique

inputs and are managed by an intermediary that combines their outputs. Since they don't interfere with one another, the network can process complex tasks more efficiently through parallel computation, making it well-suited for large, multifaceted problems [25].

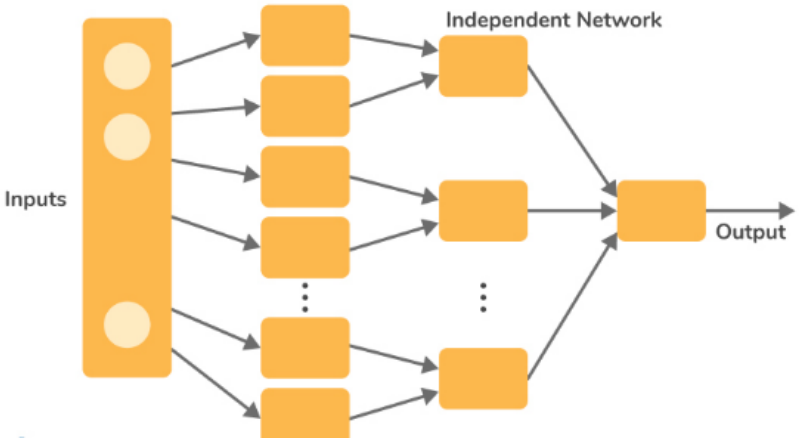

Figure II.6: Modular Neural Network [26].

II.2.4.9 Generative adversarial networks

Generative Adversarial Networks (GANs) use convolutional neural networks and deep learning techniques to uncover patterns in data through unsupervised learning. They consist of two models: a generator that creates new data and a discriminator that distinguishes between real and fake data. As the discriminator mislabels data about half the time, the generator learns to produce more realistic outputs [25].

II.3 Characteristics of Neural Network

Following are the characteristics of an ANN [27]:

- Since an ANN has a very expressive hypothesis space, it is important to choose the approximate network topology (simplistic, layered, and multi-layered) for a given problem to avoid model overfitting.
- ANN can handle redundant features because the weights are autonomous and automatically learned during the learning process. The weights for redundant features tend to be insignificant.
- Training an ANN is time-consuming particularly when the numbers of hidden layers are quite significantly large.

- ANN is quite sensitive to the perspective of noise in the training data. One approach to address this issue is to use a validation set to determine and eliminate generalization errors. Another approach is to adjust the weights by some percentages at each iteration
- ANN is a very complex system so it must be fault-tolerant. Because if any part fails it will not affect the system as much but if all parts fail at the same time the system will fail.
- ANN is an interconnected system the output of a system is a collective output of various inputs so the result is the summation of all the outputs which come after processing various inputs.

II.4 Advantages and disadvantages of Neural Network

II.4.1 Advantages

Neural networks, as a subset of artificial intelligence and machine learning, offer significant advantages [27]:

- Neural Networks have the ability to learn on their own and produce the result that is not limited to the inputs they are given.
- It is useful for tasks requiring rapid decision-making .
- ANNs can carry longer training sessions depending on factors such as the number of weights on the network, the number of training models considered, and the parameters of the various learning algorithm parameters.
- ANN learning methods are very strict on noise in training data. Training examples may contain errors, which do not affect the final result.
- Neural networks adapt to conditions in a changing environment. While neural networks may take a while to learn big changes suddenly, they are very good at adapting to the ongoing changes of information.
- Neural networks can create informative models whenever conventional methods fail. Because neural networks can handle very complex interactions they can easily display data that is very difficult to replicate in traditional ways such as unlimited statistics or system concepts.

II.4.2 Disadvantages

Neural networks also come with several disadvantages [27]:

- Many ANN systems do not describe how they solve the problems.

- The output quality of ANN is unpredictable.
- Artificial neural networks require parallel processing, by their structure.
- Particularly suitable for complex problems.
- Training time is large.
- Nature of ANN is like a Black box.

II.5 Applications in Various Sectors

Neural Networks have been a hotspot domain for researchers due to its increasing area of applications in areas where huge amounts of data are used and the main goal is to infer patterns out of it.

II.5.1 In computer science

This section covers the usage of artificial neural networks (ANNs) in the field of computer science, highlighting their roles in key areas such as image recognition, natural language processing (NLP), machine translation, automatic speech recognition, and language translation systems. We'll also go through the algorithms that power them, including the Backpropagation (BP) algorithm, the Recurrent Neural Network-Based Optimization Algorithm (RNN-OA), and advanced algorithms designed for optimising computer network routing. These discussions highlight the remarkable ability of ANNs' extraordinary capacity to convert complicated data into useful insights and choices, demonstrating their significance on a variety of computational challenges [28].

II.5.2 Image recognition

The development of ANNs has recently taken a crucial role in the computer science department, especially in the sense of creating image recognition systems. Due to their extraordinary capacities to capture and process high numbers of visual data with flawless precision, visual inspection can now be applied to multiple fields. The implementation of ANNs for image recognition within computer science is primarily based on the ability of the algorithms to detect, classify, and interpret images very quickly.

The creation of sophisticated picture recognition systems is one of the main advances made by ANNs in computer science [28].

II.5.3 Modeling

Most industrial or research problems, whether mechanical, physical, chemical, or even economic, require representation through a mathematical model that can reproduce the behavior

of the implemented process. Such tasks demand computational tools with high processing power, learning capabilities, and, most importantly, tools whose design is not heavily dependent on the complexity or size of the problem at hand. Neural networks appear to be one of the most suitable solutions for this type of problem [29].

II.5.4 Control

Controlling an industrial process involves designing a system capable of calculating the control input to be applied in order to ensure the desired dynamic behavior of the process. Neural networks provide strong performance as part of the control system due to their flexibility and self-adaptive capabilities [29].

II.5.5 Classification

Another major category of industrial problems involves automatically assigning an object to a class among several possible ones. Solving this type of problem requires representing the examples to be classified using a set of features. A system must then be designed to classify these examples based on their representation, and neural networks are particularly well-suited for this task. In fact, classification is one of the primary domains in which neural networks excel [29].

II.6 Application of Artificial Neural Networks in the petroleum industry

ANNs have demonstrated a respectable level of accuracy in numerous petroleum applications. Following a thorough examination of numerous articles regarding ANN applications in the petroleum sector [19].

In the petroleum industry, ANNs have gained significant attention for their ability to model complex, nonlinear relationships and handle large datasets with minimal explicit programming. These capabilities make them particularly useful in various upstream, midstream, and downstream applications, including reservoir characterization, production forecasting, drilling optimization, and process control. By integrating ANNs, petroleum engineers can enhance decision-making, reduce operational risks, and improve overall efficiency in exploration and production activities [19].

II.6.1 Exploration

Artificial Neural Networks (ANNs) have significantly improved exploration activities in the petroleum industry, especially where traditional methods struggle with complex, non-homogeneous subsurface environments [19].

- Subsurface Mapping: Radial Basis Function (RBF) Networks have been used to calculate point-to-point travel times, enabling accurate 3D subsurface mapping.
- Seismic Data Processing: **Hopfield Neural Networks (HNNs)** are employed for seismic velocity analysis by solving optimization problems in time-velocity semblance images, improving velocity picking accuracy.
- Parameter Identification: **Probabilistic Neural Networks (PNNs)** correlate gamma ray logs with key reservoir parameters like **Total Organic Content (TOC)** and **frackability**, aiding in the economic evaluation of reservoir zones.
- Hydrocarbon Prediction: A **dual neural network**, combining fuzzy logic and self-organizing networks, handles expert knowledge effectively and uses **homotopy learning** to achieve fast and accurate training. This enhances the precision of hydrocarbon prediction and increases the success rate of drilling operations.

II.6.2 Drilling

Artificial Neural Networks (ANNs) are widely used in drilling to enhance performance and reduce risks [19]:

- Drill Bit Monitoring: ANNs estimate bit wear in real-time, improving maintenance decisions.
- BHA Dynamics: Predicts bottom hole assembly behavior to avoid harmful vibrations.
- Trouble Prediction: Identifies potential drilling issues early using historical data.
- ROP Prediction: Improves rate of penetration forecasting for better planning and cost control.
- Report Analysis: Automates classification of drilling reports and extracts key insights.
- Geomechanics: Estimates subsurface properties to support wellbore stability.
- Bit Selection & Costing: Recommends optimal bits and predicts cost-per-foot.

II.6.3 Production

Artificial Neural Networks (ANNs) enhance various aspects of petroleum production [19]:

- Wax Prediction: ANNs accurately predict Wax Appearance Temperature (WAT), helping prevent flow blockages.
- Gravel Pack Optimization: Improve grain-size distribution estimates, enhancing gravel pack efficiency.
- Fluid Rate Prediction: Enable real-time, accurate estimation of production rates, especially in multiphase flow.
- Gas Production Forecasting: Support short- and long-term natural gas production forecasts for better planning.
- Fracture Identification: Classify fractures based on conductivity, aiding fluid flow modeling and reservoir analysis.
- Artificial Lift Optimization**:** ANNs outperform traditional methods in predicting oil flow rates in artificial lift wells.

II.6.4 Reservoir engineering

Artificial Neural Networks (ANNs) are widely used in reservoir management to improve accuracy and efficiency [19]:

- Porosity & Water Saturation: ANNs improve evaluation of shaly sand reservoirs using well log data, offering better estimates than traditional methods.
- Enhanced Oil Recovery (EOR): ANNs model complex EOR processes like Low Salinity Waterflooding (LSW), chemical flooding, and thermal EOR for better recovery predictions.
- Viscosity Prediction: Predict fluid viscosity below bubble point without full PVT data, aiding reservoir planning.
- Thermal EOR Modeling: Simulate steam injection effects by considering formation properties and injection parameters.
- Pore Pressure Forecasting: ANNs generate reliable pre-drilling and post-well pressure models.
- Additional Applications: Include reservoir simulation, history matching, rock and fluid property estimation, pore structure analysis, and well testing.

II.7 Conclusion

In this chapter, we explored neural networks from multiple perspectives, ranging from theoretical foundations to practical applications across various sectors. These computational models, inspired by the human brain, enable the processing of complex and nonlinear data, unlocking new opportunities in engineering, finance, medicine, and the petroleum industry.

Machine learning, at the heart of this technology, takes several forms such as supervised, unsupervised, and reinforcement learning. Advanced architectures like Convolutional Neural Networks (CNNs) for image analysis and Generative Adversarial Networks (GANs) for data generation have expanded the capabilities of modern artificial intelligence.

Successfully implementing neural networks requires a deep understanding of data, training algorithms, and performance evaluation criteria. Their integration into the petroleum industry, such as in permeability prediction, reservoir classification, and seismic data analysis demonstrates their potential to improve accuracy and optimize industrial processes.

In summary, neural networks represent a major advancement in artificial intelligence, offering innovative solutions to complex global challenges, while also calling for responsible and informed use.

CHAPTER III

Description of Unit 10 and GTK module of Skikda refinery

III.1 Introduction

The Skikda refinery, operated by SONATRACH, is one of the largest refining complexes in Algeria and plays a central role in the country's hydrocarbon processing infrastructure. As part of its modernization and environmental compliance initiatives, the refinery has been equipped with two Flare Gas Recovery Modules (GTK) integrated with the atmospheric distillation unit (Topping).

This installation reflects the broader upgrade and revamping programs undertaken at Skikda to enhance process efficiency and align with industry best practices. The GTK modules are integrated into the refinery's existing systems and operates in coordination with other critical components of the facility to manage hydrocarbon streams more effectively.

Commissioned during a period of increased emphasis on operational reliability and regulatory alignment, the GTK modules represent a key component in the refinery's ongoing technical development.

III.2 Overview of the Crude Distillation Unit (CDU)

The Atmospheric Distillation Unit-I (Unit 10) of the Skikda Refinery was upgraded to process 27,000 metric tons per day of Hassi Messaoud crude oil as part of the Rehabilitation Project. The Acid Water Stripping Section, located within Unit 10, was also revamped to handle the increased feed rate of acid water resulting from the renovation of Units 10 and 11 [30].

The hydrocarbon fractions present in crude oil are separated from one another through atmospheric distillation. These represent the earliest form of petroleum refining, virtually all of the first oil refineries operated as distillation towers. The process relies on the differences in the boiling points of the individual pure components found in crude oil [30].

III.2.1 Design basis

This Crude Distillation Unit forms the fundamental core of any crude oil refinery. The feedstock of the unit is crude oil, whether domestically sourced or imported. In our case, the rehabilitation design was carried out based on Hassi Messaoud crude oil.
The primary purpose of this Topping Unit is to separate the crude oil into various fractions [30].

III.2.2 Equipments

A distillation unit includes the following main equipment [30]:

- Desalter: Removal of salts.

- Distillation column: Fractionation of crude oil into various cuts.
- Stripping column: Removal of light-end products.
- Pre-flash drum: Reduces furnace duty and prevents pump cavitation.
- Charge furnace: Heats the feedstock.
- Set of: Exchangers , Drums, Pumps, Compressors.
- Stabilization column: Separates light ends from naphtha.
- Splitter column: Separation of naphtha cuts.

III.2.3 Products Obtained from the CDU

The CDU separates crude oil into several hydrocarbon fractions based on their boiling points. These include [30] :

- Fuel Gas
- LPG (Liquefied Petroleum Gas)
- C6 Cut
- Naphtha A
- Naphtha B
- Naphtha C
- Kerosene
- Light Gas Oil (LGO)
- Heavy Gas Oil (HGO)
- Reduced Crude Oil (RCO)

These streams are either sent directly to storage or directed to further downstream processing units, depending on the refinery's configuration.

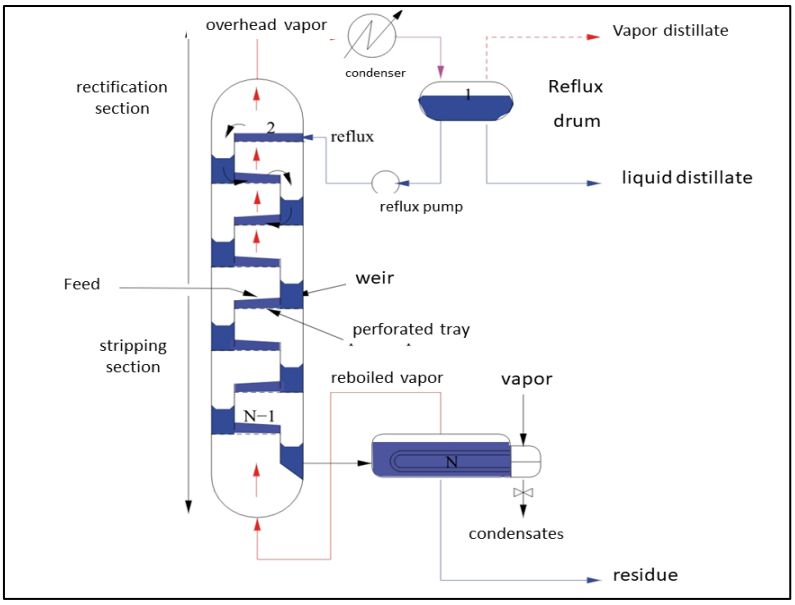

Figure III.1: colonne de distillation atmosphérique [31].

III.2.4 Process Flow Description

The crude oil feedstock is first desalted, then preheated through a series of heat exchangers using process streams. It is subsequently routed to a fired heater, where it reaches the required temperature for atmospheric separation. The heated crude enters the main distillation column, where it is fractionated into the previously mentioned products. Some of these streams, such as kerosene and gas oils, undergo further treatment via strippers to enhance product quality [30].

A simplified schematic of the CDU highlights various sections such as the preheat train, the atmospheric furnace, the main distillation column, and auxiliary equipment including stabilizers and strippers. The GTK module, although not directly involved in the separation process, is connected to several operational purge and relief points, making it essential for overall safety and environmental compliance [30].

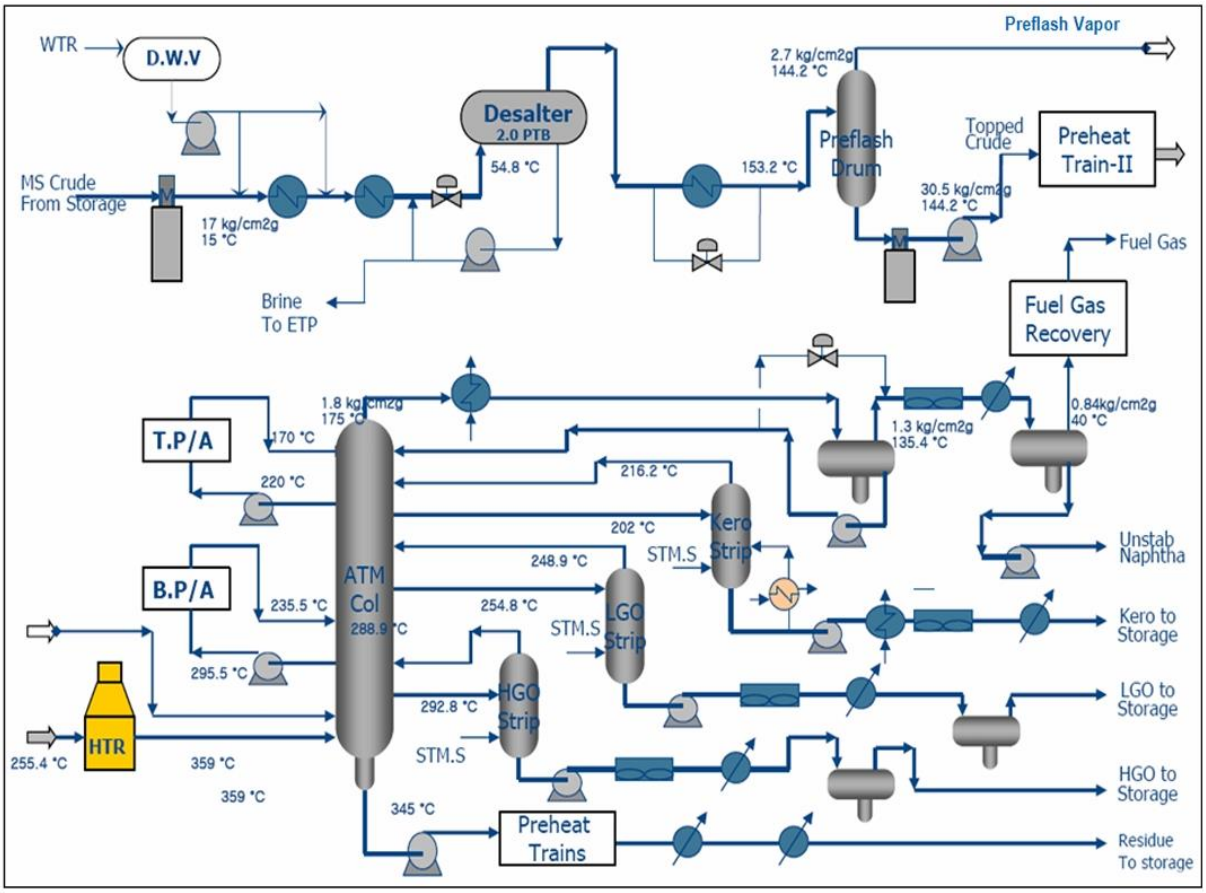

Figure III.2: Simplified diagram of CDU [30].

III.3 The GTK Module (Flare Gas Recovery System)

III.3.1 Purpose and Importance

The purpose of these two flare gas modules is to process the gas from the top of the distillation column, rather than burning it off. The aim is to recover, in particular, the fuel gas and a fraction of LPG/C5+ as separate products.

A global LPG recovery rate of at least 78 wt% is specified, along with a target molecular weight for the recovered fuel gas of less than 40 [30].

III.3.2 Location and Integration within the CDU

The GTK module is physically located within Unit 10 (CDU-I) and is integrated into the refinery's flare and fuel gas networks. It receives gases from multiple blowdown and relief valves across the CDU and processes them for reuse or safe disposal, depending on their composition and pressure.

III.3.3 Main Equipments

The GTK module typically comprises [30]:

- A flare gas compressor to raise the pressure of recovered gases
- Gas-liquid separators to remove entrained liquids
- Heat exchangers or coolers to condense heavier hydrocarbons
- Control systems to route gases either back to the fuel gas system or to storage
- Safety and monitoring devices for operational reliability

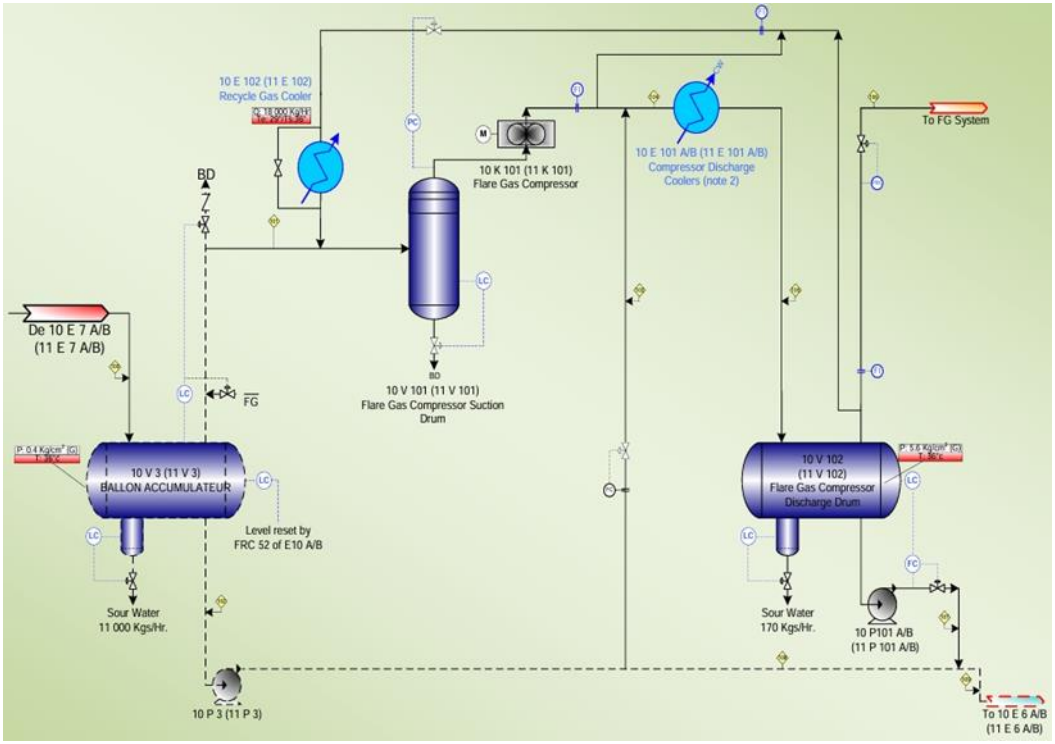

Figure III.*3*: Flare Gas Recovery Module Diagram [33].

III.3.4 Capacity

The module has a processing capacity of 8,895 kg/h, with a maximum capacity of 10,546 kg/h. The flare gas compressor compresses the gas originating from vessel V-3 from 0.4 bar to 7 bar [30].

III.3.5 Flare gas recovery process

- The fuel gas from vessel 10-V-3 (Overhead Product Drum of the Atmospheric Distillation Column) is routed to the Suction Drum of the Flare Gas Compressor (10-V-101) via the 10”-10-P1001-AA02 line [30].

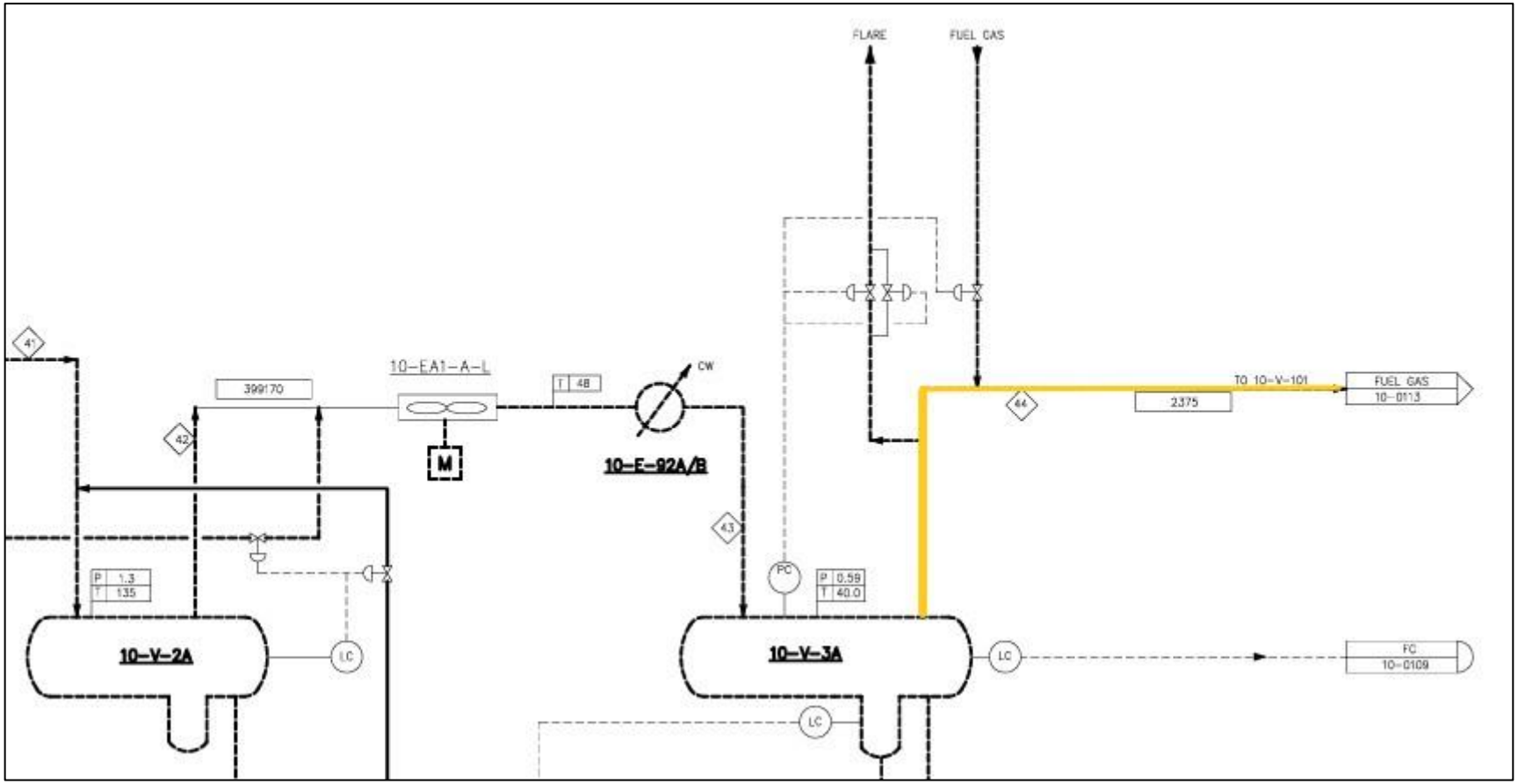

Figure III.4: Fuel Gas Recovery Section (I) [32].

- The suction drum operates at a pressure and temperature of 0.4 kg/cm²g and 39°C, respectively. The vessel 10-V-101 is equipped with a safety relief valve, 10-PSV-1102, which discharges to the blowdown system and is set to open at 4 kg/cm²g.
- The vapors from 10-V-101 are routed to the Flare Gas Compressor (10-K-101), where the gas is compressed to a discharge pressure of 6.0 kg/cm²g. The pressure regulator 10-PIC-1101 controls the compressor's suction by maintaining the suction pressure within the compressor suction drum through a discharge-side recycle loop.
- This configuration allows for reduced recycle flow when the flow from 10-V-3 increases, and increased recycle when the upstream flow decreases, thereby ensuring a relatively constant flow rate to the compressor.
- The suction and discharge pressures of the compressor are monitored by pressure indicators 10-PI-1105 and 10-PI-1106, respectively. Additionally, a safety relief valve, 10-PSV-1108, is installed on the compressor discharge line, set at 7.8 kg/cm²g, with discharge directed to the blowdown system.

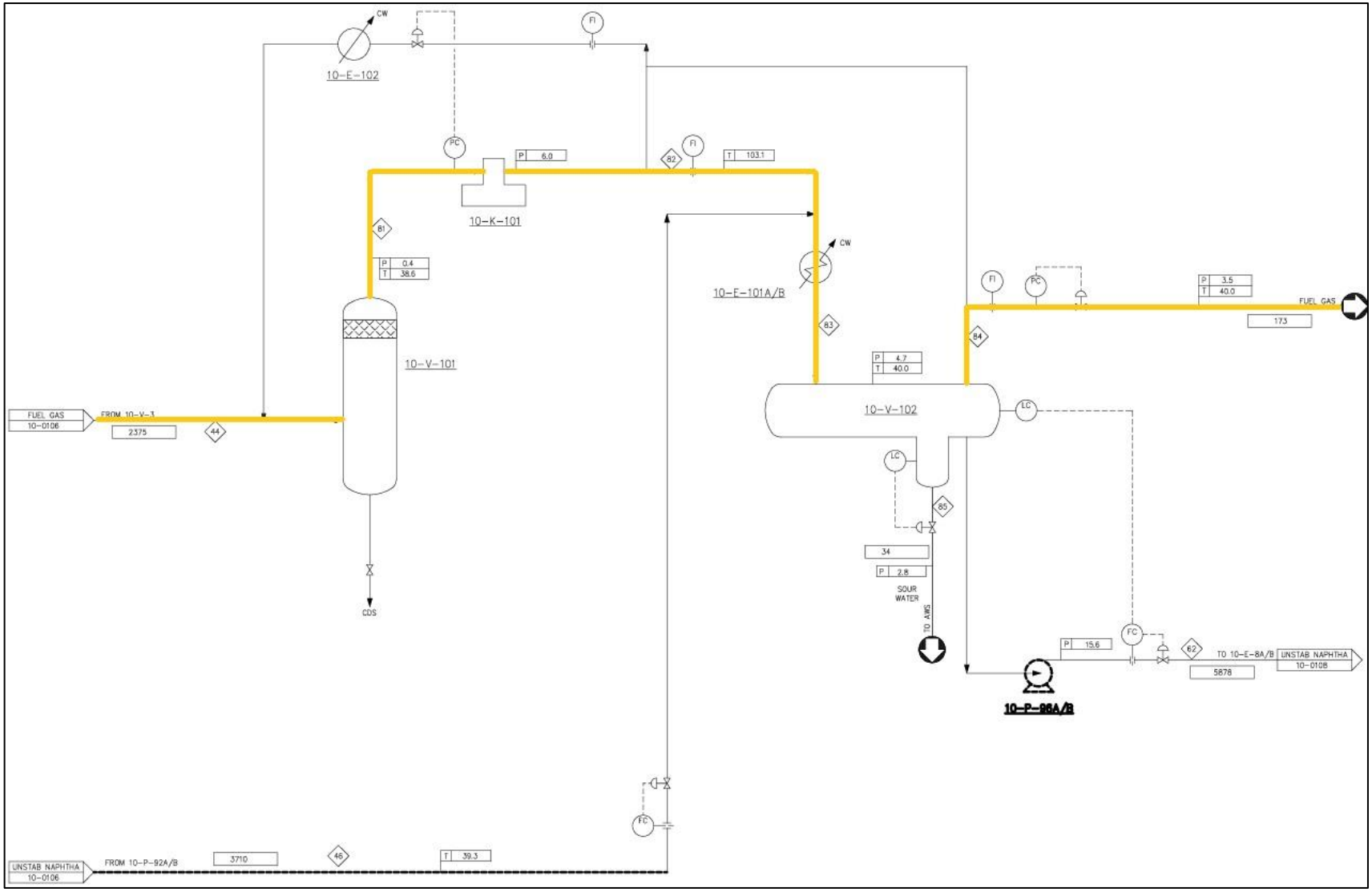

Figure III.5: Fuel Gas Recovery Section (II) [32].

- Next, the compressed gas flows through the Compressor Discharge Cooler (10-E-101A/B) on the shell side. Before entering the cooler, the compressed gas is mixed with unstabilized naphtha, sourced from vessel 10-V-3, in order to absorb C3/C4 hydrocarbons.
- The resulting mixture is cooled in the 10-E-101A/B to 40°C, then directed to the Flare Gas Compressor Discharge Drum (10-V-102) for phase separation.
- The flow of unstabilized naphtha is regulated by flow controller 10-FIC-1102, which is equipped with a low-flow alarm (10-FAL-1102) that can trigger an alert in the control room.
- Within 10-V-102, the naphtha and fuel gas are separated. The vessel operates at a pressure of 4.7 kg/cm²g and a temperature of 40°C. The separated fuel gas is sent to the fuel gas header. At the battery limits, the fuel gas conditions are maintained at 3.5 kg/cm²g and 40°C. The pressure within 10-V-102 is controlled by pressure controller 10-PIC-1112, which regulates the fuel gas flow rate to the header. By stabilizing the pressure in vessel 10-V-102, the controller helps avoid fluctuations in the fuel gas header, which could otherwise affect burner efficiency and overall process stability.

- The gas from drum V-102 has a molecular weight below 40, which makes it suitable for feeding into the existing fuel gas network. The recovery rate of liquefied petroleum gas (LPG) in the naphtha product from the original flare gas stream exceeds 91 wt% under the base case, and 89.3 wt% under the alternative case.

III.4 Conclusion

This chapter has outlined the key functions and design of Unit 10 (CDU-I) and the GTK module at the Skikda refinery. The CDU remains essential for the primary separation of crude oil, while the GTK module complements it by recovering flare gases, thus reducing losses and minimizing environmental impact.

Their integration reflects a coherent and forward-looking approach to refining combining process efficiency, energy recovery, and regulatory compliance in a unified system that supports the refinery's continuous improvement objectives.

CHAPTER IV

Simulation of Design and Real Cases of the GTK Module

IV.1 Introduction

Simulation is a powerful and widely used tool in various fields of engineering and research. It allows for the analysis of a system's behavior before real-world implementation, enabling engineers to test different solutions and operating conditions to optimize performance. The process is based on developing a model that represents the actual system and allows the execution of various scenarios to predict the behavior of the physical system under study. While these models are not exact replicas of physical reality, they are designed to capture the most important characteristics of the system being analyzed [34].

In the petrochemical industry, simulation is essential for designing, evaluating, and improving complex processes such as crude oil distillation, catalytic cracking, gas treatment, and flare gas recovery. By replicating physical and chemical operations in a virtual environment, engineers can identify inefficiencies, evaluate safety concerns, and make informed decisions without interrupting real operations. Widely used simulation tools like Aspen HYSYS, MATLAB, and CHEMCAD support the industry in reducing costs, improving safety, and enhancing environmental performance, making simulation an indispensable asset in the development and optimization of petrochemical systems.

IV.2 Definition of Aspen HYSYS Software

HYSYS software allows for the simulation of industrial processes in the gas, refining, and petrochemical industries, both in steady-state and dynamic modes [35].

- The user must specify the components of the gas, liquid, or mixture.
- A thermodynamic model must be selected.
- The necessary parameters for the calculation of each unit operation must also be specified.
- HYSYS then solves the process flow diagram and can also perform sizing for certain equipment.

There are two operating modes in a simulator: static (or stationary) and dynamic. Static simulators solve static equations that represent steady-state operation (at equilibrium), while dynamic simulators allow evaluation of how variables evolve over time by solving systems of differential equations. The most well-known industrial simulators worldwide are [34]:

- Static simulators: Aspen Plus (Aspen Technologies), Design II (from WinSim), HYSYS (Hyprotech), PRO/II (Simulation Sciences), Prosim
- Dynamic simulators: HYSYS, Aspen Dynamics (Aspen Technologies), Design II (from WinSim), Dymsym (Simulation Sciences Inc.)

These simulators are essential tools for designing new production units and optimizing industrial processes that sometimes operate far from their optimum conditions [34].

IV.3 Use of Simulation

The various tasks that a process simulator must perform include [35]:

- In Process Design (Engineering):
  - ✓ Material and energy balance analysis.
  - ✓ Equipment sizing.
  - ✓ Economic evaluation of the process.
  - ✓ Process optimization.
- In Process Monitoring:
  - ✓ Readjusting operating parameters when changes occur in the feed composition.
  - ✓ Measuring equipment performance.

IV.4 Concepts and Characteristics of the HYSYS Simulator

IV.4.1 Basic Concepts of the HYSYS Simulator

HYSYS is an object-oriented process simulation compiler. Any formal change made to an element is automatically reflected throughout the entire model. It is a conversational simulation environment based on event-driven architecture [35]:

This means that at any moment, instant access to data is possible, and any new data is processed on demand. The resulting calculations are then carried out automatically.

Furthermore, HYSYS combines the concept of modular operations with non-sequential solving. Not only is each new piece of data processed upon arrival, but it is also propagated throughout the flowsheet.

In the following sections, the main foundational concepts and associated vocabulary used during the model-building stages in HYSYS will be defined [35]:

- **Flowsheet:** A flowsheet is a collection of "Flowsheet Elements" (material streams, energy streams, unit operations, and operating variables) that represent all or part of the simulated

process and use the same thermodynamic database called a Fluid Package. HYSYS features a Multi-Flowsheet Architecture, meaning there is no limit to the number of flowsheets that can be created. It includes specific entities such as:

- A Process Flow Diagram (PFD)
- A Workbook

- **Fluid Package:** This defines the chemical components involved in the simulated process and assigns them physical and chemical properties from the pure component database. It also allows users to select thermodynamic models for calculating mixture properties and to define the reaction kinetics involved in the process.
- **Process Flow Diagram (PFD):** This diagram visually displays the streams and unit operations represented by symbols within the flowsheet, as well as the connectivity between streams, unit operations, and property tables.
- **Workbook:** A tabular interface that provides access to data related to streams and unit operations, offering a structured overview of process parameters.
- **Desktop**: The main workspace in HYSYS where different windows and tools are displayed during process design.
- **Property View**: Contains detailed information describing an object, whether a stream or a unit operation.
- **Simulation Case**: Refers to the complete set of Fluid Packages, Flowsheets, and Flowsheet Elements that make up the simulation model.

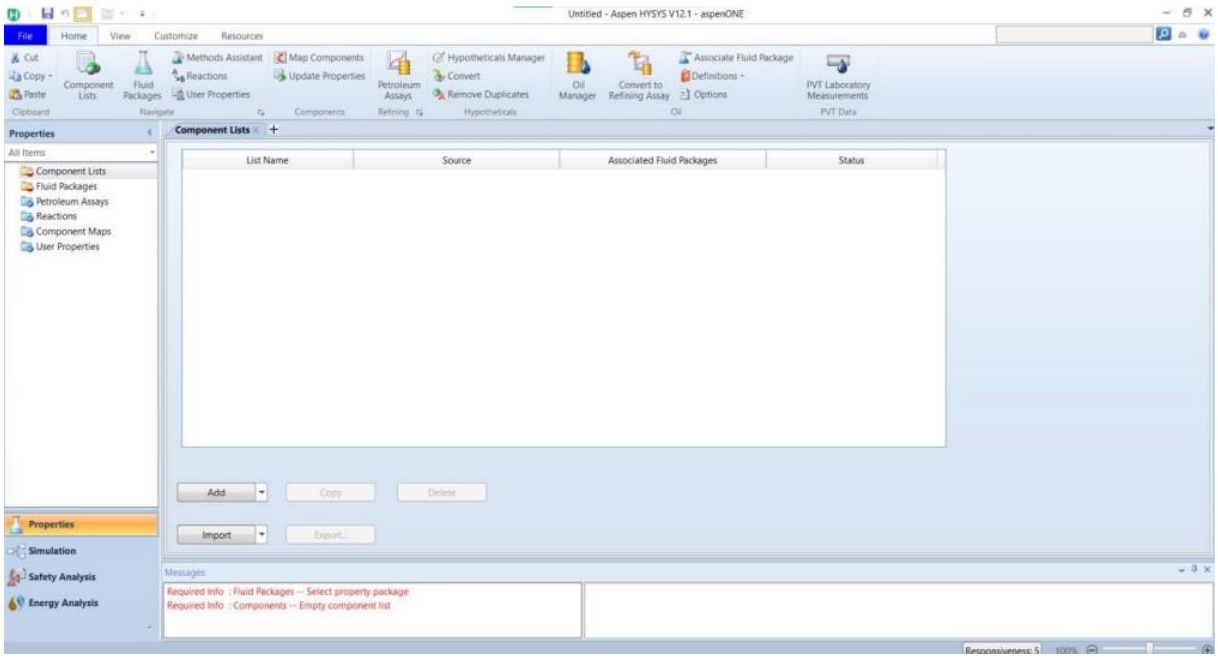

Figure IV.1: Interface of the Aspen HYSYS Simulator.

IV.5 Simulation Environment in HYSYS

There are five development environments in HYSYS used to manipulate and structure information within the simulator [35]:

1. **Basis Manager Environment**:
   This environment is used to create and modify the **Fluid Package**, including component selection and thermodynamic model setup.
2. **Oil Characterization Environment:**
   Used specifically for characterizing petroleum-type fluids, allowing the definition of pseudocomponents and crude assays.
3. **Main Flowsheet Environment :**
   This environment is used to define the topology of the main flowsheet in the simulation. It is where material and energy streams, unit operations, and **Sub-Flowsheets** are placed and configured to represent the overall process.
4. **Sub-Flowsheet Environment :**
   Allows for the creation and management of a specific sub-section of the main flowsheet (such as a particular stream, operation, or group of operations). It enables hierarchical organization of complex processes.
5. **Column Environment:**
   A specialized environment dedicated to configuring distillation columns. It has its own **Flowsheet**, **Fluid Package**, **Process Flow Diagram (PFD)**, and **Workbook**, tailored to simulate separation operations in detail.

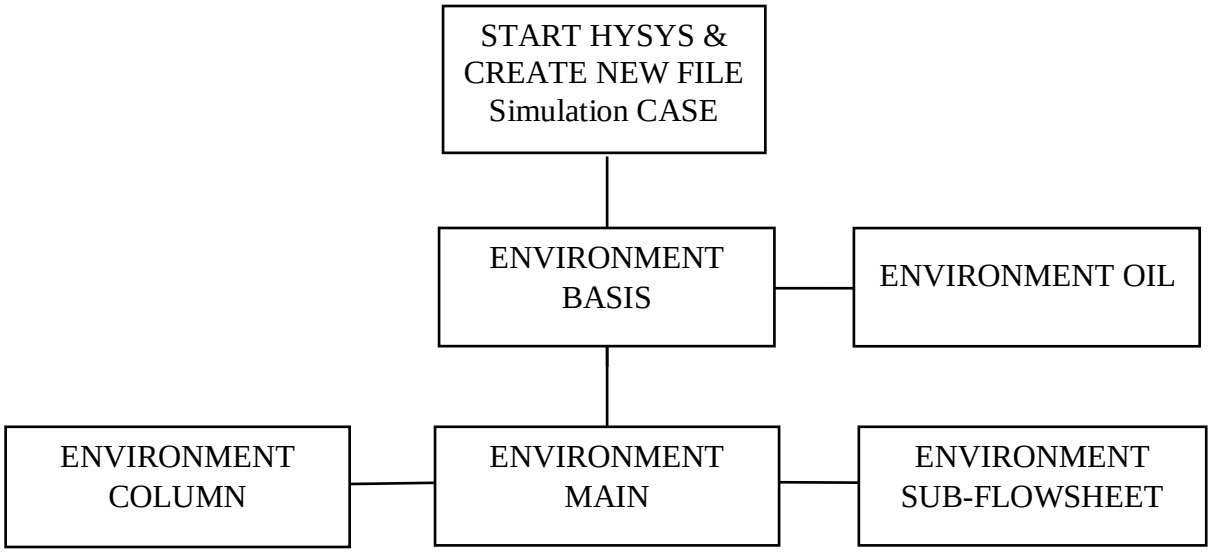

Figure IV.9: Developement environments in HYSYS [34][35].

IV.6 Key Features of HYSYS

This section briefly describes the important features that make HYSYS a powerful simulation and development platform [35].

- The Integrated Engineering Environment:

All necessary applications are used within a common simulation environment, allowing for seamless integration and workflow.

- Modeling Capability:

HYSYS supports both steady-state (or stationary) and dynamic simulations, offering flexibility for various types of process analysis.

- HYSYS Programming:

HYSYS contains an internal Macro Engine that supports the same syntax as Microsoft Visual Basic. This allows for the automation of tasks within HYSYS without the need for external programs.

Here are some characteristics of HYSYS related to how calculations are performed [35]:

- **Event-Driven Management**:

HYSYS combines interactive calculation (where calculations are executed automatically whenever new information is provided) with instant access to data (at any time, information can be accessed from any simulation environment).

- **Built-in Intelligence**:

Thermodynamic property calculations are performed instantly and automatically as soon as new information becomes available.

- **Modular Operations**:

Each stream or unit operation performs all necessary calculations, using either information provided within the operation itself or data communicated from a stream. Information flows bi-directionally through the flowsheets.

- **Non-Sequential Solving Algorithm**:

  Flowsheets can be constructed in any order, offering flexibility in how the model is built.

IV.7 Thermodynamic Model

Thermodynamic models are essential for calculating the physical properties of fluids, including hydrocarbons, over a range of operating conditions. The choice of a particular equation of state is guided by the need to strike a balance between the following three criteria [35]:

- Simplicity of the mathematical form;
- Range of applicability;
- Desired accuracy.

The thermodynamic model used is governed by the **Peng-Robinson equation**, as it is the most recommended for hydrocarbon systems. This model was adopted in the context of our simulation.

IV.8 Working methodology

For this study, we will first carry out a simulation using Aspen HYSYS V14 to verify the design case. Next, we will perform the simulation of the real case based on actual operating data from the unit, in order to validate the model.

To validate this simulation, the compressor outlet pressure was chosen as a reference parameter, as it confirms that the simulated system behaves consistently with real operating conditions. Once this validation is complete, an optimization study will be carried out, in which the fraction of the PLG that comes from the mass flow rate of the unstabilized naphtha is selected as the main **variable** to be optimized, in order to assess its impact on the performance of the GTK equipment.

IV.9 Simulations Using HYSYS Software

The HYSYS simulation begins with the following steps:

1. **Create a New Case** : Open Aspen HYSYS and start a new case by selecting *"New Case"* from the main menu.

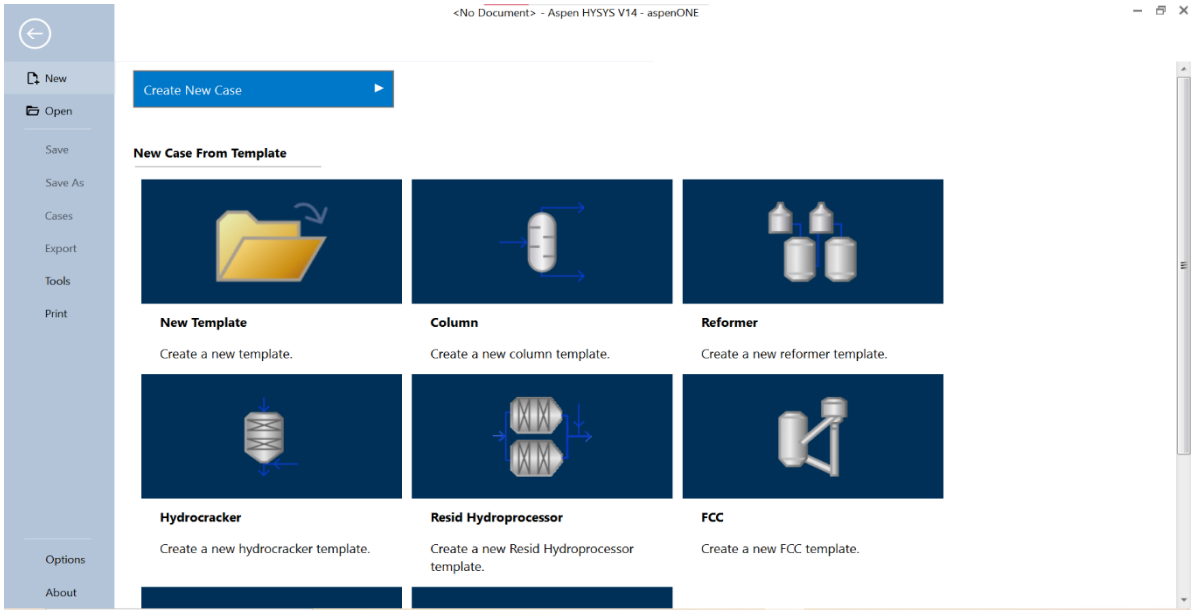

Figure IV.10: Creating a New Simulation Case.

2. **Define the Fluid Components:** Create a new component list by clicking on "Add a new component list". Then, add the fluid components (hydrocarbons, etc.) relevant to our process.

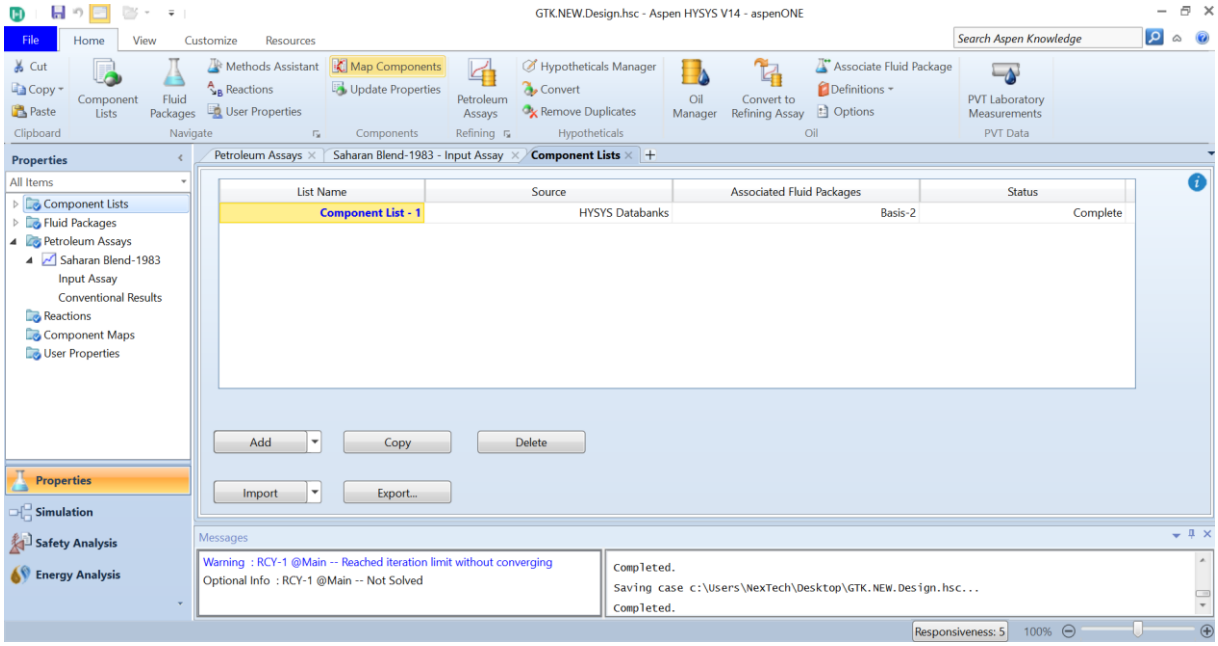

Figure IV.11: Defining Simulation Components.

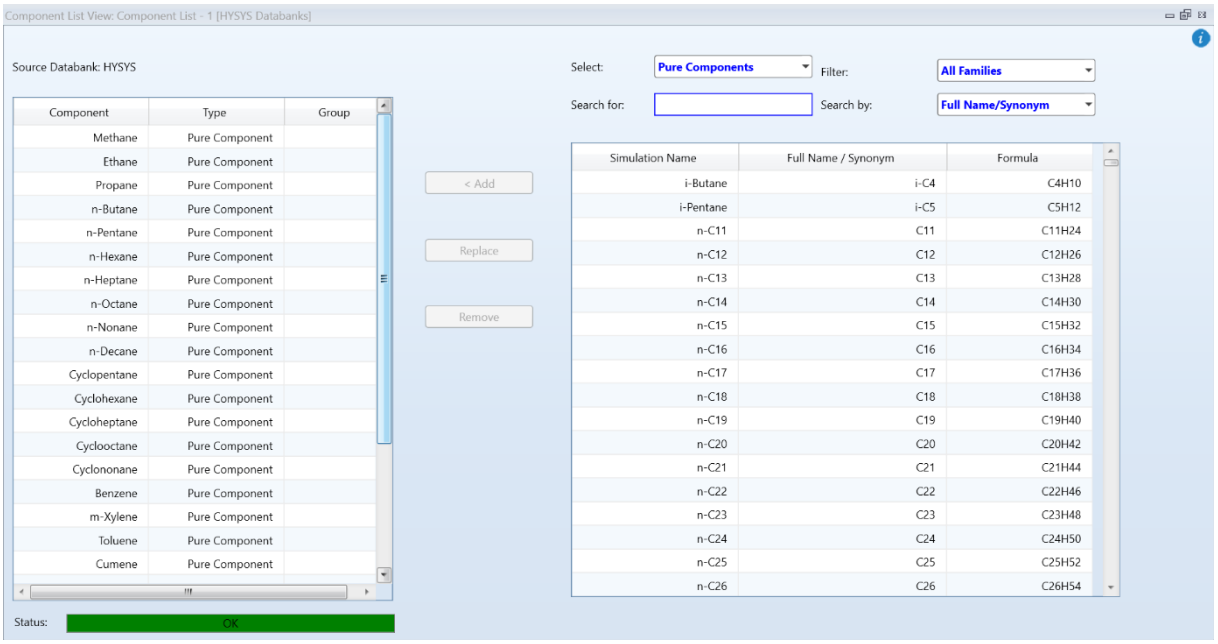

Figure IV.12: Defining Simulation Components.

3. **Select the Thermodynamic Model:** We are required to select a thermodynamic model. To do this, we click on the "Fluid Pkgs" icon, which opens a new window. In this window, we click on the "ADD" icon to specify our desired model. In hydrocarbon refining, the most commonly used thermodynamic model is Peng-Robinson.

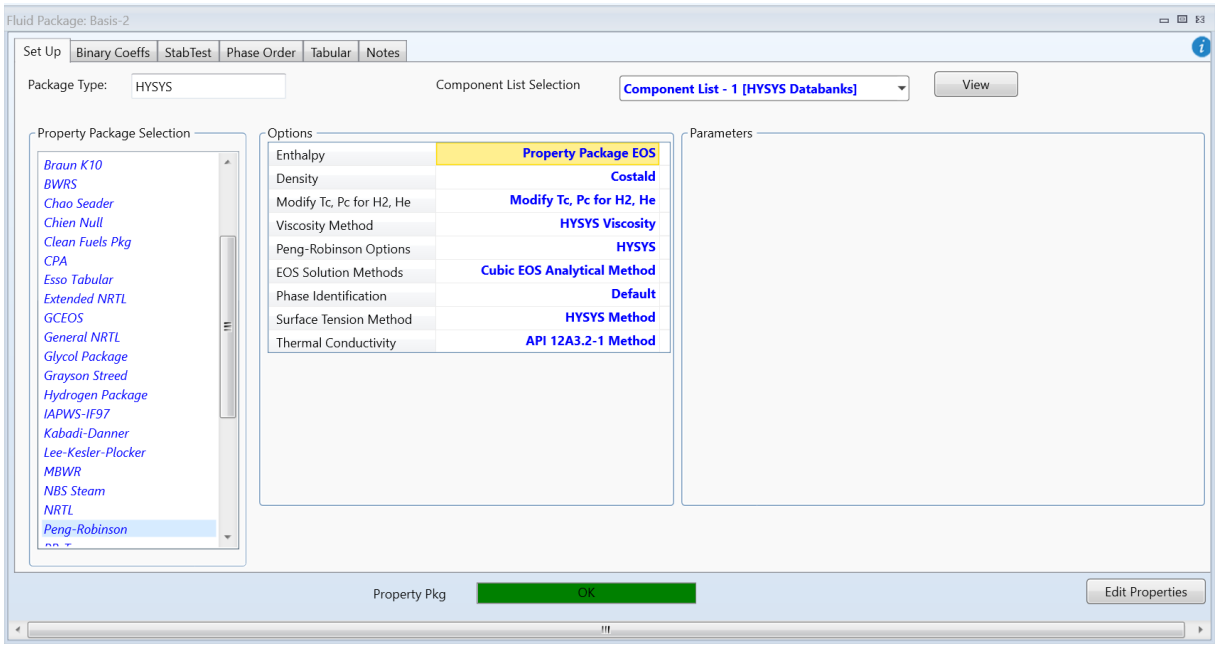

Figure IV.13: Setting the Thermodynamic Model Peng-Robinson.

- The process simulation begins with the simulation of the fuel gas feed and the feed conditions previously presented in Table.

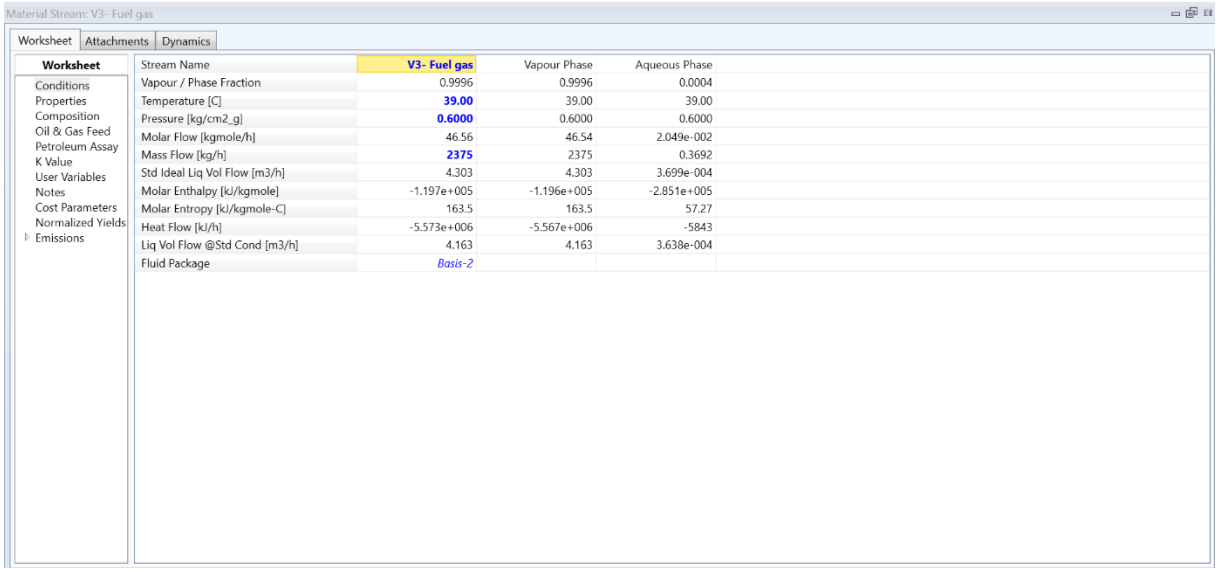

Figure IV.14: Feed Conditions.

- The composition of the fuel gas is also detailed in the table below, listing all the components present in the stream along with their respective molar fractions.

Table IV.3: Component of fuel gasV-3 (design).

Component	Molar fraction
H2O	0,043347
Methane	0,000000
Ethane	0,111070
Propane	0,392419
n-Butane	0,295723
n-Pentane	0,093939
n-Hexane	0,025186
n-Heptane	0,009118
n-Octane	0,002596
n-Nonane	0,000287
n-Decane	0,000000
Cyclopentane	0,003072
Cyclohexane	0,016843
Cycloheptane	0,000000
Cyclooctane	0,000834
Cyclononane	0,000029
Benzene	0,002707
m-Xylene	0,000245
Toluene	0,001418
Cumene	0,000000
NBP[1]151*	0,000623
NBP[1]162*	0,000383
NBP[1]173*	0,000133
Somme	1,00

- **After the simulation starts, the feed comes out of a compressor and then gets mixed with another stream called unstabilized naphtha.**

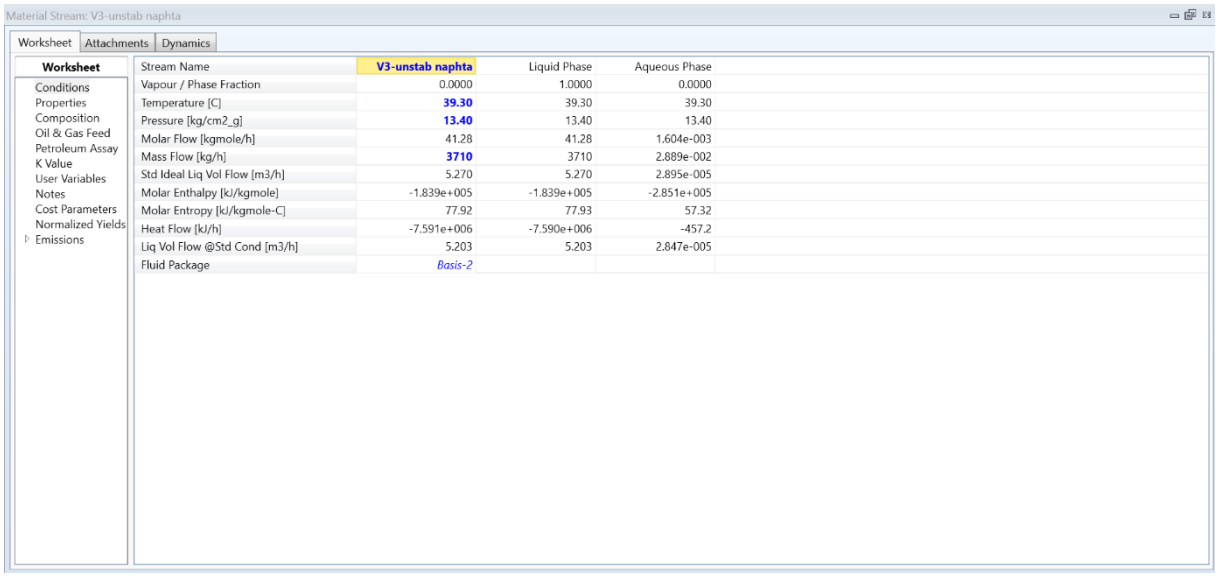

Figure IV.15: Unstabilized Naphta Conditions.

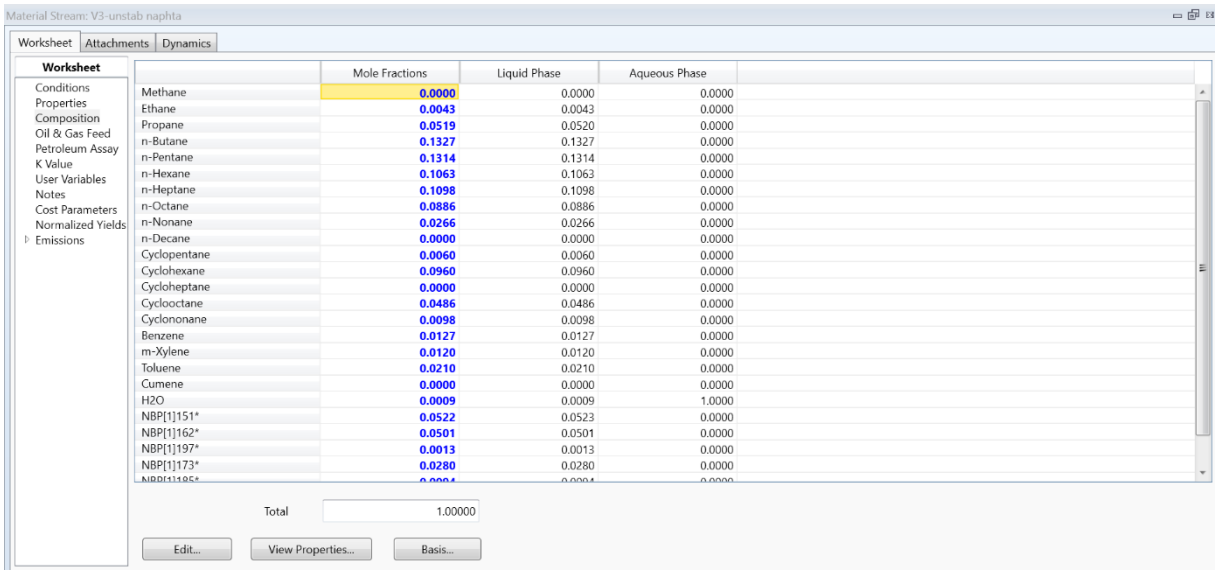

Figure IV.16: Unstabilized Naphta composition.

IV.9.1 Design Case Verification

- The feed conditions, which supply the GTK process and correspond to the fuel gas stream from V-3, are presented in the table below.

Table IV.4: Feed operating condition (design).

Operating condition	Value
Temperature (°C)	39
Pressure (kg/cm²)	0,6
Mass flow (kgmol/h)	2375

- The simulation diagram of the Design Case for the GTK equipment, part of the unit, was developed using Aspen HYSYS and is shown in the figure (IV.9) below.

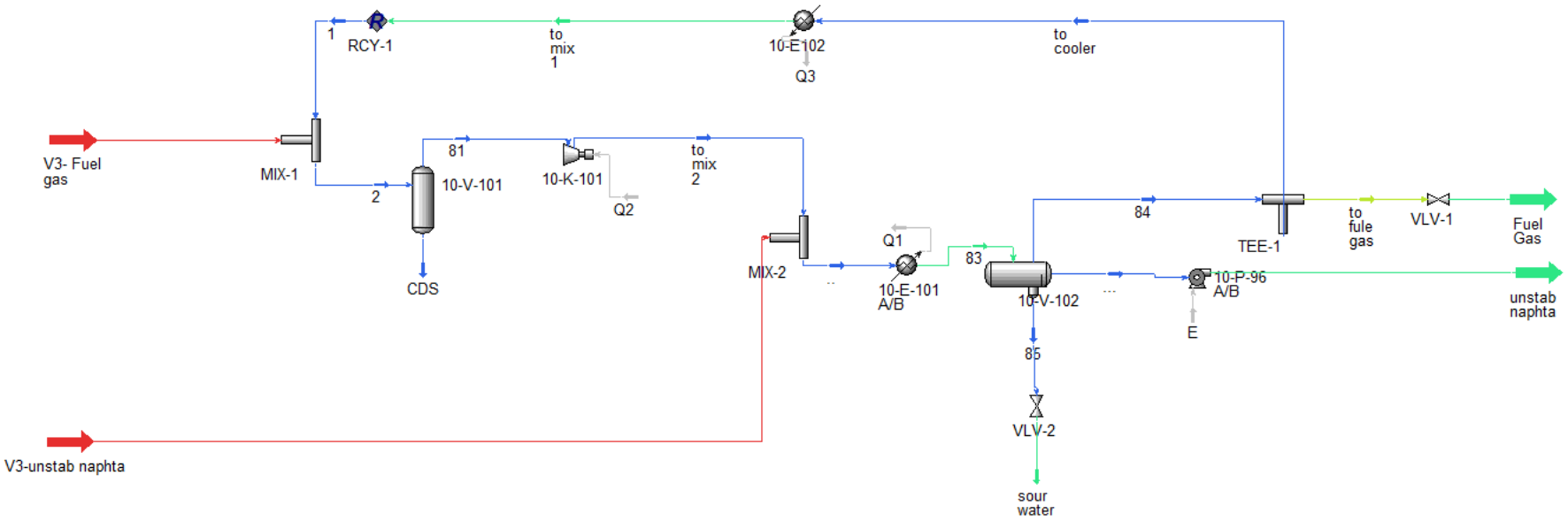

Figure IV.17: GTK Module simulation - Design Case.

- The table below shows the outlet parameters of the GTK equipment, as calculated by the manufacturer, alongside those obtained from the HYSYS simulation. The simulation results were generated using the Peng-Robinson (PR) thermodynamic model.

Table IV.5: Properties of outlets from GTK Obtained from the Design Case Simulation.

Outlets	**Temperature (°C)**			**Mass flow (Kg/h)**		
Case	Design	PR	Ecart	Design	PR	Ecart
Fuel gas	40	40	0	173	173	0
Unstabilized Naphta	41	40.65	0.85	5878	5784	1.60

The absolute error was calculated for the mass flow rates and temperatures of all the cuts using the following formula:

$$\text{Ecart} = \frac{Vdesign - V\ semulation}{Vdesign} * 100 \qquad \textbf{(1)}$$

- The simulation results shown above are very close to those provided by the manufacturer. Therefore, we can confirm that the Peng-Robinson thermodynamic model selected is valid for our simulation. For this work, Aspen HYSYS version 14 was used.

IV.9.2 Real Case Verification

To validate the simulation, the results were compared with those of the current real case. The simulation of the unit was carried out based on operating data (The feed composition, as well as the operating conditions…etc.) from December 1999.

Table IV.6: Feed operating condition (real).

Operating condition	**Value**
Temperature (°C)	37
Pressure (kg/cm²)	0,44
Mass flow (kgmol/h)	8984

- The composition of the fuel gas of the reel case is also detailed in the table below:

Table IV.7: Component of fuel gasV-3 (real).

Component	Molar fraction
Methane	0.0267
Ethane	0.1606
Propane	0.3901
i-Butane	0.0728
n-Butane	0.2142
i-Pentane	0.0478
n-Pentane	0.0556
n-Hexane	0.0294
n-heptan	0.0028

- The real case simulation diagram is shown in the figure below.

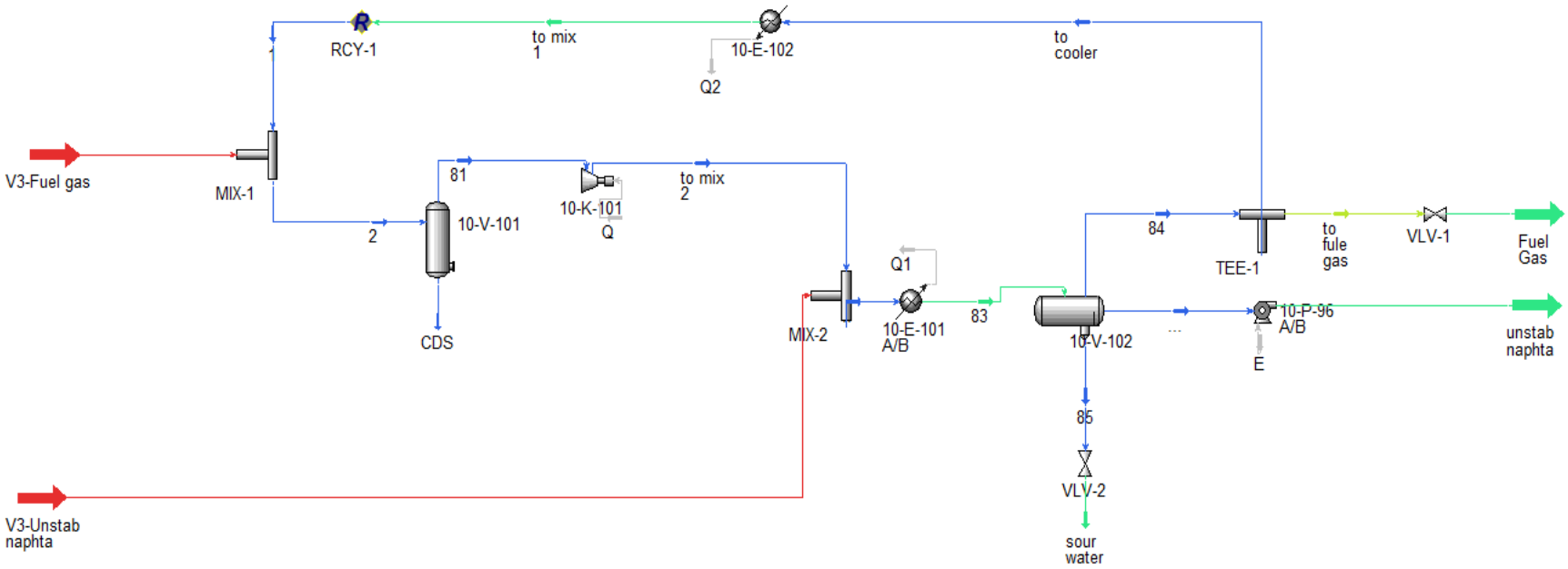

Figure IV.18: GTK Module simulation - Real Case.

Table IV.8: Properties of outlets from GTK Obtained from the real Case Simulation.

Outlets	Temperature (°C)			Mass flow(Kg/h)		
Case	Real	PR	Ecart	Real	PR	Ecart
Fuel gas	33.4	32	4.2	470.3	470.3	0
Unstabilized Naphta	33.4	32.56	2.5	28728	30310	5.5

The results obtained, after convergence, show a small deviation of less than 6% compared to the real values, in terms of Outlets and temperatures.

These results allow us to validate, first of all, the real case simulation, and then proceed to the validation of the compressor outlet pressure, followed by the optimization of **the PLG fraction** in the GTK process.

Table IV.9: Properties of outlets from GTK Obtained from the real and design Case Simulation.

Outlets	Temperature (°C)			Mass flow (Kg/h)		
Case	Design	Real	Ecart	Design	Real	Ecart
Fuel gas	40	33.4	16.5	173	470.3	63.2
Unstabilized Naphta	41	33.4	16.5	5878	28728	388.7

The results obtained show a significant difference between the design values and the real values. This is mainly due to the significant difference between the feed capacity in the real case and the design case, along with other parameters such as temperature, pressure, and others.

IV.9.3 Role of Simulation in the Study

Although the real operating data used in this work was taken from the refinery's DCS (Distributed Control System), the use of Aspen HYSYS was still very important. The goal of the simulation wasn't to exactly match the real numbers, but to better understand how the process works overall. Through the simulation, I was able to:

- Clearly identify the key inlets and outlets of the system.
- Follow the flow of materials and energy throughout the unit.
- Understand how the different pieces of equipment are connected and interact.
- Get a clearer idea of how the process behaves under different conditions.
- Validate the overall process flow logic and ensure consistency between units.
- Visualise the entire system in a more organised and structured way.
- Simulate operating scenarios that cannot be tested in real life due to safety or operational limits.
- Use the model as a base for future optimisation and performance improvement studies.
- Strengthen the interpretation of real data by comparing it to a controlled virtual environment.

IV.10 Conclusion

This chapter has demonstrated the fundamental role of process simulation in understanding, analyzing, and optimizing complex operations within the petrochemical industry. Using Aspen HYSYS V14, both the design and real operating cases of the GTK module were successfully modeled and evaluated. The selection of the Peng-Robinson thermodynamic model proved appropriate, as simulation results closely matched manufacturer specifications and real-world data, with acceptable deviations in key output parameters.

By simulating both ideal and actual conditions, the study confirmed the reliability of the developed model and highlighted discrepancies between expected and actual performance, primarily due to variations in feed conditions. These insights underscore the importance of simulation not only as a design validation tool but also as a platform for diagnostic analysis and operational improvement.

Furthermore, the simulation environment provided by HYSYS enabled a deeper understanding of the process behavior, the interactions between system components, and the effects of changing parameters insights that are difficult to obtain through real-time experimentation. This chapter thus validates the use of simulation as an indispensable asset in process engineering, laying the groundwork for future optimization studies and contributing to more efficient and safer industrial operations.

Chapter V

Optimization of the GTK Module : NN-based Modeling of the LPG Fraction

V.1 Introduction

In this chapter, we focus on using artificial neural networks (ANNs) to optimize the performance of the GTK module, which plays a key role in flare gas recovery. The main goal is to maximize the recovery of LPG-rich unstabilized naphtha, a valuable liquid product obtained through an absorption process.

By applying neural networks, we aim to better understand how different operating conditions affect the module's efficiency. The model learns from data to predict how the system behaves, and helps identify the best conditions to improve recovery rates and overall process performance.

Ultimately, this work shows how neural networks can be a powerful tool not just for modeling, but also for optimizing real industrial units like GTK—making operations smarter, more efficient, and more valuable.

V.2 Application of Neural Networks for the Optimization of the GTK Module

Neural network was used to model the behavior of unstabilized naphtha recovery within the GTK module, based on variations in operating parameters:

- Time
- Fuel Gas FLOW
- Fuel Gas PRESSURE
- Fuel Gas TEMP
- Wash Oil to E-101 A/B FLOW
- V-102 TEMP
- V-102 PRESS
- K-101 Disch FLOW
- K-101 Disch TEMP

This modeling aims to optimize the gas recovery process by taking into account the real operating conditions of the installation. The objective is to determine the optimal values of these parameters in order to maximize the recovery of LPG-rich unstabilized naphtha, thereby improving the overall efficiency of the GTK unit.

Improving the overall efficiency of the GTK unit relies primarily on maximizing the recovery of the LPG fraction. In this process, unstabilized naphtha acts as an absorbent to capture light hydrocarbons, especially LPG, from the fuel gas that would otherwise be flared. A greater quantity of recovered unstabilized naphtha indicates more effective absorption of LPG and, consequently, better recovery performance. Therefore, a higher recovery of unstabilized naphtha is a clear sign of improved LPG capture and more efficient operation of the GTK module.The dataset used for training the neural network model was extracted from the DCS data. (Look Annex)

Table V.1 summarizes the range of each variable used in the neural network, including their minimum and maximum values based on the collected DCS data.

Table V.10: Parameters Max and Min values.

		Min	Max
Operating Parameters	Fuel Gas FLOW (m^3/h)	67	130
	Fuel Gas PRESSURE (Kg/cm^2)	0,361	0,901
	Fuel Gas TEMP (°C)	31,33	49,89
	Wash Oil to E-101 A/B FLOW (m^3/h)	8,10	8,90
	V-102 TEMP (°C)	33,83	41,97
	V-102 PRESS (Kg/cm^2)	3,60	6,60
	K-101 Disch FLOW (m^3/h)	1100	1500
	K-101 Disch TEMP (°C)	138,7	184,5
K-101 Disch PRESS (Kg/cm^2)		3,11	6,92
LPG Fraction		0.165	0.399

V.2.1 Input and target data entry in MATLAB

The neural network was implemented through direct programming in MATLAB R2019a, without using the graphical interface *nntool*, in order to have better control over the training process and model configuration.

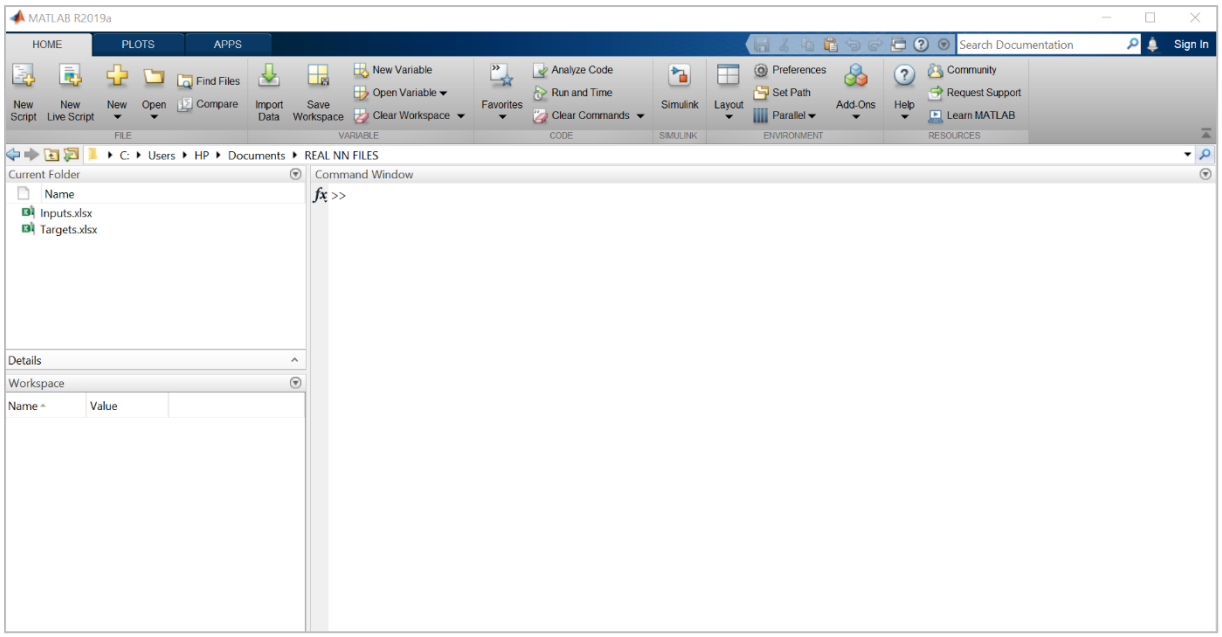

Figure V.19: MATLAB Interface.

The inputs and targets were prepared in Excel and saved as spreadsheet files. These files were then imported into MATLAB to be used as training and testing data for the neural network.

➢ The inputs are:

- The Fuel Gas flow rate is recorded in the first row (449 columns).
- The **Fuel Gas pressure** is listed in the second row (449 columns).
- The **Fuel Gas temperature** is presented in the third row (449 columns).
- The fourth row contains the values of **Wash Oil flow to E-101 A/B** (449 columns).
- The **V-102 temperature** appears in the fifth row (449 columns).
- The sixth row includes the measurements of **V-102 pressure** (449 columns).
- The **K-101 discharge flow rate** is shown in the seventh row (449 columns).
- The eighth row contains the **K-101 discharge temperature** (449 columns).

Variables - inputs

inputs

9x449 double

	1	2	3	4	5	6	7	8	9	10	11	12	13	14	15	16	17
1	v	1	2	3	4	5	6	7	8	9	10	11	12	13	14	15	16
2	126.0032	126.0048	126.0044	126.0049	126.0043	126.0058	126.0049	126.0071	126.0044	126.0045	126.0030	126.0041	126.0053	118.8112	126.0027	126.0020	126.0032
3	0.4004	0.4980	0.5624	0.5616	0.5588	0.4312	0.4410	0.5208	0.6418	0.5581	0.5550	0.6762	0.6095	0.5969	0.6278	0.5650	0.5188
4	35.4241	37.5144	39.6260	39.8004	39.3414	36.2913	36.4471	38.1847	41.6200	39.3578	38.6718	40.7713	40.4185	38.9667	38.9592	38.1319	37.0096
5	8.4040	8.4040	8.4041	8.4041	8.4040	8.4040	8.4041	8.4040	8.4040	8.4040	8.4040	8.4040	8.4040	8.4039	8.4038	8.4040	8.4041
6	36.9730	37.3049	37.7592	37.9944	38.0286	37.3958	37.3019	37.4497	38.0879	37.5795	37.5537	38.8359	39.2120	38.3548	39.4684	39.1874	39.0316
7	4.0124	4.1904	4.2244	4.2360	4.2650	4.0456	4.0717	4.2192	4.3926	4.4263	4.5016	4.9561	4.6142	5.1311	4.8213	4.5428	4.5512
8	1.4703e+03	1.4703e+03	1.4703e+03	1.4703e+03	1.4703e+03	1.4703e+03	1.4703e+03	1.4704e+03	1.4703e+03	1.4703e+03	1.4703e+03	1.4703e+03	1.4703e+03	1.4702e+03	1.4703e+03	1.4703e+03	1.4703e+03
9	146.5093	147.3121	146.9986	148.1996	149.2813	147.0300	145.6543	146.1202	150.2749	151.6685	154.1245	156.1313	154.7489	159.1287	158.1348	153.8180	152.7780

Figure V.20: Inputs Insert.

- The outputs (targets) :

Variables - targets

targets

2x449 double

	1	2	3	4	5	6	7	8	9	10	11	12	13	14	15	16	17
1	4.3600	4.5900	4.6800	4.6900	4.7100	4.4100	4.4400	4.6400	4.9000	4.8400	4.8900	5.3800	5.0400	5.4500	5.2200	4.9400	4.9000
2	0.2801	0.2641	0.2555	0.2548	0.2583	0.2760	0.2736	0.2584	0.2404	0.2444	0.2430	0.2118	0.2315	0.2090	0.2207	0.2378	0.2404

Figure V.21: Targets Insert.

V.3 Neural Network direct prediction

V.3.1 Used Experimental Data

Four hundred forty-nine 449 sample have been collected. The logistic sigmoid function was used as the activation (transfer) function in the hidden layer and the mean square error (MSE) automatically calculated was employed as a measure of fitness. Each network topology was trained 3 times to compensate the effects of random initialization of the neural network weights, and the best performances were recorded.

To prevent overlearning of the neural networks, the early-stopping technique was applied during the training of the neural networks by using 67 random data points (15%) among the training set as the validation data.

The root-mean-square error RMSE, which indicates the degree of generalization accuracy, was estimated (eq 1) then used to determine the optimal neural network topology. The errors between these predictions and the corresponding experimental results were recorded [36].

$$RMSE = \sqrt{\frac{1}{n}\sum_1^n (p_i - t_i)^2} \qquad (1)$$

The coefficient of determination (R2) was also calculated (eq 2) to indicate the fitness of the model [36].

$$R^2 = 1 - \frac{\sum_1^n (p_i - t_i)^2}{\sum_1^n (t_i - \bar{t})^2} \qquad (2)$$

In eqs (1) and (2), p_i and t_i are the predicted and target (experimental) values respectively.

V.3.2 Constructing the Optimal Neural Network Model

To find the best neural network model representing the database, several network topologies were tested and compared according to their RMSEs for testing and training (Figure 3).

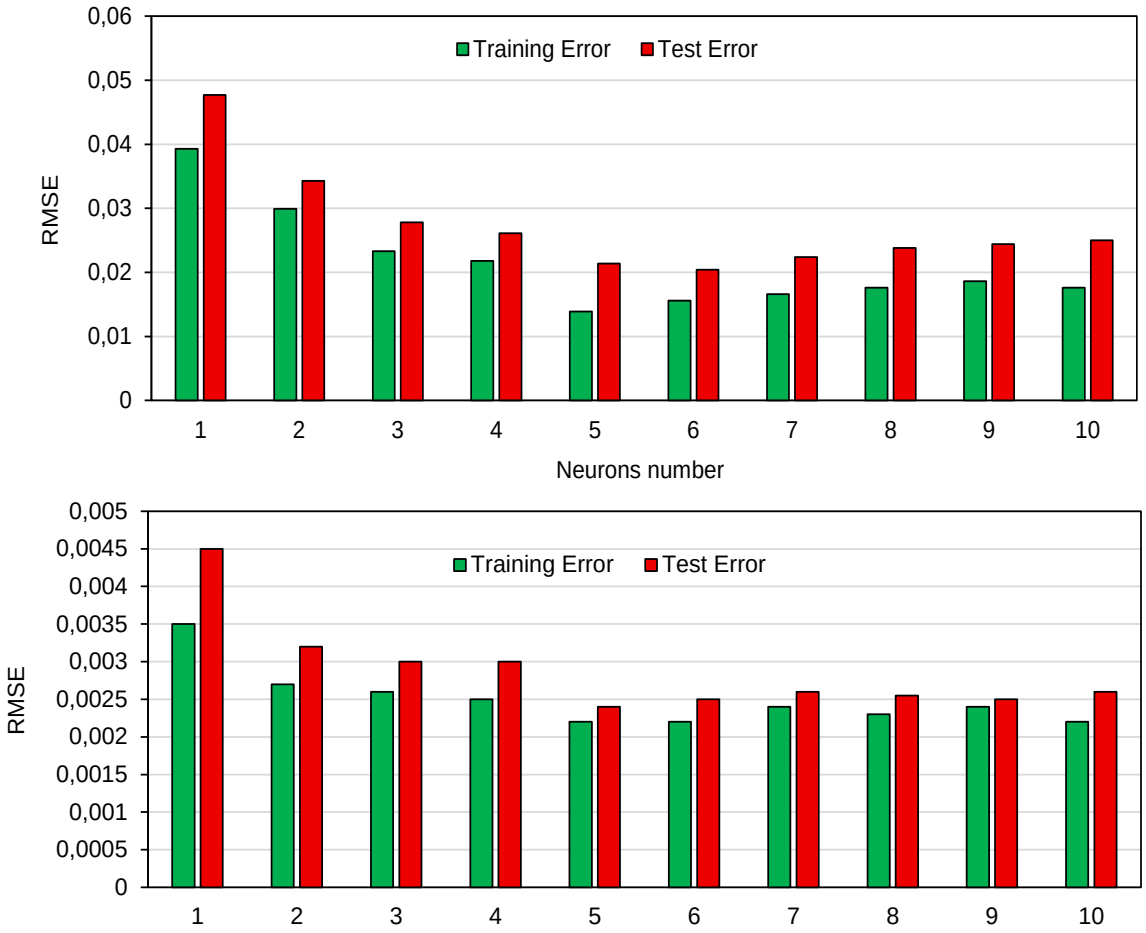

Figure V.22: Comparison of errors for various neural network topologies.

As the network size increases, the training error generally decreases because of the use of more weights. The testing error, on the other hand, has the tendency to decrease first and then to increase as the network gets larger, because of the increase in the degree of overlearning.

Because our purpose was to find a successful knowledge-extraction model with the ability to predict the results of a new set of conditions using existing data, the testing error should be as small as possible. Hence, the network architecture (5 neurons) with the lowest RMSE of testing (values in table V.1.) was chosen as optimal and used in the remaining parts of the work. R2 was also calculated to give some idea of the suitability of the database to construct a single model, although it was not used in decision making.

Table V.11: RMSE and R Values.

Target	**Number 1**		**Number 1**	
Section	**Training**	**Test**	**Training**	**Test**
RMSE	0,0139	0,0214	0,0022	0,0024
R^2	0,9961	0,9889	0,9937	0,9807

V.3.3 Testing the Optimal Network to Predict the Unseen

The diagram below illustrates the neural network architecture used in this study. The model was trained using 9 input process variables relevant to the GTK module, and its objective is to estimate the LPG Fraction and the Compressor discharge pressure.

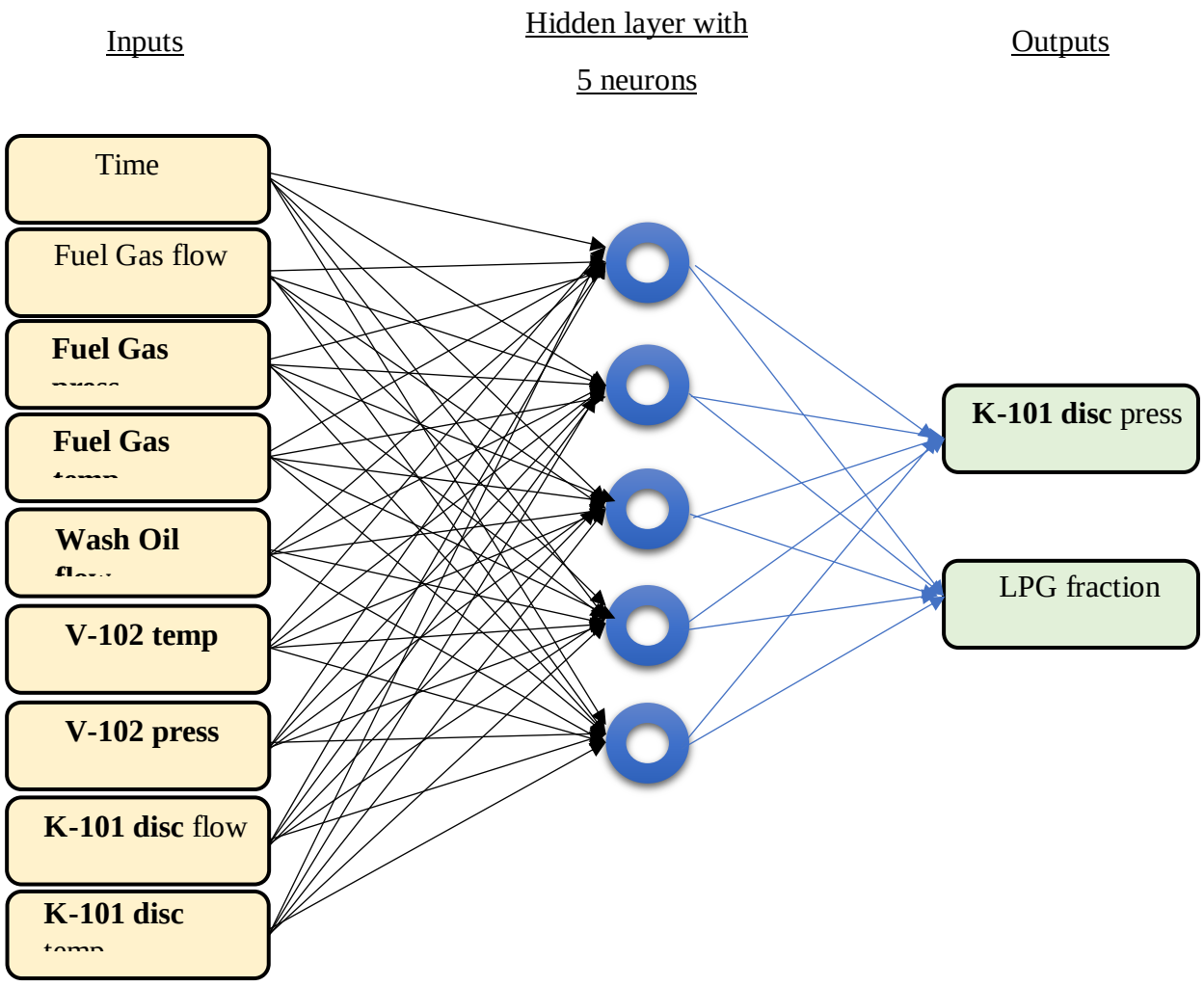

Figure V.23: Optimal Diagram for Modeling the LPG Fraction.

V.3.3.1. Neural Network Training

The neural network was implemented and trained using custom MATLAB code, allowing for flexible configuration adapted to LPG fraction modeling.

- By executing the MATLAB code, a panel appears that displays the network's defined properties and indicates that the neural network training process has been initiated.

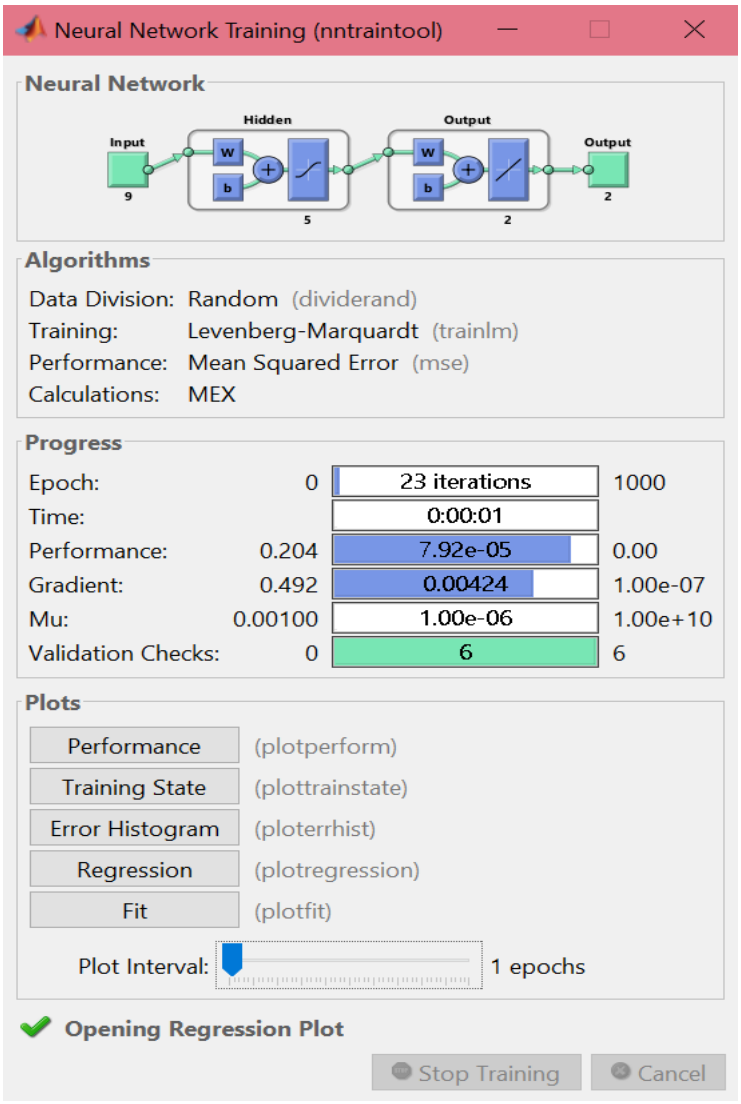

Figure V.24: The Neural Network Creation Process for the LPG Fraction.

- Linear regressions of the input data can be plotted. The figure V.7 shows the regressions of the results predicted by the neural network.

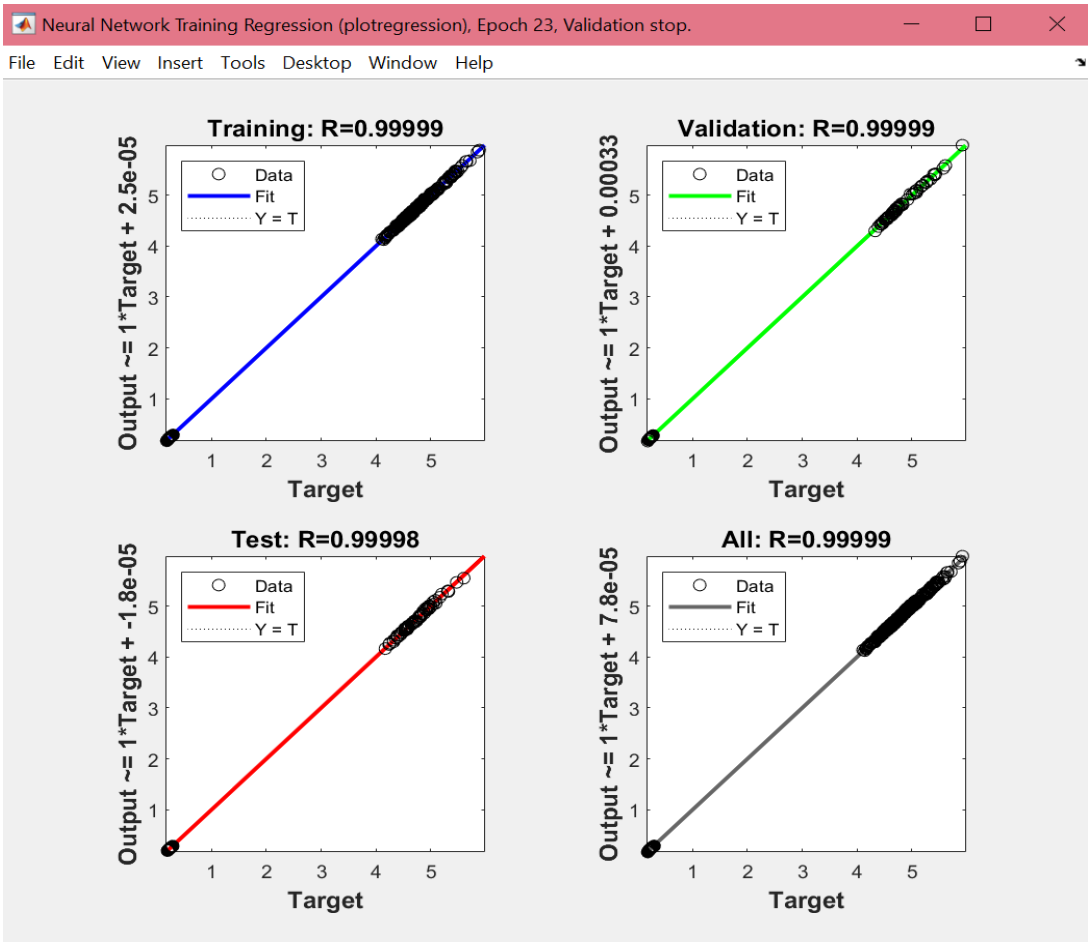

Figure V.25: the regression of the results predicted by the neural network.

- **The blue plot:** illustrates the regression corresponding to the 70% of the dataset used for training. The results demonstrate that the neural network model achieves highly accurate predictions of the LPG fraction for the majority of the input data. The correlation coefficient of R = 0.99999 confirms the excellent linear relationship between the predicted and target values, highlighting the network's capacity to capture the underlying trend.
- **The green plot** represents the regression for the 15% of the data allocated to validation. The outcomes indicate that the training process generalizes effectively to data unseen during training. The high correlation factor of R = 0.99999 provides further evidence of the linearity and reliability of the model's predictions for the LPG fraction.
- **The red plot:** shows the regression for the 15% of the dataset designated for testing. This additional verification step confirms that the trained network maintains its predictive performance on completely independent data. The correlation coefficient of R = 0.99998 reinforces the consistency and robustness of the model in estimating the LPG fraction.

Further simulation results will be examined later in this work to assess the prediction capabilities on new input scenarios beyond the training set.

- **The black plot:** presents the regression for all data combined (training, validation, and test). The global correlation coefficient of R = 0.99999 demonstrates the overall effectiveness of the neural network in modeling the LPG fraction, indicating a strong agreement between the predicted and actual target values across the entire dataset.

The chosen network structure was used to predict the results of all 449 sample .

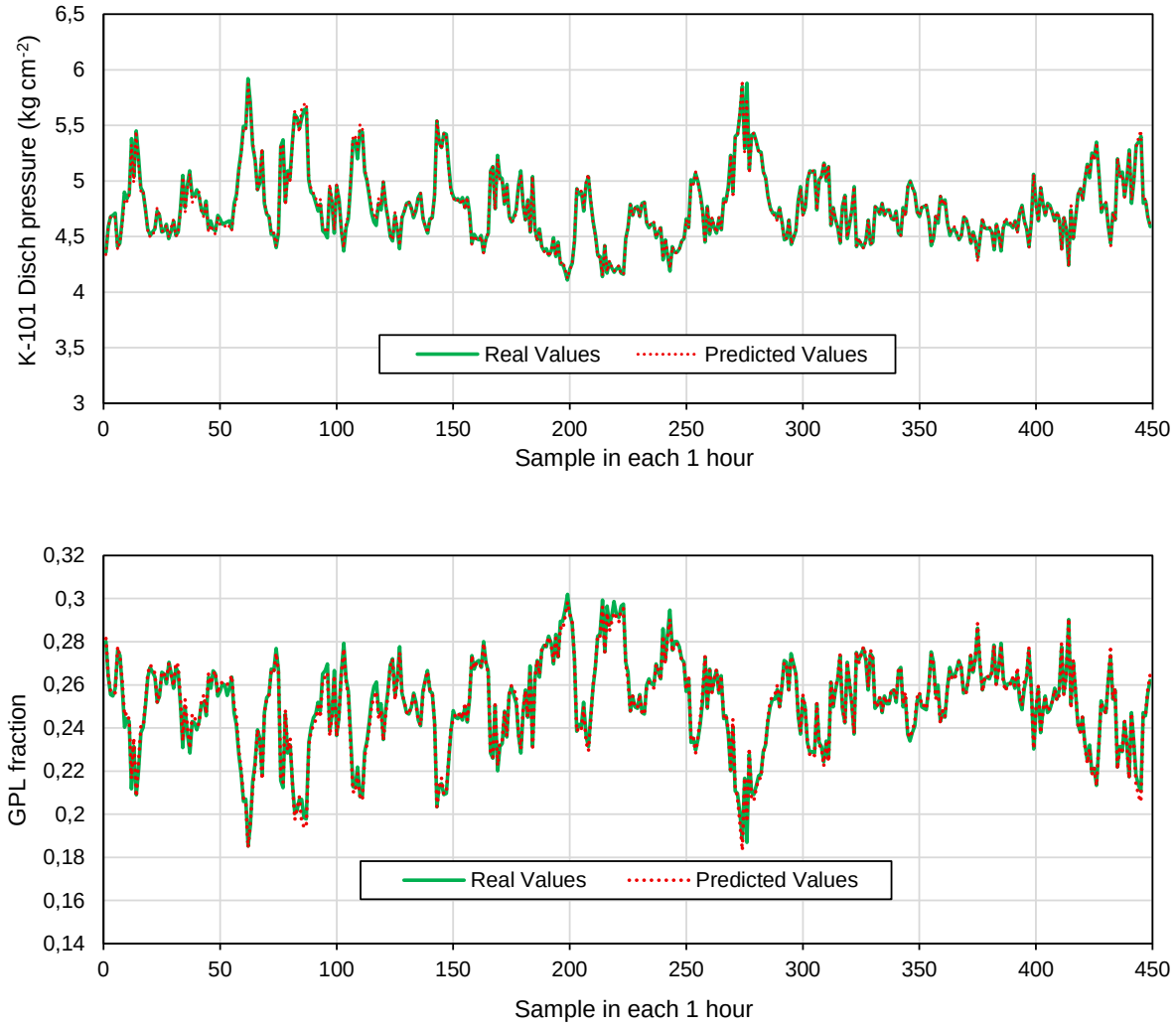

Figure V.26: Comparison between the Real LPG fractions values and the values predicted by Neural Network.

A mathematical optimization of the process can be performed at this point to maximize the GPL fraction. However, in practice, this cannot be considered, given that we are dealing with a real-time dynamic system.

V.4 Development of the Dynamic Model Using LSTM neural networks

To simulate the real-time evolution of the process variables, a dynamic model based on Long Short-Term Memory (LSTM) neural networks was developed. This model allows the prediction of future values of the system inputs, step by step, using only the historical values of the process. The training and implementation were conducted according to the following structured steps:

a. Secure Data Loading

The input dataset (Inputs1.xlsx) was loaded using MATLAB's readmatrix function. A validation check ensured the file contained exactly 8 rows corresponding to the 8 process variables used in the dynamic modeling. An automatic transposition was applied if necessary.

b. Verification of Vector Orientation

The data structure was verified to ensure each row represents a distinct process variable and each column a time step. If the orientation did not match expectations, the matrix was transposed.

c. Data Partitioning

The time series data was split into two subsets:

- 90% for training
- 10% for testing

This split ensures the model generalizes well to unseen data.

d. Data Normalization

To improve convergence during training and avoid bias due to variable scale differences, each variable was normalized to zero mean and unit variance using the training set statistics.

e. LSTM Input Preparation

The training inputs (XTrain) were defined as the normalized data at time *t*, while the training outputs (YTrain) were the values at time *t+1*. This transformation frames the problem as a sequence-to-sequence prediction task.

f. Conversion to Sequence Format

As LSTM models in MATLAB require sequences to be formatted as cell arrays, both inputs and outputs were converted accordingly.

g. LSTM Model Definition

The model architecture consists of:

- A sequence input layer with 8 features (one per variable)
- A hidden LSTM layer with 100 units
- A fully connected layer with 8 output neurons
- A regression layer for continuous prediction

h. Model Training

The model was trained using the Adam optimizer over 600 epochs with scheduled learning rate drops. A gradient threshold was set to prevent gradient explosion.

i. Multi-step Forecasting on Test Set

After training, the model was used to perform multi-step forecasting on the test data by iteratively feeding back predicted values as input for the next time step, simulating real-time evolution.

j. Denormalization of Predictions

The predicted values were transformed back to the original scale using the stored mean and standard deviation from the training set.

k. Evaluation

The model performance was assessed by computing the Root Mean Square Error (RMSE) between the predicted and true values for each variable. Trend plots were also generated to visually compare forecasted and observed data.

The figure below shows the window of the training progress of Dynamic Model Using LSTM neural networks. After 300 iteration the loss was reduced to almost zero with confirms the accuracy of the training.

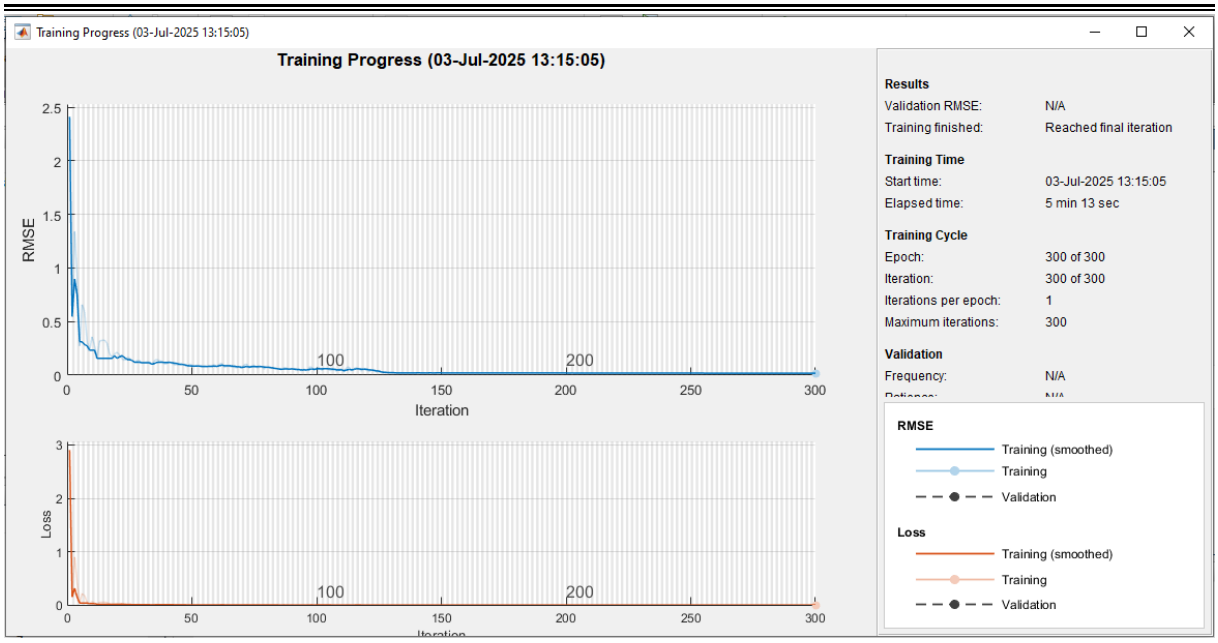

Figure V.9: Window of the training progress of Dynamic Model Using LSTM neural networks.

The prediction performance was evaluated by plotting the trends of the different inputs and outputs over a range of 0 to 45 consecutive hours selected for “Testing” (Figure V.27*)*.

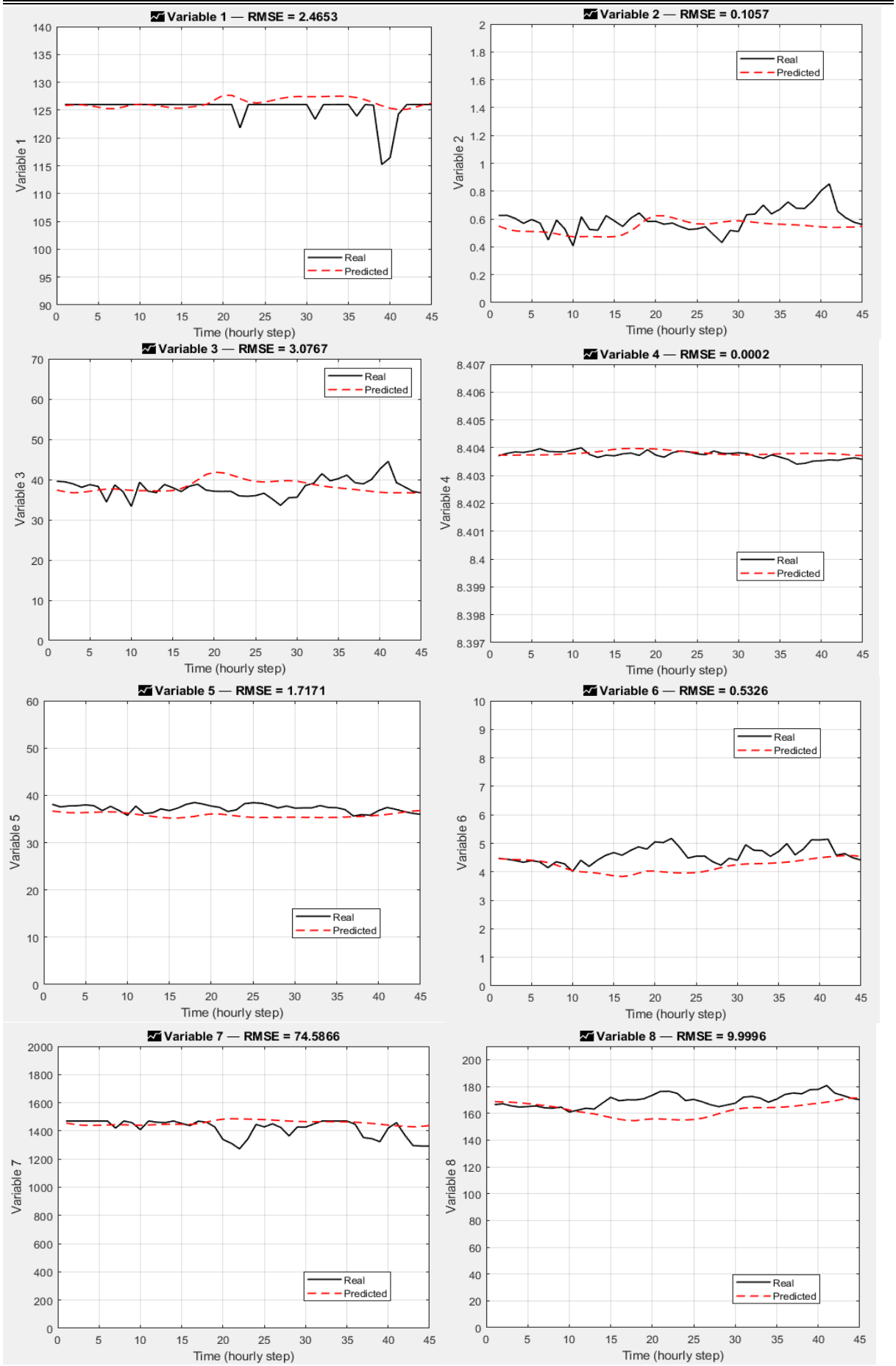

Figure V.28: Trends of the different inputs predicted by Dynamic Model Using LSTM ANN.

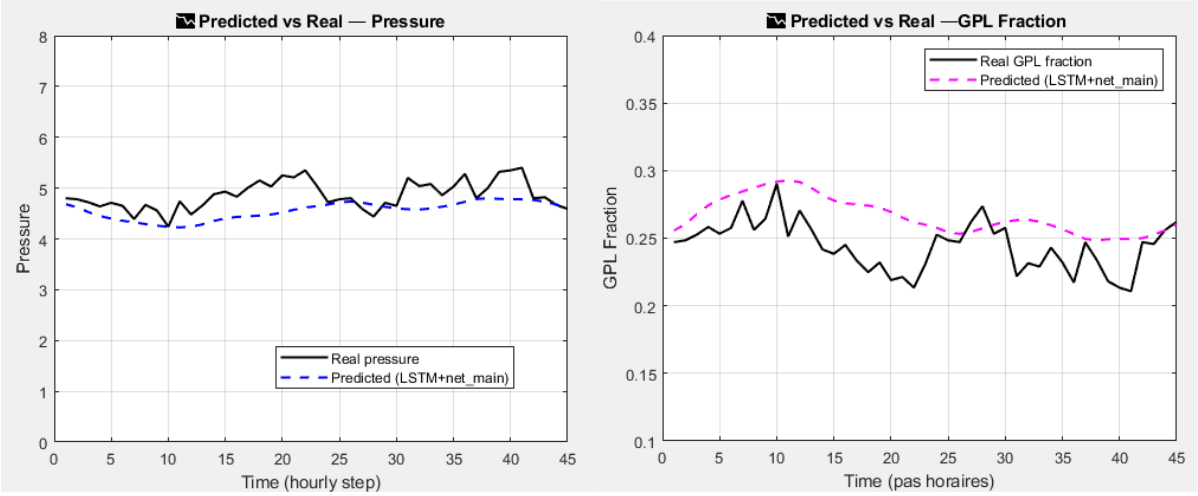

Figure V.29: Trends of the tow target variables predicted by Dynamic Model Using LSTM neural networks.

To extend the prediction capabilities beyond process variable forecasting, the trained dynamic model (LSTM) was combined with a secondary neural network, hereafter referred to as the **main prediction network**. This network is a feedforward model previously trained to map 8 process variables at time *t* to the two main output targets of the refinery unit (similar to the first Neural Network direct prediction).

The integration follows these steps (Shown on the App interface) :

a. Initialization with Arbitrary or Real Process State

A set of initial values for the 8 input variables is selected. This vector acts as the starting point (t = 0) for the dynamic prediction. These values can be either:

- Taken from real plant data (e.g., the last measured values),
- Or generated arbitrarily to explore operational scenarios.

b. Iterative Forecasting with LSTM

The LSTM model is used to predict future values of the 8 variables from t = 1 to t = N (e.g., N = 400 steps). The forecast at each time step is recursively computed using the predicted state from the previous step.

c. Prediction of the Main Outputs

For each predicted time step (t = 1 to N), the 8 dynamic variables are fed into the trained net_main network to compute the corresponding values of the two main output targets:

- **Target 1**: K-101 Discharge Pressure
- **Target 2**: GPL Fraction

d. Trend Analysis

The full sequence of predictions (both inputs and outputs) is stored and visualized to assess system behavior over time. This allows tracking of how variations in operating conditions influence critical output parameters.

e. Optimization Insight

The evolution of the second output (GPL fraction) can be analyzed to identify the optimal time step where it reaches its maximum. At this optimal point, the corresponding predicted values of:

- The first output (pressure),
- and all 8 input variables are extracted and recorded, potentially guiding optimization or control strategies.

VI. Conclusion

In this chapter, the optimization of the GTK module was successfully addressed through the application of Artificial Neural Networks (ANNs), particularly feedforward and LSTM models. By leveraging real operational data and implementing a structured modeling approach in MATLAB, a highly accurate neural network was developed to predict and enhance the recovery of LPG-rich unstabilized naphtha. The model demonstrated excellent predictive performance, as shown by high R^2 values and low RMSE, validating its reliability. Moreover, the introduction of dynamic modeling using LSTM allowed the simulation of future scenarios and provided insights into optimal operational strategies over time. These results confirm the significant potential of neural networks in refining process optimization and supporting smart decision-making in petrochemical industries.

GENERAL CONCLUSION

This thesis set out to explore the potential of turning a conventional petroleum refining unit, the GTK module, into a smart, optimized system by combining process simulation, real-time industrial data, and the power of artificial intelligence. Through the integration of Aspen HYSYS simulation and actual DCS data from the Skikda refinery, we first validated both design and real operational scenarios of the atmospheric distillation unit. This allowed for a precise understanding of product yields, cut points, and the behaviour of unstabilized naphtha under varying conditions.

With a foundation built on accurate modeling, the work then moved into the realm of machine learning. Artificial Neural Networks (ANNs), specifically feedforward and LSTM architectures, were developed and trained using real operational data in MATLAB. These models demonstrated strong predictive performance in forecasting key recovery metrics, particularly the recovery of LPG-rich unstabilized naphtha, a crucial economic and environmental target.

Beyond static predictions, the use of LSTM networks introduced a dynamic dimension to the optimization, allowing for future scenario simulations and smarter, time-sensitive decision-making strategies. This shift from traditional process control to intelligent, predictive modelling represents a meaningful step towards Industry 4.0 in the petrochemical sector.

More than just a technical study, this project was also an exploration of transformation, from raw data to actionable insight, from traditional operation to intelligent optimisation, and from industrial complexity to user-friendly tools. All of this effort was ultimately crystallised into a digital application, a smart interface that brings together the predictive power of neural networks and the practical demands of refinery operations, offering an intuitive decision-support system for engineers and operators alike.

BIBLIOGRAPHY

[1]. Zadakbar, O., et al. (2008, November). Flare gas recovery in oil and gas refineries. *Oil & Gas Science and Technology - Revue de l'IFP*.

[2]. Emam, E. A. (2016, February 4). Environmental pollution and measurement of gas flaring. *International Journal of Scientific Research in Science, Engineering and Technology*.

[3]. Hana, B. (2019). *Étude de la possibilité de récupération des gaz torchés au niveau des champs de Haoud Berkaoui* [Master's thesis, Université de Ouargla].

[4]. Feldman, L., et al. (2024). *Flaring accountability: Global gas flaring by major oil and gas companies*.

[5]. United Nations Economic and Social Commission for Western Asia. (2020). *Reducing gas flaring in Arab countries: A sustainable development necessity*. Beirut.

[6]. Lorenzato, G., et al. (2022). *Financing solutions to reduce natural gas flaring and methane emissions*. Washington, DC: World Bank.

[7]. Ismail, S., et al. (2012, June). Global impact of gas flaring. *Energy and Power Engineering*.

[8]. Advancing environmental and social performance www.ipieca.org Global Gas Flaring Reduction Partnership Flaring management guidance for the oil and gas industry Climate change. (n.d.). www.ipieca.org

[9]. King & Spalding LLP**.** (2020, March 13). *Overview of the new Algerian hydrocarbons law*. Lexology. Retrieved June18,2025. https://www.lexology.com/library/detail.aspx?g=179e2721-6859-4a35-982b-b4a590f2808e

[10]. Kolmetz, K. (2020, January). *Flare systems safety, selection, sizing and troubleshooting*. KLM Technology.

[11]. Hagos, F. Y., et al. (2021, November). Recovery of gas waste from the petroleum industry: A review. *Environmental Chemistry Letters*.

[12]. Brennan, D., & Fisher, P. W. (2002, June). Minimize flaring with flare gas recovery. *Hydrocarbon Processing*.

[13]. GeeksforGeeks. (n.d.). *Neural networks: A beginner's guide*. https://www.geeksforgeeks.org/neural-networks-a-beginners-guide/

[14]. Kaushik, V. (2021, August 27). 8 applications of neural networks. *Analytics Steps*. https://www.analyticssteps.com/blogs/8-applications-neural-networks

[15]. Roth, M. W. (1988). Neural-network technology and its applications. *Johns Hopkins APL Technical Digest*, *9*(3), 242–253.

[16]. Y. T., et al. (2022, March 21). Artificial neural network.

[17]. Sammut, C., & Webb, G. I. (2011). *Encyclopedia of machine learning* (2nd ed.).

[18]. Adamowski, J., Fung, H., Prasher, S. O., Ozga, B., & Sliusarieva, A. (n.d.) Comparison of multiple linear and nonlinear regression, autoregressive integrated moving average, artificial neural network method for urban water demand. *Advancing Earth and Space Science*.

[19]. Noor, R. K. F. H. (2024). Applications of artificial neural networks in the petroleum industry: A review. *Iraqi Journal of Oil & Gas Research*, *4*(2), 53–60.

[20]. Creately Team. (n.d.). Neural network diagram. *Creately*. https://creately.com/diagram/example/gvt0PxHTJ8L/neural-network-diagram

[21]. Qamar, R., & Roheen, B. A. Z. (2023, August). Artificial neural networks: An overview. *Mesopotamian Journal of Computer Science*, 131–139.

[22]. Sears-Collins, A. (2019, July 30). Artificial feedforward neural network with backpropagation from scratch. *Automatic Addison*. https://automaticaddison.com/artificial-feedforward-neural-network-with-backpropagation-from-scratch/

[23]. B. J., et al. (2024). A comparative survey between cascade correlation neural network (CCNN) and feedforward neural network (FFNN) machine learning models for forecasting suspended sediment concentration. *Scientific Reports*.

[24]. F. A., et al. (2022, July 22). Sentiment analysis of public social media as a tool for health-related topics. *IEEE Access*.

[25]. Spiceworks. (n.d.). What is a neural network? *Spiceworks*. https://www.spiceworks.com/tech/artificial-intelligence/articles/what-is-a-neural-network/

[26]. Free Time Learning. (n.d.). What is modular neural network? *Free Time Learning*. https://www.freetimelearning.com/software-interview-questions-and-answers.php?What-Is-Modular-Neural-Network?&id=4165

[27]. D. K., et al. (2021, June). Survey on artificial neural network. *International Research Journal of Modernization in Engineering Technology and Science*, *3*(6).

[28]. Vasileiadis, A., Alexandrou, E., Paschalidou, L., Chrysanthou, M., & Hadjichristoforou, M. (n.d.). Artificial neural network and its applications [Unpublished manuscript].

[29]. Ghadjati, M. (2012). *Applications des réseaux de neurones aux systèmes de communications numériques* [Master's thesis, Université 8 Mai 1945 – Guelma, Algérie].

[30]. Skikda Refinery. (n.d.). *Operating manual of the atmospheric distillation unit (U10)*.

[31]. École des Mines d'Albi. (n.d.). Schéma de distillation simple. Retrieved April 20, 2025, from https://nte.mines-albi.fr/Thermo/fr/co/uc_SchemaDistillationSimple.html

[32]. Sonatrach. (2023). *PFD (Process Flow Diagram) of the Atmospheric Distillation Unit (U10)* [Process Flow Diagram]. Refining Division, Skikda Refinery.

[33]. Bahloul, I., & Abdennebi, R. (2019). *Calcul de vérification du module de récupération des gaz torchés de l'unité de topping à la RA1K* [Unpublished master's thesis]. Algerian Petroleum Institute, Boumerdes.

[34]. Orantes Molina, A. (2005). *Méthodologie pour le placement des capteurs à base de méthodes de classification en vue du diagnostic* [Doctoral dissertation, Institut National des Sciences Appliquées de Toulouse]. HAL Open Science.

[35]. Bentitraoui, T. (2022). *Étude du processus de liquéfaction et séparation des gaz de l'air* [Unpublished master's thesis]. University of M'Hamed Bougara Boumerdes.

[36]. Gunay, M. E., & Yildirim, R. (2011). Neural network analysis of selective CO oxidation over copper-based catalysts for knowledge extraction from published data in the literature. *Industrial & Engineering Chemistry Research, 50*(22), 12488–12500.

1 Annex 01: GTK Module PFD (Process Flow Diagram).

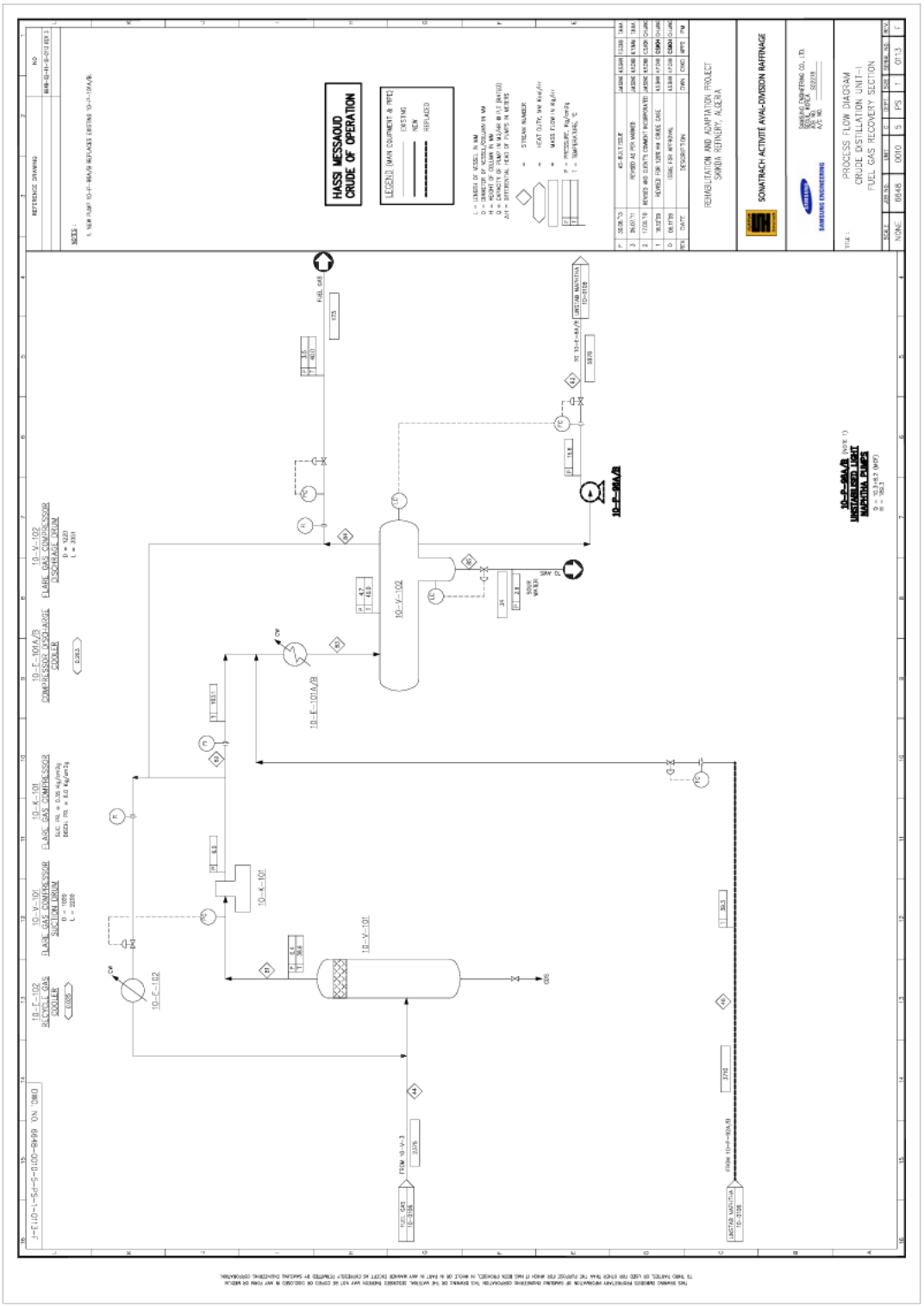

2 Annex 2: GTK Module Streams Composition and Parametrs “Design Case”.

SKIKDA REFINERY REHABILITATION ADAPTATION PROJECT

STREAM SUMMARY FOR CRUDE DISTILLATION UNIT - I

Doc. No : 6648-0010-5-PS-SS-0001-F SHEET: 11 of 26

REV.

STREAM ID	UNIT	41	42	43	44	45
NAME		2nd VAPOR_2	CR OVHD	CR OVHD_92	GAS	UNSTAB_NAP
PHASE		MIXED	WET VAPOR	WET LIQUID	WET VAPOR	WET LIQUID
TEMPERATURE	C	135	135	40	39	39
PRESSURE	KG/CM2G	1.3	1.3	0.8	0.6	0.6
* TOTAL STREAM *						
RATE	KG/HR	980442	399170	399170	2375	380249
RATE	KG-MOL/HR	10254.8	5147.9	5147.9	45.4	4184.1
ENTHALPY	M*KCAL/HR	-436.159	-190.290	-248.264	-1.326	-184.344
(BULK) DENSITY	KG/M3	13.3	5.5	691.1	3.3	683.9
MW	KG/KG MOLE	95.6	77.5	77.5	52.4	90.9
WT FRAC LIQUID		0.5	0.0	1.0	0.0	1.0
CRIT. TEMP	C	294.4	270.6	270.6	140.7	249.3
CRIT. PRES.	KG/CM2	46.9	66.3	66.3	47.6	31.7
RVP	PSIA	9.86	19.54	19.54	126.49	18.60
* VAPOR PHASE *						
RATE	KG/HR	399192	399170	---	2375	---
STD. RATE	M3/HR	121725.1	121720.3	---	1072.4	---
ENTHALPY	KCAL/KG	-476.705	-476.713	---	-558.570	---
DENSITY	KG/M3	5.483	5.482	---	3.311	---
MW	KG/KG MOLE	77.5	77.5	---	52.4	---
VISCOSITY	CP	0.01	0.01	---	0.01	---
THERMAL COND.	KCAL/HR-M-C	0.019	0.019	---	0.015	---
CP	KCAL/KG-K	0.493	0.493	---	0.419	---
COMPRESS. (Z)		0.95	0.95	---	0.97	---
CP/CV RATIO		1.07	1.07	---	1.11	---
* LIQUID PHASE *						
RATE	KG/HR	581250	---	399170	---	380249
ACT.RATE	M3/HR	888.9	---	577.6	---	556.0
ENTHALPY	KCAL/KG	-422.989	---	-621.949	---	-484.797
STD. DENSITY	KG/M3	756.415	---	705.831	---	698.096
DENSITY	KG/M3	653.9	---	691.1	---	683.9
MW	CP	113.8	---	77.5	---	90.9
VISCOSITY	CP	0.22	---	0.37	---	0.34
THERMAL COND.	KCAL/HR-M-C	0.089	---	0.100	---	0.096
CP	KCAL/KG-K	0.595	---	0.528	---	0.505
SURF. TENS	DYNE/CM	12.9	---	---	---	17.3
CRIT. TEMP.	C	318.4	---	---	---	249.3
CRIT. PRES.	KG/CM2	27.3	---	---	---	31.7
* FREE WATER *						
RATE	KG/HR	---	---	16578	0	0

SKIKDA REFINERY REHABILITATION ADAPTATION PROJECT

STREAM SUMMARY FOR CRUDE DISTILLATION UNIT - I

Doc. No : 6648-0010-5-PS-SS-0001-F SHEET: 12 of 26

REV.

STREAM ID	UNIT	46	47	48	49	50
NAME		UNSNAP_P	SOUR_WATER	UNSTAB_P	STM_HGO	STM_LGO
PHASE		WET LIQUID	WATER	WET LIQUID	WATER VAPOR	WATER VAPOR
TEMPERATURE	C	39	39	39	330	330
PRESSURE	KG/CM2G	13.4	0.6	13.4	2.9	2.9
* TOTAL STREAM *						
RATE	KG/HR	3710	16547	376539	1527	4396
RATE	KG-MOL/HR	40.8	918.5	4143.3	84.8	244.0
ENTHALPY	M*KCAL/HR	-1.797	-62.593	-182.380	-4.686	-13.490
(BULK) DENSITY	KG/M3	685.1	996.8	685.1	1.4	1.4
MW	KG/KG MOLE	90.9	18.0	90.9	18.0	18.0
WT FRAC LIQUID		1.0	1.0	1.0	0.0	0.0
CRIT. TEMP	C	249.3	374.1	249.3	374.1	374.1
CRIT. PRES.	KG/CM2	31.7	224.5	31.7	224.5	224.5
RVP	PSIA	18.60	---	18.60	---	---
* VAPOR PHASE *						
RATE	KG/HR	---	---	---	1527	4396
STD. RATE	M3/HR	---	---	---	2004.2	5769.7
ENTHALPY	KCAL/KG	---	---	---	-3068.728	-3068.728
DENSITY	KG/M3	---	---	---	1.397	1.397
MW	KG/KG MOLE	---	---	---	18.0	18.0
VISCOSITY	CP	---	---	---	0.02	0.02
THERMAL COND.	KCAL/HR-M-C	---	---	---	0.040	0.040
CP	KCAL/KG-K	---	---	---	0.489	0.489
COMPRESS. (Z)		---	---	---	0.99	0.99
CP/CV RATIO		---	---	---	1.30	1.30
* LIQUID PHASE *						
RATE	KG/HR	3710	16547	376539	---	---
ACT.RATE	M3/HR	5.4	16.6	549.6	---	---
ENTHALPY	KCAL/KG	-484.358	-3782.858	-484.358	---	---
STD. DENSITY	KG/M3	698.096	997.986	698.096	---	---
DENSITY	KG/M3	685.1	996.8	685.1	---	---
MW	CP	90.9	18.0	90.9	---	---
VISCOSITY	CP	0.34	0.66	0.34	---	---
THERMAL COND.	KCAL/HR-M-C	0.096	0.542	0.096	---	---
CP	KCAL/KG-K	0.504	1.031	0.504	---	---
SURF. TENS	DYNE/CM	17.2	69.7	17.2	---	---
CRIT. TEMP.	C	249.3	374.1	249.3	---	---
CRIT. PRES.	KG/CM2	31.7	224.5	31.7	---	---
* FREE WATER *						
RATE	KG/HR	---	16547	---	---	---

SKIKDA REFINERY REHABILITATION ADAPTATION PROJECT

STREAM SUMMARY FOR CRUDE DISTILLATION UNIT - I

Doc. No : 6648-0010-5-PS-SS-0001-F SHEET: 19 of 26

REV.

STREAM ID	UNIT	81	82	83	84	85
NAME		GAS_COMP_IN	GAS_COMP_OUT	E-101_SS	FUEL_GAS	WAT_V102
PHASE		WET VAPOR	WET VAPOR	MIXED	WET VAPOR	WATER
TEMPERATURE	C	39	103	40	40	40
PRESSURE	KG/CM2G	0.4	6.0	4.7	4.7	4.7
* TOTAL STREAM *						
RATE	KG/HR	2375	2375	6085	173	34
RATE	KG-MOL/HR	45.4	45.4	86.2	3.9	1.9
ENTHALPY	M*KCAL/HR	-1.326	-1.264	-3.324	-0.100	-0.127
(BULK) DENSITY	KG/M3	2.8	12.6	233.5	10.4	996.1
MW	KG/KG MOLE	52.4	52.4	70.6	44.0	18.0
WT FRAC LIQUID		0.0	0.0	1.0	0.0	1.0
CRIT. TEMP	C	140.7	140.7	192.2	97.2	374.1
CRIT. PRES.	KG/CM2	47.6	47.6	40.1	45.2	224.5
RVP	PSIA	126.49	126.49	69.82	239.82	---
* VAPOR PHASE *						
RATE	KG/HR	2375	2375	173	173	---
STD. RATE	M3/HR	1072.4	1072.4	93.0	93.0	---
ENTHALPY	KCAL/KG	-558.570	-532.361	-577.128	-577.128	---
DENSITY	KG/M3	2.816	12.596	10.375	10.375	---
MW	KG/KG MOLE	52.4	52.4	44.0	44.0	---
VISCOSITY	CP	0.01	0.01	0.01	0.01	---
THERMAL COND.	KCAL/HR-M-C	0.015	0.021	0.017	0.017	---
CP	KCAL/KG-K	0.418	0.497	0.439	0.439	---
COMPRESS. (Z)		0.97	0.92	0.92	0.92	---
CP/CV RATIO		1.11	1.12	1.16	1.16	---
* LIQUID PHASE *						
RATE	KG/HR	---	---	5878	---	34
ACT.RATE	M3/HR	---	---	9.3	---	0.0
ENTHALPY	KCAL/KG	---	---	-526.889	---	-3781.716
STD. DENSITY	KG/M3	---	---	639.838	---	997.986
DENSITY	KG/M3	---	---	629.0	---	996.1
MW	CP	---	---	73.1	---	18.0
VISCOSITY	CP	---	---	0.23	---	0.65
THERMAL COND.	KCAL/HR-M-C	---	---	0.086	---	0.543
CP	KCAL/KG-K	---	---	0.539	---	1.031
SURF. TENS	DYNE/CM	---	---	12.9	---	69.5
CRIT. TEMP.	C	---	---	192.6	---	374.1
CRIT. PRES.	KG/CM2	---	---	35.5	---	224.5
* FREE WATER *						
RATE	KG/HR	---	---	34	0	34

3 Annex 03: GTK Streams Composition and Parameters “Real Case”.

Hyprotech's Process Simulator HYSIM - Licensed to Brown & Root Condor
Date 99/12/20 Version STD|C2.63 Case Name U11-3-21.SIM
Time 12: 0:09 Prop Pkg PR

Stream Name		Gas(V3)	Wash-Oil	Fuel-Gas	Naphta
Vapour_Frac		1.00	0.00	1.00	0.00
Temperature	C	37.0	30.0	33.4	33.4
Pressure	kg/cm2_g	0.44	16.00	5.65	19.00
Flow	kgmole/h	181.8	237.7	13.1	356.2
Mass_Flow	kg/h	8984.6	21811.0	470.3	28728.0
Volume_Flow	m3/h	3159.9	31.2	47.5	43.2
Mole_Weight		49.41	91.74	35.87	80.66
Methane	Mole frac.	0.0267	0.0000	0.2263	0.0000
Ethane	Mole frac.	0.1606	0.0048	0.3338	0.0228
Propane	Mole frac.	0.3901	0.0459	0.2957	0.0946
i-Butane	Mole frac.	0.0728	0.0203	0.0304	0.0378
n-Butane	Mole frac.	0.2142	0.0886	0.0743	0.1534
i-Pentane	Mole frac.	0.0478	0.0580	0.0120	0.0837
n-Pentane	Mole frac.	0.0556	0.0944	0.0138	0.1281
n-Hexane	Mole frac.	0.0294	0.1296	0.0110	0.1085
n-Heptane	Mole frac.	0.0028	0.1071	0.0027	0.0775
n-Octane	Mole frac.	0.0000	0.1057	0.0000	0.0591
n-Nonane	Mole frac.	0.0000	0.0619	0.0000	0.0376
n-Decane	Mole frac.	0.0000	0.0369	0.0000	0.0173
n-C11	Mole frac.	0.0000	0.0011	0.0000	0.0016
Cyclopentane	Mole frac.	0.0000	0.0059	0.0000	0.0052
Cyclohexane	Mole frac.	0.0000	0.0206	0.0000	0.0158
Mcyclopentan	Mole frac.	0.0000	0.0213	0.0000	0.0159
Cycloheptane	Mole frac.	0.0000	0.0717	0.0000	0.0489
Cyclooctane	Mole frac.	0.0000	0.0292	0.0000	0.0308
Cyclononane	Mole frac.	0.0000	0.0250	0.0000	0.0183
Cyclodecane	Mole frac.	0.0000	0.0057	0.0000	0.0034
Benzene	Mole frac.	0.0000	0.0104	0.0000	0.0083
Toluene	Mole frac.	0.0000	0.0154	0.0000	0.0106
E-Benzene	Mole frac.	0.0000	0.0285	0.0000	0.0136
Cumene	Mole frac.	0.0000	0.0120	0.0000	0.0070
H2O	Mole frac.	0.0000	0.0000	0.0000	0.0000
Methane	kg/h	77.8034	0.0000	47.5993	0.0000
Ethane	kg/h	878.2587	34.3148	131.5985	244.4061
Propane	kg/h	3127.7681	481.2044	170.9594	1485.5457
i-Butane	kg/h	769.6397	280.5171	23.1666	783.2357
n-Butane	kg/h	2263.5220	1224.3259	56.6209	3176.4556
i-Pentane	kg/h	626.4331	994.8972	11.3516	2150.2737
n-Pentane	kg/h	729.9649	1619.2809	13.0543	3292.2854
n-Hexane	kg/h	460.2011	2655.2705	12.4286	3330.2002
n-Heptane	kg/h	50.9626	2551.4480	3.5472	2764.8750
n-Octane	kg/h	0.0000	2870.5864	0.0000	2402.6191
n-Nonane	kg/h	0.0000	1887.4974	0.0000	1719.1780
n-Decane	kg/h	0.0000	1248.2264	0.0000	877.5066
n-C11	kg/h	0.0000	40.8786	0.0000	89.1580
Cyclopentane	kg/h	0.0000	98.3773	0.0000	130.0119
Cyclohexane	kg/h	0.0000	412.1742	0.0000	474.0323
Mcyclopentan	kg/h	0.0000	426.1898	0.0000	477.0433
Cycloheptane	kg/h	0.0000	1673.7472	0.0000	1711.6573
Cyclooctane	kg/h	0.0000	778.9589	0.0000	1232.0254
Cyclononane	kg/h	0.0000	750.2933	0.0000	823.5300
Cyclodecane	kg/h	0.0000	190.0822	0.0000	170.0132
Benzene	kg/h	0.0000	193.1292	0.0000	231.1159
Toluene	kg/h	0.0000	337.3499	0.0000	348.1793
E-Benzene	kg/h	0.0000	719.3466	0.0000	514.7181
Cumene	kg/h	0.0000	342.9035	0.0000	299.9342
H2O		0.0000	0.0000	0.0000	0.0000

4 Annex 04: DCS DATA “15/04/2025”.

SKIKDA REFINERY REHABILTATION AND ADAPTATION PROJECT

PERFORMANCE TEST LOG SHEET FOR CDU-I (UNIT 10)

DOCUMENT NO.	6648-0010-5-PS-PT-0001-0
Commencement Date	
Commencement Time	
PERIOD	

RECORDED DATE	SECL CHECKED BY	SECL APPROVED BY	SONATRACH CHECKED BY	SONATRACH APPROVED BY
15/04/2025				

15/04/2025 12:00 AM

04/15/25

00:00

Format edited: 12 Dec. 2012

CHARGE AND PREHEAT TRAIN

TIME	FLOW 10FI4 PV P-71A/B DISCHARGE m3/hr	FLOW 10FIC2 PV P-72A/B/C DISCHARGE m3/hr	TEMP 10TI1161 PV CRUDE AT B/L DegC	10TI1454 PV 10-E-107-5A/B SHELL OUTLET DegC	10TI1152 PV 10-E-72A/B OUTLET DegC	10TI171 PV 10-V-51 INLET DegC	10TI170 PV 10-V-51HDR OUTLET DegC	10TI1153 PV E-93A-H OUTLET DegC	10TI11 PV V-1 PREFLASH DRUM LIQUID DegC	10TI1159 PV E-82A OULET DegC	10TI17 PV E-82B OUTLET DegC	10TI1456 PV E-61A-D OUTLET DegC
00:00	1260	1347,5	25,60	45,68	72,7	72,9	73,1	146,7	141,0	143,4	150,1	171,8
01:00	1264	1347,4	25,60	45,40	72,2	72,5	73,0	146,8	141,0	143,5	150,3	171,8
02:00	1256	1347,4	25,22	45,33	72,4	72,6	72,5	146,8	140,8	143,3	150,1	171,8
03:00	1268	1346,4	25,22	45,40	72,5	72,7	73,0	146,9	141,1	143,5	150,3	172,1
04:00	1261	1346,7	25,16	45,17	72,2	72,4	72,5	146,8	140,8	143,3	150,1	171,7
05:00	1254	1347,0	25,09	45,23	72,5	72,7	72,8	147,0	140,9	143,4	150,2	171,8
06:00	1260	1347,3	25,05	45,41	72,7	72,9	73,0	146,9	140,9	143,3	150,1	171,8
07:00	1260	1347,5	25,21	45,38	72,5	72,7	72,7	146,7	140,9	143,3	150,1	171,6
08:00	1254	1347,0	25,50	45,63	72,8	73,0	73,2	147,2	141,5	143,9	150,7	172,2
09:00	1272	1346,7	25,71	45,93	72,8	73,0	73,2	146,4	140,9	143,4	150,2	172,0
10:00	1293	1347,2	25,85	45,81	72,4	72,6	72,9	146,4	141,0	143,4	150,1	171,7
11:00	1278	1347,0	25,90	45,93	72,5	72,7	72,8	146,6	141,2	143,6	150,3	172,0
12:00	1255	1346,3	25,84	46,56	73,6	73,8	73,6	146,9	141,3	143,7	150,5	172,1
13:00	1265	1346,8	26,11	46,62	73,5	73,7	74,1	147,1	141,7	144,1	150,8	172,6
14:00	1285	1346,4	26,25	46,62	73,2	73,4	73,6	146,2	141,1	143,6	150,3	172,1
15:00	1266	1347,6	26,16	46,74	73,6	73,8	73,9	146,7	141,4	143,8	150,4	172,1
16:00	1246	1347,5	25,96	46,50	73,5	73,7	74,0	146,2	142,3	144,7	151,3	173,0
17:00	1231	1346,6	25,87	46,35	73,6	73,8	73,8	143,3	143,5	145,9	152,6	174,4
18:00	1246	1346,8	25,74	46,04	73,1	73,3	74,0	148,2	142,9	145,4	152,1	174,2
19:00	1276	1347,4	25,34	45,05	71,7	71,9	72,2	146,2	141,0	143,4	150,2	172,6
20:00	1267	1346,5	25,17	44,37	71,0	71,2	71,8	147,3	141,8	144,2	151,0	172,7
21:00	1277	1347,4	25,55	44,41	70,8	71,1	71,1	146,9	141,7	144,1	151,0	172,9
22:00	1266	1346,3	25,58	44,91	71,6	71,9	71,9	147,4	141,9	144,3	151,2	173,1
23:00	1253	1346,2	25,57	45,41	72,2	72,4	72,1	146,0	141,1	143,6	150,4	172,6
Average	1263	1347,0	25,53	45,67	72,6	72,8	73,0	147,0	141,4	143,8	150,6	172,3
Total	30307	32327,2	614,25	1036,00	1741,4	1746,9	1751,0	3521,7	3393,7	3452,0	3614,7	4136,4
Maximum	1295	1347,8	26,25	46,74	73,6	73,8	74,1	148,2	143,5	145,9	174,4	152,6
Minimum	1231	1346,2	25,05	44,37	70,8	71,1	71,1	146,0	140,8	143,3	150,1	171,6

CHARGE AND PREHEAT TRAIN / PRESS / F-1A ATM HEATER

TIME	TEMP 10TI1160 PV E-83A OUTLET DegC	10TI18 PV E-83B OUTLET DegC	10TI10 PV E-91 OUTLET DegC	10TI12 PV E-90A/B OUTLET DegC	10TI1460 PV E-62 OUTLET DegC	10TI1461 PV E-63A/B OUTLET DegC	PRESS 10PI1152 PV CRUDE AT B/L kg/cm2	10PDI213 PV DESALTER MIXING VALVE DE kg/cm2	10PI40 PV V-51 DESALTER OUTLET kg/cm2	10PIC1351 PV LV-2 INLET PRESSURE kg/cm2	10PIC1 PV V-1 PREFLASH DRUM VAPOR kg/cm2	FLOW 10FIC2A PV PASS-A m3/hr
00:00	176,5	184,4	194,3	222,7	235,7	240,8	0,505	0,623	8,30	5,42	3,000	86,0
01:00	176,5	184,3	194,3	222,7	235,7	240,7	0,486	0,625	8,29	5,42	3,000	86,0
02:00	176,5	184,3	194,4	222,9	235,9	240,9	0,630	0,617	8,36	5,46	3,001	86,1
03:00	176,3	184,7	194,7	223,1	236,0	241,1	0,630	0,629	8,38	5,48	3,000	85,9
04:00	176,4	184,1	194,2	222,7	235,7	240,7	0,630	0,622	8,34	5,45	3,001	86,0
05:00	176,5	184,3	194,4	222,8	235,8	240,8	0,630	0,616	8,38	5,47	2,999	85,9
06:00	176,6	184,4	194,4	222,8	235,8	240,9	0,630	0,622	8,37	5,47	3,000	86,0
07:00	176,3	184,1	194,2	222,5	235,6	240,6	0,630	0,620	8,37	5,47	3,001	85,9

C-1 ATMOSPHERIC COLUMN

TIME	TEMP 10TI90 PV RESIDUE AT C-1 BOTTOM DegC	10TI89 PV FLASH ZONE DegC	10TI86 PV BPA DRAW TEMP DegC	10TI87 PV BPA RETURN TEMP DegC	10TI85 PV TPA DRAW TEMP DegC	10TI83 PV TPA RETURN TEMP DegC	10TI81 PV ATM COLUMN TOP DegC	10TIC1180 PV V-2 DegC	10TI1955 PV V-3 DegC	10TI82 PV KEROSENE DRAW DegC	10TI84 PV LGO DRAW DegC	10TI86 PV HGO DRAW DegC
00:00	330,0	336,5	293,7	231,7	216,4	161,9	166,7	123,6	38,77	201,7	258,7	293,7
01:00	330,0	336,5	293,8	231,7	216,8	162,1	166,2	123,7	37,87	202,1	259,1	293,8
02:00	330,2	336,6	294,1	231,8	216,8	162,1	167,0	123,5	37,54	202,4	259,2	294,1
03:00	330,0	336,4	293,8	231,8	216,8	162,1	166,3	123,7	39,95	201,9	258,7	293,8
04:00	330,0	336,5	293,7	231,6	216,7	162,0	166,3	123,5	37,73	202,3	259,2	293,7
05:00	330,1	336,5	293,8	231,8	216,9	162,1	166,8	123,7	37,83	202,2	259,0	293,8
06:00	330,2	336,6	293,8	231,8	216,7	162,0	166,8	123,7	40,09	201,6	258,5	293,8
07:00	330,1	336,5	293,7	231,7	216,7	162,0	167,0	123,5	39,07	202,0	258,9	293,7
08:00	330,1	336,6	293,9	231,9	216,9	162,3	167,0	130,1	40,14	202,5	259,2	293,9
09:00	329,2	335,8	293,3	231,6	216,4	161,8	166,6	129,3	40,57	201,5	258,3	293,3
10:00	330,0	336,6	293,3	231,8	216,8	162,0	166,6	129,3	40,15	202,3	259,3	293,9
11:00	329,9	336,2	293,9	231,8	217,0	162,1	166,4	129,3	39,04	202,6	259,5	293,9
12:00	330,0	336,3	293,9	231,8	216,9	162,1	166,3	129,9	38,09	201,9	258,8	293,9
13:00	329,8	336,1	293,9	231,9	216,8	162,3	166,2	130,1	37,85	201,8	258,6	293,9
14:00	329,8	336,1	293,9	231,6	216,4	161,9	165,7	129,2	36,99	201,1	258,1	293,9
15:00	329,8	336,2	293,8	231,7	216,5	162,1	166,2	129,8	36,74	201,5	258,4	293,8
16:00	330,0	336,2	294,0	232,1	217,2	162,6	167,6	131,2	37,51	202,9	259,4	294,0
17:00	330,1	336,2	294,1	232,3	217,6	163,2	168,3	132,5	38,51	202,3	259,1	294,1
18:00	330,1	336,1	294,0	231,9	217,0	162,6	167,2	131,9	37,40	200,3	257,7	294,0
19:00	329,8	335,8	293,8	231,0	216,0	160,8	165,7	129,8	37,13	199,0	256,8	293,6
20:00	330,0	336,5	294,0	231,5	216,7	161,7	166,4	130,6	40,84	201,2	258,6	294,0
21:00	330,5	336,9	294,8	232,0	217,3	162,0	166,3	130,1	39,66	202,1	259,6	294,8
22:00	330,5	336,5	294,5	231,9	217,3	162,1	166,4	130,9	43,48	201,6	259,0	294,5
23:00	330,2	336,6	294,2	231,7	216,5	161,6	165,2	129,3	39,46	201,7	259,3	294,2
Average	330,0	336,4	293,9	231,8	216,8	162,1	166,5	130,0	38,81	201,8	258,8	293,9
Total	7920,3	8073,0	7054,0	5562,4	5203,0	3889,8	3997,8	3120,1	931,42	4842,8	6210,9	7054,0
Maximum	330,5	336,9	294,8	232,3	217,6	163,2	168,3	132,5	43,48	202,9	259,6	294,8
Minimum	329,2	335,8	293,3	231,0	216,0	160,8	165,2	129,2	36,74	199,0	256,8	293,3

C-1 ATMOSPHERIC COLUMN / SIDE STRIPPERS

TIME	PRESS 10PI14 PV FLASH ZONE kg/cm2	10PI13 PV ATM COLUMN TOP kg/cm2	10PIC15 PV V-3 kg/cm2	10PI2056 PV RESIDUE TO STORAGE (B/L) kg/cm2	FLOW 10FIC3 PV KERO TO STORAGE OR U-20 m3/hr	10FIC2051 PV EXCESS KERO TO LGO m3/hr	10FIC47 PV LGO TO STORAGE m3/hr	10FIC46 PV HGO TO STORAGE m3/hr	10FIC1851 PV MP STEAM TO C-3 kg/hr	10FIC1852 PV MP STEAM TO C-4 kg/hr	TEMP 10TI2 PV KERO TO STORAGE DegC	10TI1855 PV LGO TO STORAGE DegC
00:00	1,715	1,288	0,595	2,73	141,1	0,03	285,2	68,6	1398	750	60,46	30,67
01:00	1,702	1,273	0,562	2,74	140,9	0,03	283,9	69,3	1401	751	60,24	30,33
02:00	1,689	1,260	0,541	2,76	141,6	0,03	283,2	71,1	1397	752	59,43	29,92
03:00	1,744	1,311	0,630	2,79	141,0	0,03	286,3	70,6	1400	748	59,58	30,05
04:00	1,701	1,271	0,545	2,77	140,8	0,03	283,1	68,4	1401	749	58,96	29,58
05:00	1,698	1,267	0,543	2,81	141,0	0,03	284,8	70,0	1397	754	58,78	29,49
06:00	1,749	1,323	0,638	2,87	140,9	0,03	288,9	64,0	1399	751	59,28	29,90
07:00	1,728	1,300	0,602	2,84	141,2	0,03	285,5	61,8	1399	751	59,78	30,06
08:00	1,743	1,324	0,637	2,84	141,4	0,04	283,7	62,2	1401	747	61,27	30,96
09:00	1,759	1,336	0,674	2,85	141,5	0,04	287,5	61,8	1397	750	62,41	31,99
10:00	1,754	1,330	0,655	2,77	141,7	0,04	283,3	61,5	1396	747	62,33	32,26
11:00	1,704	1,274	0,578	2,83	141,6	0,04	282,2	61,1	1399	753	62,51	32,25
12:00	1,700	1,268	0,567	2,75	141,0	0,04	287,1	61,5	1405	751	61,81	32,48
13:00	1,689	1,257	0,558	2,82	141,3	0,04	287,4	61,3	1399	754	62,03	32,54
14:00	1,678	1,245	0,558	2,84	140,6	0,04	283,6	61,4	1401	749	61,56	32,47
15:00	1,670	1,236	0,537	2,88	140,7	0,03	287,8	60,4	1404	755	61,51	32,47
16:00	1,702	1,265	0,524	2,86	141,7	0,04	281,6	61,5	1395	750	61,43	32,15
17:00	1,733	1,288	0,486	2,61	142,5	0,04	280,9	61,6	1404	749	61,14	31,98
18:00	1,717	1,267	0,452	2,80	141,9	0,03	284,2	61,6	1401	748	59,32	31,60
19:00	1,714	1,265	0,479	2,90	141,2	0,04	285,7	62,8	1403	751	57,97	30,51
20:00	1,803	1,365	0,573	2,91	142,5	0,04	277,7	66,3	1398	751	59,07	29,67
21:00	1,786	1,346	0,534	2,99	143,5	0,03	275,4	63,9	1402	752	59,29	29,37
22:00	1,876	1,444	0,664	3,05	143,2	0,03	278,4	62,5	1400	753	59,53	29,91
23:00	1,738	1,309	0,586	3,11	143,8	0,03	280,3	62,1	1400	748	60,13	30,20

	C-8 ACID WATER STRIPPER								K-101 FLARE GAS COMPRESSOR SECTION			
	FLOW		TEMP				PRESS		FLOW			
TIME	10FI49	10FIC50	10TI3106	10TI103	10TI3104	10TI3107	10PIC19	10PI3108	10FI1101		10FI1103	10FIC1102
	PV	PV	PV	PV	PV	PV	PV	PV	PV		PV	PV
	ACID GAS TO 10-F-1A/B AND 1	STIPPING LP STEAM TO C-8	FEED TO C-8	OUTLET OF EA-12	C-8 BOTTOM	STRIPPED WATER TO V-52	V-17	STRIPPED WATER TO V-52	K-101 DISCHARGE		FLARE GAS TO FUEL GAS HEA	UNSTABILIZED NAPHTHA TO E-101 A/B
	Nm3/hr	m3/hr	DegC	DegC	DegC	DegC	kg/cm2	kg/cm2	Nm3/hr		Nm3/hr	m3/hr
00.00	25,0	15	18,6	22,9	18,9	36,0	0,000	3,145	1470		126,0	8,404
01.00	25,2	14	18,4	22,1	18,6	36,5	0,000	3,145	1461		126,0	8,404
02.00	25,0	13	18,2	22,2	18,6	35,0	0,000	3,144	1466		126,0	8,404
03.00	24,9	14	18,0	21,9	18,5	36,1	0,000	3,146	1470		126,0	8,404
04.00	24,2	14	17,8	22,3	18,3	36,7	0,000	3,144	1468		126,0	8,404
05.00	24,0	14	17,6	22,4	18,1	35,3	0,000	3,151	1470		126,0	8,404
06.00	25,4	13	17,4	22,0	18,0	35,9	0,000	3,151	1470		126,0	8,404
07.00	25,7	13	17,3	21,8	17,9	36,5	0,000	3,151	1470		126,0	8,403
08.00	27,8	13	17,5	22,7	18,1	37,4	0,000	3,140	1468		126,0	8,403
09.00	30,0	13	17,6	24,7	18,3	37,7	0,000	3,122	1470		126,0	8,403
10.00	31,2	14	18,3	26,7	18,7	38,6	0,000	3,123	1470		126,0	8,403
11.00	31,3	14	18,9	27,2	19,4	37,8	0,000	3,053	1443		125,5	8,403
12.00	31,5	15	19,7	26,5	19,9	36,8	0,000	2,680	1470		126,0	8,403
13.00	32,0	15	20,3	26,3	20,8	36,7	0,000	3,113	1470		126,0	8,403
14.00	31,3	15	20,7	26,3	20,8	36,2	0,000	3,122	1470		126,0	8,403
15.00	31,3	15	21,1	26,4	20,9	35,7	0,000	3,138	1446		126,0	8,403
16.00	31,1	15	21,4	26,4	21,2	35,6	0,000	3,143	1410		126,0	8,404
17.00	30,8	15	21,7	25,5	21,4	36,5	0,000	3,145	1389		126,0	8,404
18.00	29,6	15	21,9	24,4	21,5	36,3	0,000	3,146	1418		126,0	8,404
19.00	26,0	15	21,7	24,0	21,2	34,2	0,000	3,131	1439		126,0	8,404
20.00	23,7	15	20,7	20,8	20,5	35,1	0,000	3,138	1470		126,0	8,404
21.00	24,9	13	19,9	19,5	20,2	37,0	0,000	3,143	1468		126,0	8,404
22.00	25,1	13	19,4	20,8	19,8	37,6	0,000	3,140	1470		126,0	8,404
23.00	24,3	14	19,0	21,9	19,6	39,0	0,000	3,128	1470		126,0	8,404
Average	27,6	14	19,3	23,7	19,5	36,5	0,000	3,116	1458		126,0	8,404
Total	662,4	342	463,1	567,8	468,9	876,3	-0,002	74,786	34989		3023,5	201,685
Maximum	32,0	16	21,9	27,2	21,5	39,0	0,000	3,151	1470		126,0	8,404
Minimum	23,7	13	17,3	19,5	17,9	34,2	0,000	2,680	1389		125,5	8,403

	K-101 FLARE GAS COMPRESSOR SECTION						UTILITY AT BIL				
	FLOW	TEMP			PRESS			COOLING WATER			
TIME	10FIC1105	10TI1111	10TI1101	10TI1110	10PI1104	10PI1107	10PIC1112	10FI172	10FIS101	10FIS105	10TIS102	10TIS104
	PV	PV	PV	PV	PV	PV	PV	PV	PV	PV	PV	PV
	NAPHTHA FROM P-96A/B	K-101 SUCTION	K-101 DISCHARGE	V-102	K-101 SUCTION	K-101 DISCHARGE	V-102	FLOW (EXISTING HEADER)	FLOW (NEW HEADER)	PUMP CW RETURN HEADER F	SUPPLY TEMP. (EXISTING HEA	SUPPLY TEMP. (NEW HEADER)
	m3/hr	DegC	DegC	DegC	kg/cm2	kg/cm2	kg/cm2	m3/hr	m3/hr	m3/hr	DegC	DegC
00.00	14,63	35,43	167,3	39,11	0,5105	4,74	4,44	594	982	-1,0	23,47	22,94
01.00	14,63	35,43	166,5	38,59	0,4819	4,66	4,37	609	990	-1,0	23,24	22,71
02.00	14,63	34,11	165,1	38,54	0,4657	4,65	4,38	597	993	-1,0	23,04	22,52
03.00	14,63	36,73	164,0	39,16	0,5339	4,73	4,39	600	996	-1,0	22,83	22,37
04.00	14,63	35,55	163,6	38,52	0,4620	4,53	4,23	611	1002	-1,0	22,76	22,24
05.00	14,63	34,66	162,4	38,29	0,4595	4,51	4,21	608	1009	-1,0	22,54	22,02
06.00	14,63	36,63	163,6	38,61	0,5406	4,76	4,42	613	1006	-1,0	22,35	21,83
07.00	14,63	36,14	166,0	37,73	0,5127	4,70	4,38	611	1018	-1,0	22,38	21,86
08.00	14,63	36,75	169,4	38,00	0,5513	4,95	4,65	606	964	-1,0	22,74	22,20
09.00	14,63	36,80	169,8	38,64	0,5816	5,00	4,68	586	-23	-1,0	23,44	22,88
10.00	14,63	36,52	169,3	38,71	0,5654	4,94	4,63	584	-23	-1,0	23,87	23,31
11.00	14,48	34,53	170,1	38,26	0,5068	4,83	4,63	533	-23	-1,0	24,07	23,50
12.00	14,63	34,51	166,5	38,62	0,4893	4,72	4,44	602	-23	-1,0	24,06	23,50
13.00	14,63	34,16	165,2	38,55	0,4803	4,68	4,40	598	-23	-1,0	24,01	23,43
14.00	14,63	32,95	166,3	38,11	0,4867	4,76	4,50	607	-23	-1,0	24,03	23,46
15.00	14,63	32,90	167,2	38,10	0,4712	4,77	4,53	608	-23	-1,0	24,07	23,50
16.00	14,63	33,96	168,6	37,94	0,4622	4,78	4,55	592	-23	-1,0	24,09	23,53
17.00	14,63	34,39	168,0	37,77	0,4263	4,65	4,43	598	-23	-1,0	24,10	23,54
18.00	14,63	34,25	163,8	37,56	0,3895	4,42	4,15	596	-23	-1,0	23,95	23,30
19.00	14,63	31,88	164,4	37,90	0,4115	4,48	4,23	613	860	-1,0	23,73	23,20
20.00	14,63	35,04	165,6	38,37	0,4886	4,68	4,38	610	1477	-1,0	23,46	22,94
21.00	14,63	35,18	163,1	38,85	0,4573	4,62	4,35	586	1339	-1,0	23,37	22,83
22.00	14,63	40,07	164,2	39,31	0,5628	4,86	4,51	601	1409	-1,0	23,37	22,84
23.00	14,63	37,42	165,5	38,78	0,5061	4,78	4,50	603	1417	-1,0	23,34	22,81